ADDIS ABABA UNIVERSITY

ADDIS ABABA INSTITUTE OF TECHNOLOGY

CENTER OF ENERGY TECHNOLOGY

DESIGN OF COOLANT HEATER FOR AN EMERGENCY ELECTRIC GENERATOR DRIVE DIESEL ENGINE BY SOLAR ENERGY FOR A CEMENT INDUSTRY

BY

TADESSE MELETA

NOVEMBER 2016

ADDIS ABABA,

ETHIOPIA

Addis Ababa University

Addis Ababa Institute of Technology

Center of Energy Technology

Design of Coolant Heater for an Emergency Electric Generator Drive Diesel Engine by Solar Energy for a Cement Industry

A thesis submitted to Addis Ababa Institute of Technology, Energy Center, in Partial Fulfillment of the Requirements for the Degree of **Master of Science in Energy Technology**

By:

Tadesse Meleta

Advisor:

Dr.Ing. Demis Alemu

November 2016

Addis Ababa, Ethiopia

Addis Ababa University

Addis Ababa Institute of Technology

Center of Energy Technology

Design of Coolant Heater for an Emergency Electric Generator Drive Diesel Engine by Solar Energy for a Cement Industry

By:

Tadesse Meleta

APPROVED BY BOARD OF EXAMINERS

1.	**Mr. Fitsum Salehu**	_____	_____
	Chairman, Graduate Committee,	Signature	Date
2.	**Dr.-Ing. Demiss Alemu**	_____	_____
	Theses Advisor	Signature	Date
3.	**Dr.-Ing. Edessa Dirbsa**	_____	_____
	Internal Examiner	Signature	Date
4.	**Dr. Tesfaye Dama**	_____	_____
	External Examiner	Signature	Date

DECLARATION

I hereby declare that this thesis is my own work towards MSc in Energy Technology and that, to the best of my knowledge, it contains no material previously published by another person nor material which has been accepted for the award of any other degree of the University, except where due acknowledgement has been made in the text.

Declared by:

Name: Tadesse Meleta

Signature: _____

Date: _____

Place: Addis Ababa Institute of Technology, Addis Ababa University, Addis Ababa, Ethiopia

This thesis has been submitted for examination with my approval as a University Advisor.

Confirmed by:

Advisor's Name: Dr.-Ing. Demiss Alemu

Signature: _____

Date: _____

This thesis is dedicated to the memory of my father, Meleta Dadi and my brother Debebe Meleta.

ACKNOWLEDGEMENT

First, I thank my advisor Dr.-Ing. Demis Alemu,for his continuous support during this thesis work period. My special thanks also go to Diriba Korecha (PhD), National Climate Scientist-Ethiopia, USGS/Famine Early Warning Systems Network and Girma Bacha, Mugher Cement Factory Maintenance Engineering Division Head, who engaged me in a number of discussions and document preparation in all the stages of the study that helped me to identify the appropriate horizon of research tools, input variables and overall approaches. I am indebted to my course teachers, who shared their professional knowledge, and provided lively and highly interactive lectures during my stay in this post graduate study.

I gratefully acknowledge the full scholarship granted to me from my company, Mugher Cement Factory, which enabled me to pursue my study without any time and financial constraints. I wish to extend my thanks to all of my relatives and friends. It is impossible to list all of their names here. I thank them all for being a source of strength and for their enjoyable friendships.

Last, but not least, I thank my wife, Alem Tajebe, and my lovely kids, Siddise and Solan, for their valuable endurance during my absence from them to attend the courses and their encouragement to concentrate on my study.

LIST OF ACRONYMS

$^{\circ}C$	Degree Celsius	Hz	Hertz
N	North	V	Volt
E	East	KVA	Kilo Volt Ampere
m	metre	A	Ampere
U.S.	United States	DC	Direct Current
i.e.	that is	LED	Light Emitting
C_2S	Dicalcium Silicate		Diode
C_3S	Tricalcium Silicate	KV	Kilo Volt
tpd	tones per day	MVA	Mega Volt Ampere
MJ/kg	Mega Joule per kilo gram	EEPCO	Ethiopian Electric
Kcal/kg	Kilo calorie per kilogram		Power Corporation
L/D	Length to Diameter	AC	Alternating Current
°F	Degree Fahrenheit	MCC	Motor Control
α	alpha		Cabinet
β	beta	VFD	Variable Frequency
γ	gamma		Drive
MgO	Magnesium Oxide	Genset	Generator set
CaO	Calcium Oxide	deg.C	degree Celsius
mm	millimeter	W	Watt
Hp	Horse power	L	Liter
Rpm	Revolution per minute	”	inch
Kw	Kilo watt		

TABLE OF CONTENTS

Table of Contents **Page**

LIST OF TABLES

List of tables Page

LIST OF FIGURES

List of Figures Page

ABSTRACT

This study explored the application of the solar thermal technology to the engine circulating coolant and lubricant to attain the optimum operating temperature without delay in an industry using diesel engine to drive emergency electric generator in attaining its rated power capacity for one of the diesel engine driven emergency electric generator installed for Mugher Cement Factory. The result will serve for avoiding the cement production equipment of the rotary kiln and related drive systems from thermal gradient deformation immediately after unexpected main grid failure.

In order to improve the circulating coolant temperature and the pre-heating time requirement, electric heater has been installed. To measure the improvement of engine efficiency during starting up period after main grid failure, temperature data are collected from the generator set controller and measuring instruments both before and after installation of electric heater. These data have been collected when this experiment was made on site in Mugher Cement Factory. The data contain readings of temperatures [°C] obtained from measuring instruments and installed controller.

The analysis of the system has been done by using controller performance display readings and performance measuring instruments. Besides, temperature reading data has been analyzed by using some statistical methods, particularly to investigate the improvements achieved or the severity of the existing problem. From the performance improvements, the results computed from observed data as well as from test instruments, the generator set shows that its performance has been clearly improved by using heater to heat the coolant. Besides these, it can be deduced, even if not tested, that coupling of the solar thermal technology can further improve its performance. Based on these preliminary results, a solar water heater of 100 litre capacity, with provision of auxiliary electrical heater in addition to solar heater, in comparison with the cases of electrical heater, is designed in detail to be locally fabricated and installed for the case of Mugher Cement Factory. Generally, selecting and adopting proper solar water heating technology for the circulating coolant of emergency electric generator drive diesel engine has improved preheating time in attaining engines thermostat opening temperature in a lesser time to avoid the rotary kiln and related drive-driven systems thermal gradient deformation immediately after the main grid failure of a cement industry. This is an indication of the applicability of the result of this thesis.

The output of the research shall contribute reliability for industry's production processing equipment, especially the key equipment that operate at high process temperature, by avoiding rapid cooling that causes the thermal gradient deformation and leads to complete equipment damage and consequently loss of production, revenue and employee lay off due to inefficiency of the engine. The finding of this research can be used as the potential of making the diesel engine driven electric generator that enable to attain its full load immediately by adopting similar technologies for institutions that require immediate back up. Furthermore, it creates an opportunity in looking at heating water by harnessing energy from the sun for industrial and commercial firms in order to overcome the rising of oil prices as well as utilization of environmental-friendly alternative sources of energy, specifically renewable energy technologies and promoting green energy technology.

Key words: Engine coolant, heating time, delay time, heater, emergency generator, kiln, cooler, solar radiation, solar collector.

CHAPTER ONE

INTRODUCTION

1.1. Background

The Diesel generator owes its roots to mainly two inventors. One of these is the creator of the first generator Michael Faraday and the other is the creator of the Diesel engine Rudolph Diesel. The first of these two has contributed greatly to life today with all his discoveries in electricity.

It was his discovery of electromagnetic induction in the year 1831 that led to the development of the modern generator. He used what he termed induction ring to discover the electromagnetic induction. This was the generation or induction of electricity in a wire by the use of the electromagnetic effect of the current in another wire. This was the first transformer and followed closely with the discovery of the magneto-electric induction process which is the production of a steady electric current.

According to Barney L. Capehart et al, in the diesel generator set, diesel engine is the prime mover, which drives an alternator to produce electrical energy. To make a decision on the type of engine, which is most suitable for a specific application, the factors that need to be considered are, power and speed of the engine, the cooling system, lubrication system, abnormal environmental conditions (dust, dirt, etc.), fuel quality, speed governing (fixed or variable speed), control system, starting equipment, drive type, ambient temperature, altitude, humidity, etc. The power requirement is determined by the maximum load. The engine power rating should be 10–20 % more than the power demand by the end use. This prevents overloading the machine by absorbing extra load during starting of motors or switching of some types of lighting systems or when wear and tear on the equipment pushes up its power consumption.

The general feeling has been that a water cooled Diesel generator set is better than an air cooled set, as most users are worried about the overheating of engines during summer months and delay of heating up to attain the proper operating temperature during start up. This is to some extent true and precautions have to be taken to ensure that the cooling water temperature does not exceed the prescribed limits. However, from performance and

maintenance point of view, proper care should be taken on all the circulating cooling water to ensure operating temperature within limits.

Hot water and steam form an integral part of various industrial and commercial applications and with rising oil prices, there has never been a better time to look at heating water by harnessing energy from the Sun [4].

The main components of a typical solar water heating system are:

I. Solar Collectors: functions as the primary heating source;
II. Insulated hot water tank: for storing hot water;
III. Insulated piping: regulate flow of water between components; and
IV. Air vent: to release trapped air from hot water tank.

Based on experience over a decade in installing large capacity systems, requiring different features that enable to customize and design solar water heating systems to suit specific site/industry requirements are carried out.

According to Thammasat (2008), solar collector oriented due south in the northern hemisphere and tilted at an angle of $\pm 5^{o}$ more or less than the local geographic latitude is best recommended to heat the water to the maximum temperature for the site.

The intent of this research is to apply the solar thermal technology to the engine circulating coolant and lubricant to attain the optimum operating temperature without delay in an industry using engine to drive emergency electric generator.

1.2. Problem Statement

This research is to find out the problems of the delay of diesel engine driven emergency electric generator in attaining its rated power capacity that suits the purpose for which it is intended and seek solution, specifically for one of the diesel engine driven emergency electric generator installed at Mugher Cement Factory as a case study. The main problem in the conversion process of the installed emergency electric generator in this Factory is the delay of required capacity electric power generation to avoid the rotary kiln and related drive systems from thermal gradient deformation immediately after unexpected main grid failure.

1.3. Hypothesis

The delay of the system in attaining the required capacity is due to low start up operating temperature of drive engine including the circulating coolants and lubricants.

The performance of the engine's coolants and lubricants shall be improved by providing a hotter circulating coolant always readily available by installing a solar water heater that improves the engine's preheating time in attaining its thermostat opening temperature of $75^{\circ}C$ in a lesser time.

1.4. Objective

1.4.1. Major Objective

The major objective of this research is to investigate the potential of making the diesel engine driven electric generator fully attains its full load immediately, without longer period of pre-heating time requirement of engine, for the intended purpose by adopting similar technologies of the findings of the research for institutions that require immediate back up.

1.4.2. Specific Objectives

This research has the following specific objectives:-

I. Selecting and adopting proper solar water heating technology for the circulating coolant of emergency electric generator drive diesel engine that shortens the preheating time in attaining its thermostat opening temperature of $75^{\circ}C$ in a lesser time to avoid the rotary kiln and related drive-driven systems thermal gradient deformation immediately after the main grid failure of a cement industry.

II. Carrying out analysis of the performance parameters improvement achieved.

1.5. Significance of the Research

The research shall contribute reliability for industry's production processing equipment, especially the key equipment that operate at high process temperature, by avoiding rapid cooling that causes the thermal gradient deformation and leads to complete equipment damage and consequently loss of production, revenue and employee lay off.

1.6. Limitation of the Study

Lack of engine tuning equipment, engine and generator output performance measuring instruments, lack of solar panel/solar water heater for practical testing and comparing of the improvements achieved, as well as lack of the running fuel for onsite testing the engine, which the industry may not be willing to allow the experiment out of their plan due to cost incursion, are assumed to be the limitation of the study.

1.7. Scope of the Study

This study is planned to be carried out in Mugher Cement Factory, a state owned cement producing industry in Ethiopia. Its geographic location is (9°40'60")N latitude, (37°58'60")E longitude at an altitude/elevation of 2496m above sea level, 90 kilo meter away west of the capital city, Addis Ababa. The factory has an average daily production capacity of five thousand tone of clinker with three production lines.

1.8. Organization of the Study

This thesis is organized as follows:

I. Chapter Two, shall discuss about the literature review relating to this research.
II. In Chapter Three, Materials used, data and methodology employed in this research shall be presented.
III. In Chapter Four, the main results of this research shall be discussed.
IV. In Chapter Five, the finding of the research shall be summarized with necessary recommendations.

CHAPTER TWO

LITERATURE REVIEW

2.1. Electric Generator and Diesel Engine

The Diesel generator owes its roots to mainly two inventors. One of these is the creator of the first generator Michael Faraday and the other is the creator of the Diesel engine Rudolph Diesel. The first of these two has contributed greatly to life today with all his discoveries in electricity. It was his discovery of electromagnetic induction in the year 1831 that led to the development of the modern generator. He used what he termed his induction ring to discover the electromagnetic induction. This was the generation or induction of electricity in a wire by the use of the electromagnetic effect of the current in another wire. This was the first transformer and followed closely with the discovery of the magneto-electric induction process which is the production of a steady electric current.

According to Barney L. Capehart et al (2007), in the Diesel generator set, Diesel engine is the prime mover, which drives an alternator to produce electrical energy. To make a decision on the type of engine, which is most suitable for a specific application, the factors that need to be considered are, power and speed of the engine, the cooling system, lubrication system, abnormal environmental conditions (dust, dirt, etc.), fuel quality, speed governing (fixed or variable speed), control system, starting equipment, drive type, ambient temperature, altitude, humidity, etc. The power requirement is determined by the maximum load. The engine power rating should be 10 – 20 % more than the power demand by the end use. This prevents overloading the machine by absorbing extra load during starting of motors or switching of some types of lighting systems or when wear and tear on the equipment pushes up its power consumption.

The temperature of engine intake air and cooling air or water (as applicable) can have a substantial engine performance impact. Atmospheric pressure, especially as determined by altitude, is also a major factor. Even humidity can be significant to engine operation. Therefore, the ambient conditions are an important part of engine performance data.

According to U.S. Nuclear Regulatory Commission of Draft Regulatory Guide DG-1172 (2006), an emergency diesel generator selected for use in an onsite electric power system should have the capability to:

I. Start and accelerate a number of large motor loads in rapid succession, while maintaining voltage and frequency within acceptable limits,
II. Provide power promptly to engineered safety features if a loss of offsite power (loop) and a design-basis event occur during the same time period, and
III. Supply power continuously to the equipment needed to maintain the plant in a safe condition if an extended.

Knowledge of the characteristics of each load is essential to establish the bases for selection of an emergency diesel generator that is able to accept large loads in rapid succession. The majority of these emergency loads are large induction motors. At full voltage, this type of motor draws a starting current of five to eight times its rated full-load current. These sudden large increases in current drawn from the diesel generator as a result of the startup of induction motors can result in substantial voltage reductions. This lower voltage could prevent a motor from starting (i.e., accelerating its load to rated speed in the required time), or could cause a running motor to coast down or stall. Other voltage-sensitive loads might also be lost because of low voltage or if their associated contactors drop out. Recovery from the transient caused by starting large motors, or from the loss of a large load, could cause diesel engine over speed that, if excessive, might result in a trip of the engine (i.e., loss of the safety-related power source). These same consequences can also result from the cumulative effect of a sequence of more moderate transients if the system is not permitted to recover sufficiently between successive steps in a loading sequence [6].

The general feeling has been that a water cooled Diesel generator set is better than an air cooled set, as most users are worried about the overheating of engines during summer months and delay of heating up to attain the proper operating temperature during start up. This is to some extent true and precautions have to be taken to ensure that the cooling water temperature does not exceed the prescribed limits. However, from performance and maintenance point of view, proper care should be taken all the circulating cooling water to ensure operating temperature within limits.

2.2. Solar Radiation and Its Estimation

2.2.1. The Sun-Earth Relations

2.2.1.1. Sun-Earth and Geometric Radiation-Plane Angles

As the earth rotates about the sun, it spins about an axis which points to the North Star and is inclined at approximately 23.45^o to the orbital plane as illustrated in fig 2.1

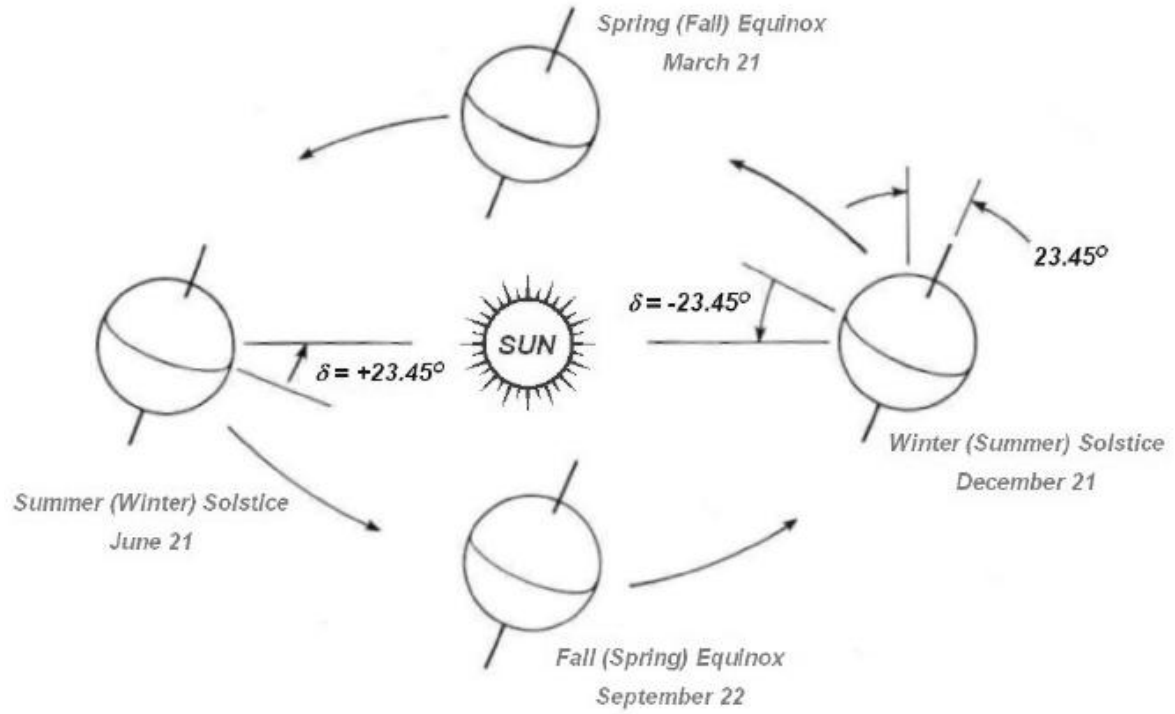

Figure 2.1: Northern (Southern) Hemisphere Earth-Sun Relationship (Source: Dr.Ing Abebayehu Assefa's lecture note)

At about June 21, we observe that the noon time sun is at its highest point in the sky and the declination angle (δ) = +23.45^o. We call this condition summer solstice and it marks the beginning of summer in the northern hemisphere. The winter solstice occurs on about December 22, when the northern hemisphere is tilted away from the sun. The noon time sun at its lowest point in the sky, that is, the declination angle (δ) = -23.45^o. In between, on about September 23 (Autumnal equinox) and March 22 (Vernal equinox), the line from the earth to the sun lies on the equatorial plane and δ=0^o.

Therefore, the angle between the earth's equatorial plane and earth-sun line varies between +/-23.45^{o} throughout the year. This angle is called the declination, δ. Declinations north of the equator are positive (summer in the Northern Hemisphere); those south are negative. This declination of the earth-sun line has an effect on the amount of radiation striking the solar collector besides the effect of other factors like cloud, which depends on the season.

The declination angle (δ) of the sun varies daily and is calculated from the following relation:

$$\delta = 23.45 sin\left[\frac{360}{365}(284 + N)\right] \quad \textit{(2.1)}$$

Where; N = the day in the year (day number); and for monthly average days, dates and declinations, see table 2.1 below.

Table 2.1: Recommended average days for months and values of N by months (Duffie and Beckman, 1991)

Month	N for ith day of month	For the average day of the month		
		date	Day of year N	Declination δ
January	i	17	17	-20.9
February	31+i	16	47	-13.0
March	59+i	16	75	-2.4
April	90+i	15	105	9.4
May	120+i	15	135	18.8
June	151+i	11	162	23.1
July	181+i	17	198	21.2

Month	N for i^{th} day of month	For the average day of the month		
		date	Day of year N	Declination δ
August	212+i	16	228	13.5
September	243+i	15	258	2.2
October	273+i	15	288	-9.6
November	304+i	14	318	-18.9
December	334+i	10	344	-23.0

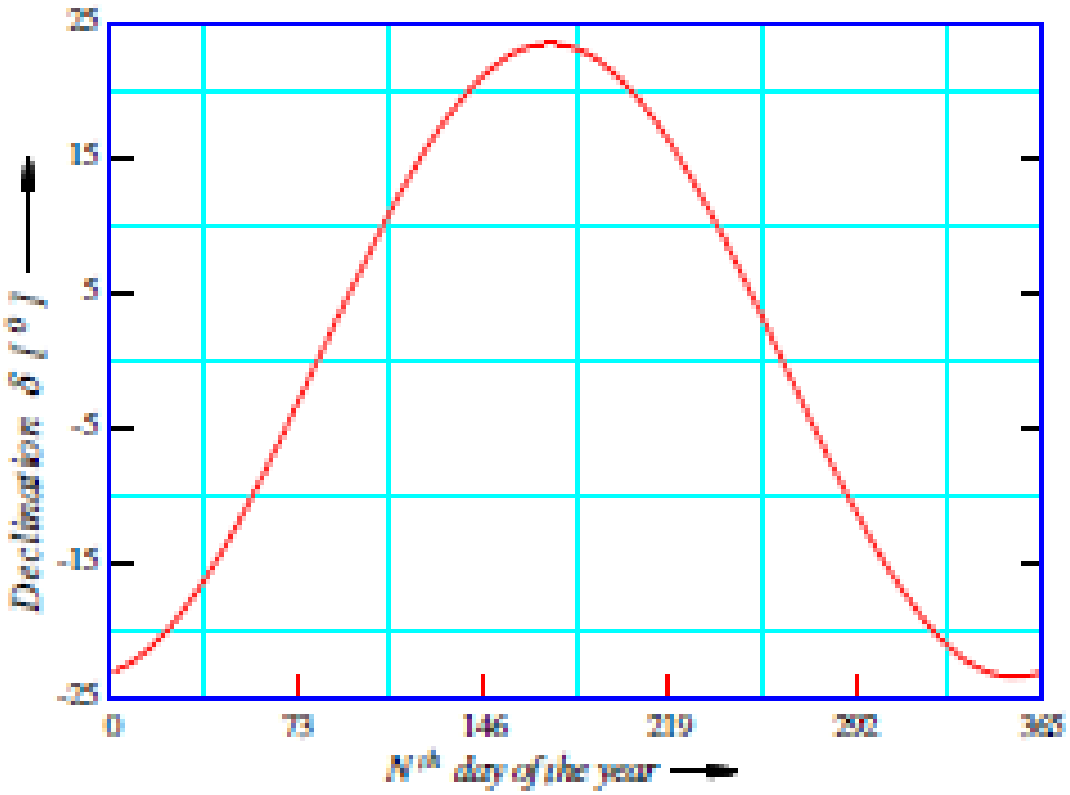

Figure 2.2: Variation of declination angle, δ, with N^{th} day of year (Source: Dr.Ing Abebayehu Assefa's lecture note).

2.2.1.2. Environmental Variables of Direction of Radiations

The geometric relationships between any fixed or movable plane of any particular orientation relative to the earth at any time and the incoming beam solar radiation with respect to the position of the sun relative to that plane can be described in terms of several angles [Duffie, J.A. and Beckman, (1991)]. Some of the angles are defined as follows:

I. The solar altitude, α_s at a point on the earth is the angle between the line passing through the point and the sun and the line passing through the point tangent to the earth and passing below the sun, ($\alpha = 90-\theta_z$). It shows the sun's location in the sky relative to a point on the earth's surface.

II. The solar azimuth, γ_s, as illustrated in fig 2.3 is the angle between the line under the sun and the local meridian pointing to the equator, or due south in the Northern Hemisphere, The solar zenith angle is the angle between a solar ray and local vertical direction, is the complements of θ_z. It shows the sun's location in the sky relative to a point on the earth's surface.

III. ϕ= latitudes for the specified solar measurement stations of area of required installation of the project.

IV. $\delta = 23.45sin\left[\frac{360}{365}(284+N)\right]$ the sun's declination As defined on equation 2.1 above.

V. β = the collector's tilt measured towards the horizontal plane.

VI. γ = the solar collector's azimuth angle = deviation from south, positive towards west, negative towards east in the Northern hemisphere and vice versa in the Southern hemisphere.

VII. γ_s = the sun's azimuth angle.

VIII. ω = the sun's hour angle measured in degrees (15°/h) from the meridian; positive in the afternoon, negative in the morning. Both hour angle (ω) and solar time (ST) are related as $\omega = (\mathrm{ST}-12)\times 15^{\circ}$ as defined on equation 2.3 below. The solar hour angle is the angular displacement of the sun east or west of the local meridian; morning negative, afternoon positive. The solar hour angle is equal to zero at solar noon and varies by 15 degrees per hour from solar noon. For example at 7 a.m. (solar time2) the solar hour angle is equal to –75° (7 a.m. is five hours from noon; five times 15 is equal to 75, with a negative sign because it is morning).

IX. θz = the sun's zenith angle = 90°-α_s (Solar altitude angle).

X. N = the day in the year (day number); for monthly average days, dates and declination, see table 2.1 above.

XI. θ = angle of incidence = angle between the solar collector normal and the beam radiation. It is a function of the following variables:

$$cos\theta = sin\delta\, sin\phi\, cos\beta - sin\delta\, cos\phi\, sin\,\beta\, cos\gamma + cos\delta\, cos\phi cos\beta cos\omega + cos\delta\, sin\phi\, sin\beta\, cos\gamma\, cos\omega + cos\delta\, sin\beta\, sin\gamma\, sin\omega \quad \ldots\ldots\ldots\ldots\ldots\ldots\ldots (2.2)$$

XII. The above equation (2.2) shows that there are a set of important relationships relating the angle of incidence of beam radiation θ to the other angles.

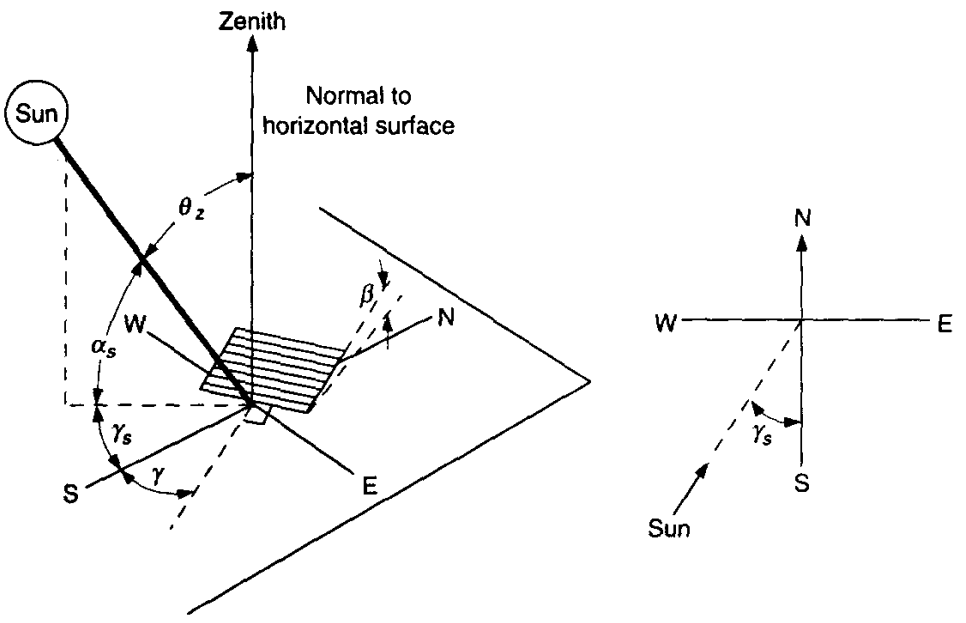

Figure 2.3: Zenith angle, slope, surface azimuth angle, solar azimuth angle for a tilted surface and plan view showing solar azimuth angle (Source: Duffie, J.A. and Beckman, W.A., Solar Engineering of Thermal Processes, 1991.)

The sun's location in the sky is a function of the location on the earth, the time of year and the time of day. The location on the earth is specified by the latitude,ϕ, which can be read from the atlas for specific location, which is (9°40'60")N latitude, (37°58'60")E longitude at an altitude/elevation of 2496m above sea level for our case. The time of year is specified by the solar declination, δ.

The time of day specified by the hour angle, ω, is defined as zero at local solar noon (γs), and, decreases by 15° for each hour before local solar noon and increases by 15° for each hour after solar noon. Hour angle (ω) and solar time (ST) are related as:

$$\omega = (ST - 12) \times 15^{\circ} \quad \text{..... (2.3)}$$

From figure 2.5 below, the hour angle ω of a point on the earth's surface which is defined as the angle through which the earth would turn to bring the meridian of the point directly under the sun.

The concept of solar time is used in predicting the direction of sun rays relative to a point on the earth. Solar time is the time used in all sun-earth angle relationships; it does not coincide with local clock time.

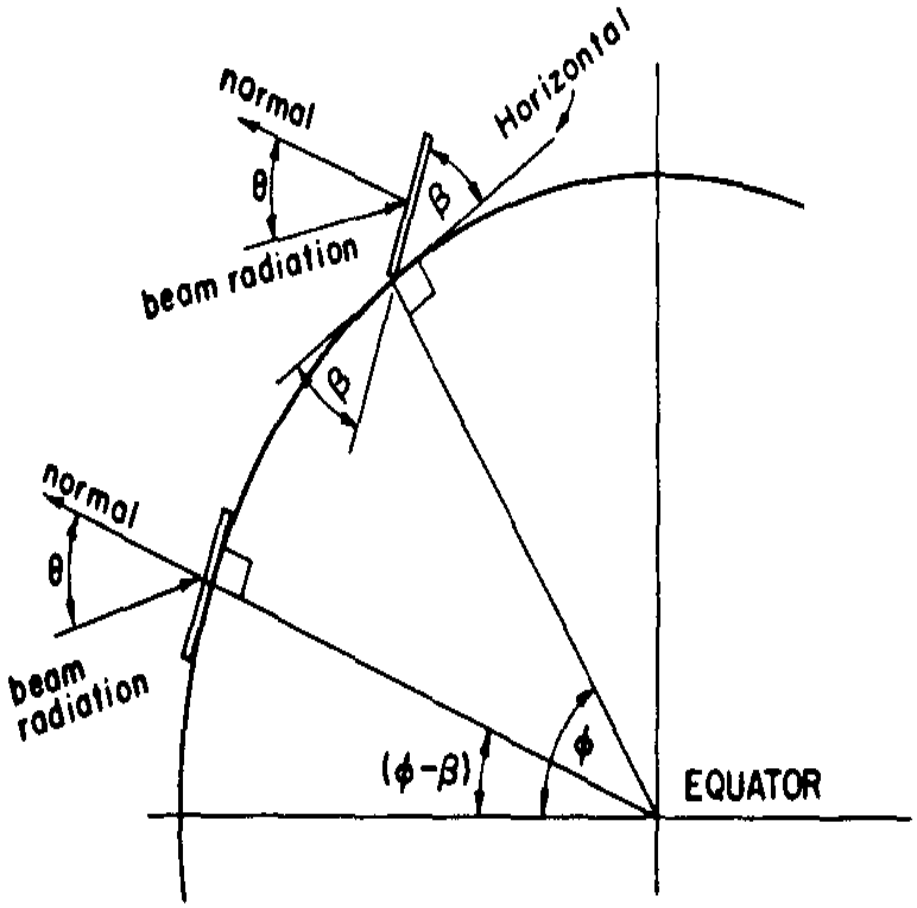

Figure 2.4: Section of earth showing β, θ, ϕ and (ϕ-β) for a south-facing surface (Source: Duffie, J.A. and Beckman, W.A., Solar Engineering of Thermal Processes, 1991.)

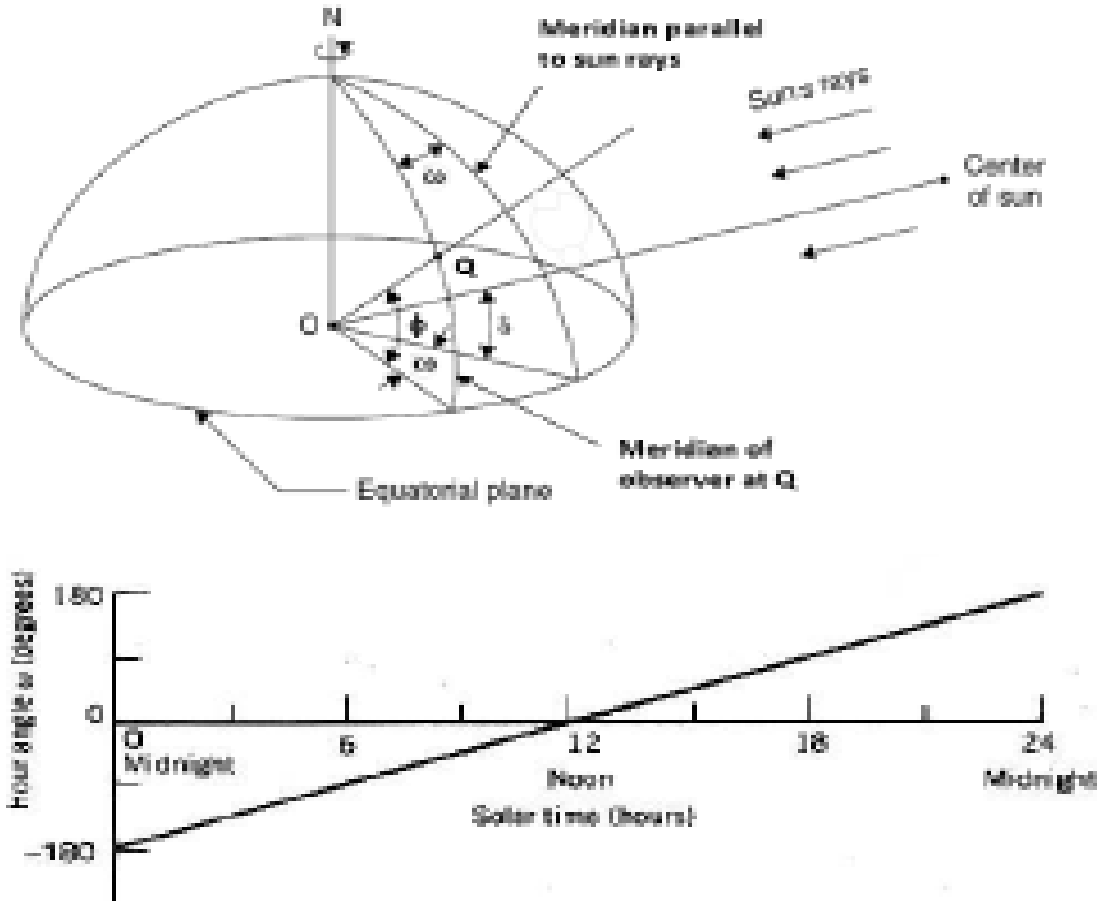

Figure 2.5: Hour angle (ω) and its variation (Source: Dr.Ing Abebayehu Assefa's lecture note).

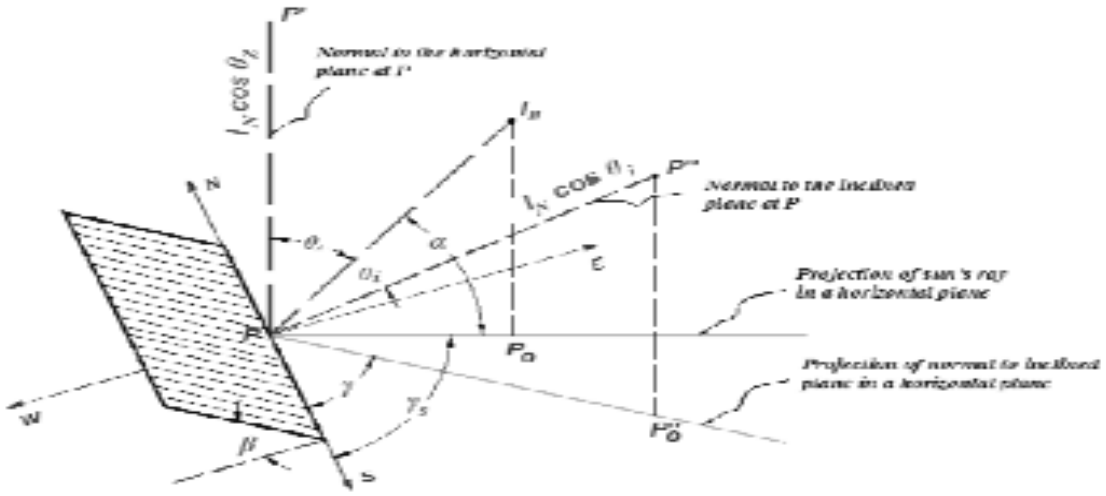

Figure 2.6: Views of various Sun-Earth Angles (Source: Dr.Ing Abebayehu Assefa's lecture note).

South tilted surface (for a surface facing due south, the azimuth angle $\gamma = 0$) with tilt β at latitude ϕ has the same incident angle θ as a horizontal surface at latitude $(\phi - \beta)$:

$$cos\theta = cos(\phi - \beta)\, cos\delta\, cos\omega + sin(\phi - \beta)sin\delta \quad \ldots\ldots (2.4)$$

This can be rewritten as:

$$cos\,\theta = (cos\,\emptyset\, cos\,\beta + sin\,\emptyset\, sin\,\beta)\, cos\,\delta\, cos\,\omega + sin\,\delta(sin\,\emptyset\, cos\,\beta - cos\,\emptyset\, sin\,\beta) \ldots (2.5)$$

For a horizontal plane facing due south; $\gamma = 0$, $\beta = 0$ and $\theta = \theta_z$ (Zenith angle):

$$cos\,\theta_z = cos\,\emptyset\, cos\,\delta\, cos\,\omega + sin\,\delta\, sin\,\emptyset \quad \ldots\ldots (2.6)$$

For a vertical surface facing due south; $\gamma = 0$, $\beta = 90°$ and $\theta = \theta_z$ (Zenith angle):

$$cos\,\theta = cos\,\delta\, cos\,\omega\, cos\,\emptyset + sin\,\delta\, sin\,\emptyset \quad \ldots\ldots (2.7)$$

Similarly, the sunrise and sunset hour angle (ω_s) is defined as follows:

ω_s = the sunrise and sunset hour angle is the hour angle at the time of sunrise (or sunset). It is the hour angle when the altitude angle is zero. The relationship for the sunrise and sunset hour angles and day-length could be obtained from the relation of zenith angle θ_z, which gives the angle between the sun's rays and the normal to the horizontal surface. At sunrise and sunset, the zenith angle $\theta_z = 90°$ and the corresponding hour angles are denoted as sunrise hour angle and sunset hour angle ω_s. Solving equation (2.7) above for the sun rise or sunset hour angle with $\omega = \omega_s$ and $\theta_z = 90°$:

$$0 = \cos\emptyset\cos\delta\cos\omega + \sin\delta\sin\emptyset$$

$$Or\, 2\omega_s = 2\, cos^{-1}(-tan\,\emptyset\, tan\,\delta) \quad \ldots\ldots (2.8)$$

$$\omega_s = cos^{-1}(-tan\,\emptyset\, tan\,\delta) \quad \ldots\ldots (2.9)$$

The number of daylight (sunshine) hours N_s is given by (since 15°= 1hour):

$$N_s = \frac{2}{15} cos^{-1}(-tan\,\emptyset\, tan\,\delta) \quad \ldots\ldots (2.10)$$

The following figure clearly shows the variation of daylight (sunshine) hours in northern hemisphere for the months of June 21, December 21, March 21 and September 21 for different latitudes.

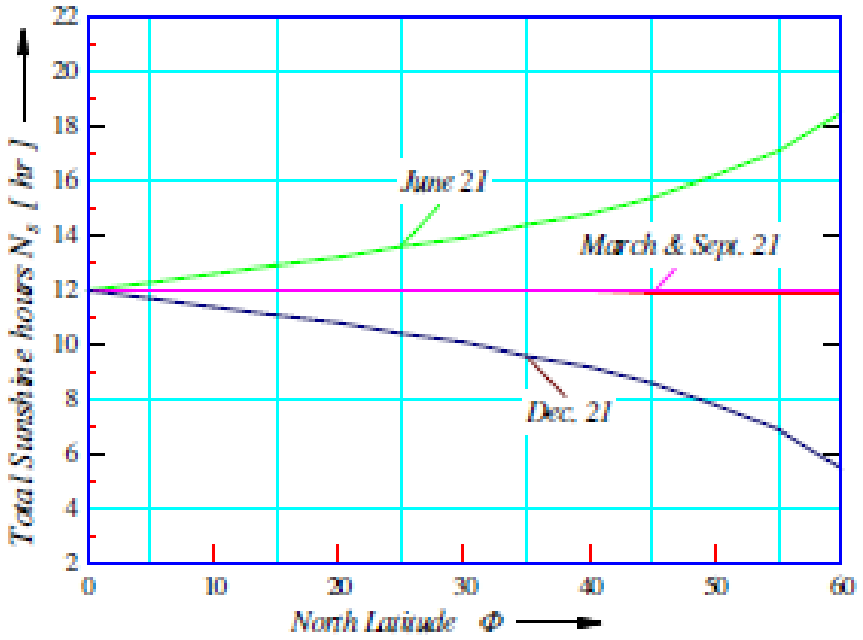

Figure 2.7: Variations of N_s with latitude for different days of the year (Source: Dr.Ing Abebayehu Assefa's lecture note).

2.2.2. Measurement of Solar Radiation

The prediction of the available solar energy at a given location and at a given time is necessary for the accurate design of any system for providing useful energy from the sun. The presentation of the basic information available to design the collector along with the methods of measurement commonly used and the methods of calculating or approximating site-specific data from the sparse information available is very important.

The motion of the sun is described from the point of view of a terrestrial observer as it moves around the earth. Using this convention, the amount of solar radiation striking a surface situated at Mugher at the specified tilt angle will be calculated. Since the calculation method to be used is used to estimate the amount of radiation energy available require only a single average value per month, monthly averaged total solar radiation, calculations will be presented.

Before the calculation of the amount of solar radiation which strikes the collector, it is necessary to define some terms related to solar radiation.

Beam or Direct Insolation, I_b: - is the solar radiation that reaches the surface of the earth directly from the sun without being scattered in the earth's atmosphere

Diffuse Insolation, I_d: - is the solar radiation that reaches the earth's surface after being scattered or diverted from its original path in the atmosphere.

Reflected Radiation, I_r: - is the solar radiation reflected from the ground and surroundings.

Global Insolation: - is the sum of all solar radiation on a surface. This includes not only the beam and diffuse insolation but also any insolation reflected from surrounding objects.

Air Mass: - is the ratio of the distance that solar radiation travels through the earth's atmosphere (path length), to the distance (path length) it would travel if the sun were directly overhead.

The solar constant (I_{sc}):- is the total amount of electromagnetic energy that falls on a unit area normal to the sun in unit time at the top of the earth's atmosphere when the earth is at its mean distance from the sun.

Irradiance (W/m^2): - is the rate at which radiant energy is incident on a surface per unit area of surface.

Irradiation or radiant exposure (J/m^2): - is the incident energy per unit area on a surface, found by the integration of irradiance over a specified time, usually an hour or a day.

Insolation: - is a term applied specifically to solar energy irradiation.

The symbol H: - is used for insolation for a day and **I** for insolation for an hour. Both H and I can represent beam, diffuse or total and can be on surfaces of any orientation.

2.2.2.1. Terrestrial and Extraterrestrial Regions

Figure 2.8 below shows the positions of terrestrial and extraterrestrial regions. In between, x-rays and extreme ultra-violet radiations of the sun are absorbed highly in the ionosphere by nitrogen, oxygen and other atmospheric gases. Ozone and water vapors largely absorb ultraviolet ($\lambda < 0.40$ μm) and infrared radiations ($\lambda > 2.3$ μm), respectively. There is almost

complete absorption of short wave radiations ($\lambda < 0.29$ μm) in the atmosphere. Hence, the energy in wavelength radiation below $\lambda = 0.29$ μm and above $\lambda = 2.3$ μm of the spectra of the solar radiation, incident on the earth's surface is negligible.

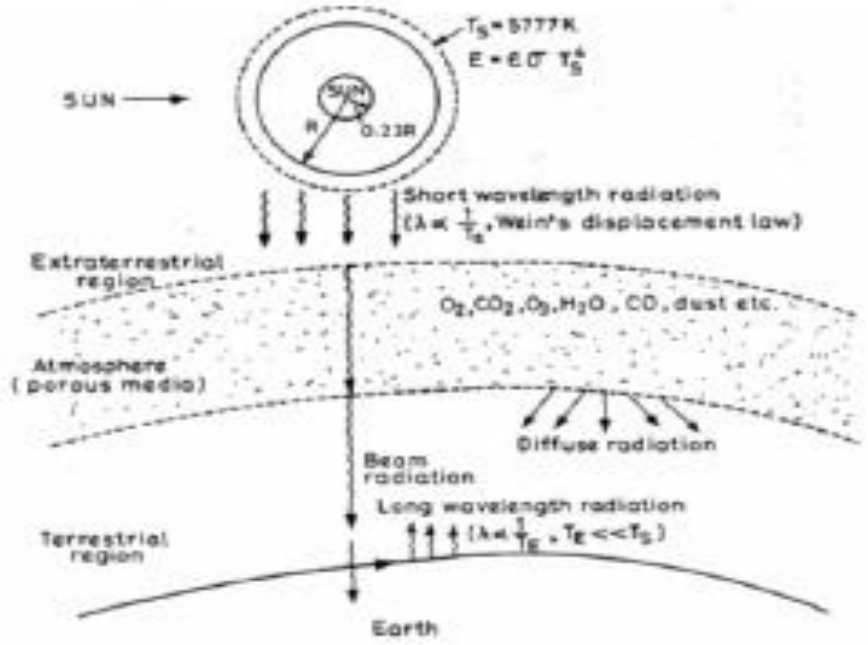

Figure 2.8: Positions of terrestrial and extraterrestrial regions (Source: Dr.Ing Abebayehu Assefa's lecture note).

2.2.2.1.1. Extraterrestrial Solar Radiation

Solar radiation outside the earth's atmosphere is called extraterrestrial radiation. The intensity of the extraterrestrial radiation outside a planet varies inversely to the square of the distance of the planet from the sun. If the intensity of the radiation at a point and the distance of the point from the sun are known, then the intensity at another point can be calculated. As per figure 2.9 below, the earth revolves around the sun every 365.25 days in an elliptical orbit – called the ecliptic plane, with a mean earth-sun distance of 1.495×10^{11} m defined as an astronomical unit (1 AU = 149.5 million km). The earth's orbit reaches a maximum distance from the sun, or Aphelion, of 1.52×10^{11} m on about the 3rd day of July. The minimum earth-sun distance, the Perihelion, occurs on about January 2nd, when the earth is 1.47×10^{11} m from the sun. The distance between the sun and the earth varies every day and is a minimum on January 2 and a maximum on July 3.

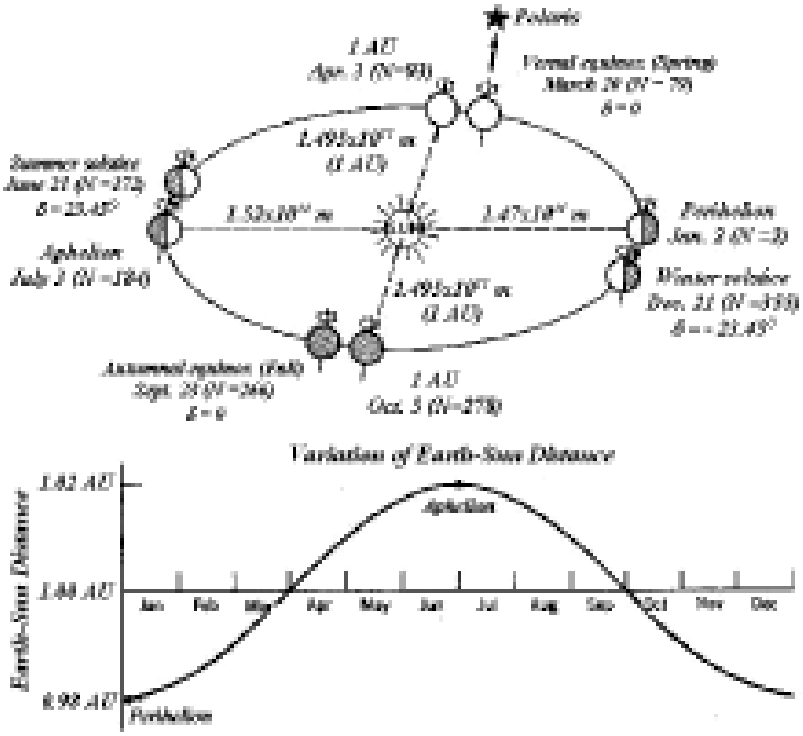

Figure 2.9: Variation of Earth-Sun distance (Source: Dr.Ing Abebayehu Assefa's lecture note).

Solar irradiance varies by ±3.4% with the maximum irradiance occurring at the Perihelion (where the earth is closest to the sun) and the minimum at the Aphelion (where the earth is farthest from the sun). The current accepted value of solar constant (I_{sc}) is 1367 W/m^2 and the top of the atmosphere is about 40 km from the earth's surface [9].

A study of the extraterrestrial radiation is important because of the following features:

I. It indicates the maximum possible radiation that could be expected on the earth's surface (on an extremely clear day).
II. The extraterrestrial radiation on top of the earth's atmosphere could be used as a reference in the absence of solar radiation data on the earth's surface. Expressions related to the extraterrestrial radiation can be applied to generate solar radiation data at any place on the earth's surface.
III. Knowledge of the spectral distribution and the radiation intensity identifies in what wavelength energy is greater.

The intensity of extraterrestrial radiation falling on a surface normal to the sun's rays at 1 AU (mean sun earth distance) is given by solar constant (I_{sc}). The intensity of extraterrestrial radiation I_{ext} measured on a plane normal to a surface on the N^{th} day of the year is given in terms of solar constant (I_{sc}) as follows (Duffie and Beckman, 1991):

$$I_{ext} = I_o = I_{SC}\left[1 + 0.033\,cos\left(\frac{360N}{365}\right)\right]\left[{}^{W}/_{m^2}\right] \quad \text{(2.11)}$$

An important concept, that is, often used in solar irradiance models is the extraterrestrial solar irradiance falling on a horizontal surface can be done by considering a flat surface just outside the earth's atmosphere and parallel to the earth's surface illustrated on figure 2.10 below.

The rate of solar energy falling on both surfaces A and B is the same. However, the area of surface A is greater than its projection (hypothetical surface B), making the rate of solar energy per unit area, that is the solar irradiance, falling on surface A less than on surface B. The extraterrestrial solar irradiance falling on a surface parallel to the ground is:

$$I_{o,h} = I_o\,cos\,\theta_z \quad \left[{}^{W}/_{m^2}\right] \quad \text{(2.12)}$$

Where: Io is the extraterrestrial solar irradiance, and

θ_z the angle between the two surfaces

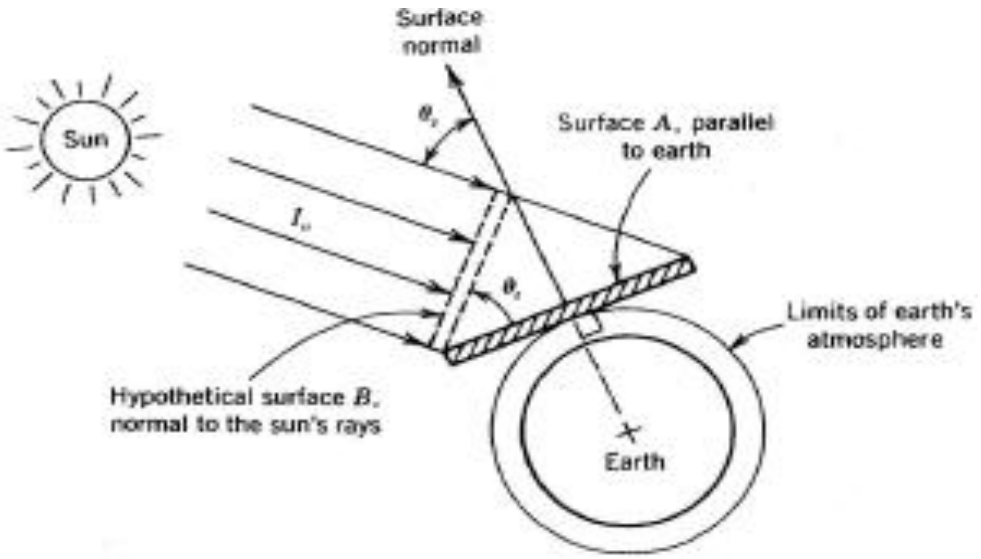

Figure 2.10: The cosine effect as related to the concept of extraterrestrial horizontal irradiance (Source: Dr.Ing Abebayehu Assefa's lecture note).

Reduction of radiation by the cosine of the angle between the solar radiation and a surface normal is called the cosine effect. The cosine effect is an extremely important concept in optimizing the orientation of solar collectors. Graphically, the variation of the extraterrestrial solar radiation with respect to the time of the year (N^{th} day) is illustrated on figures 2.11a and 2.11b below.

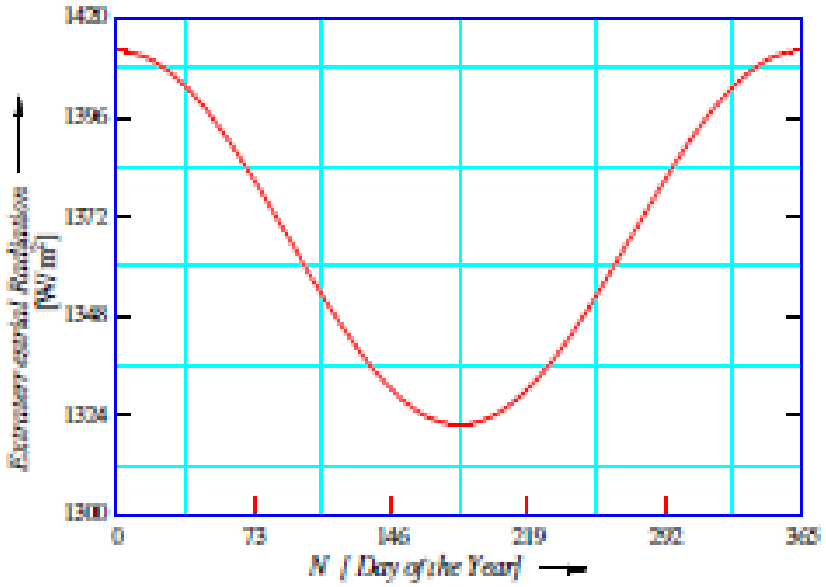

Figure 2.11a: Variation of extraterrestrial solar radiation with time of the year (Source: Dr.Ing Abebayehu Assefa's lecture note).

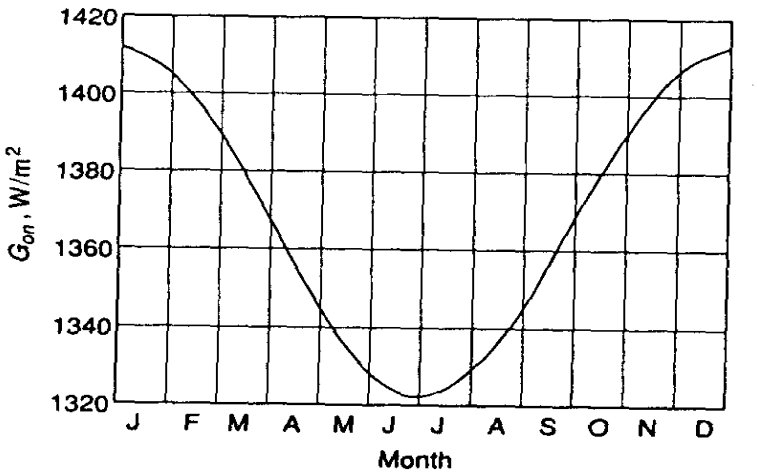

Figure 2.11b: Variation of extraterrestrial solar radiation with months of the year (Source: Duffie and Beckman, 1991).

Where: G_{an} is the extraterrestrial solar irradiance, and J=January, June, July, F=February, M= March, May, A= April, August, S=September, O=October, N=November, D=December

The daily extraterrestrial radiation on a horizontal surface, Ho, can be computed for the day of year N from the following equation:

$$H_o = \frac{24 \times 3600 I_{SC}}{\pi} \left\{1 + 0.033 cos\left(2\pi \frac{N}{365}\right)\right\} (cos\, \emptyset\, cos\, \delta\, sin\, \omega_s + \omega_s\, sin\, \emptyset\, sin\, \delta) \text{........ } (2.13)$$

Where: the variables and constants have the same meanings and values described above.

2.2.2.1.2. Terrestrial Solar Radiation on a Surface

Before reaching the surface of the earth, radiation from the sun is attenuated by the atmosphere and the clouds. The ratio of solar radiation at the surface of the earth to extraterrestrial radiation is called the clearness index.

Air mass is the ratio of the distance that solar radiation travels through the earth's atmosphere (path length), to the distance (path length) it would travel if the sun were directly overhead. Radiation coming from directly overhead, therefore, is said to pass through an air mass of 1.0 at sea level. Solar irradiance coming from a zenith angle of 60 degrees would pass through approximately twice the perpendicular path length and hence an air mass of 2.0. Large value of air mass indicates that solar radiation travel greater distance in atmosphere. An expression for air mass, referring figure 2.12 below is:

$$Air\ mass = \frac{\overline{AB}}{\overline{AC}} = sec\, \theta_z = \frac{1}{cos\, \theta_z} \text{.. } (2.14)$$

The following expression has been developed by Kasten and Young (1989) to approximate air mass at any zenith angle:

$$Air\ mass = \frac{1}{cos\, \theta_z + 0.50572 \times (96.07985 - \theta_z)^{-1.6364}} \text{... } (2.15)$$

At sunset ($\theta_z = 90^o$), equation (2.15) gives a value of 37.92 and that is why there is very little solar radiation reaching the earth's surface at sunset. For altitudes other than sea level, the air mass calculated above is reduced by the ratio of the local atmospheric pressure to standard sea-level atmospheric pressure.

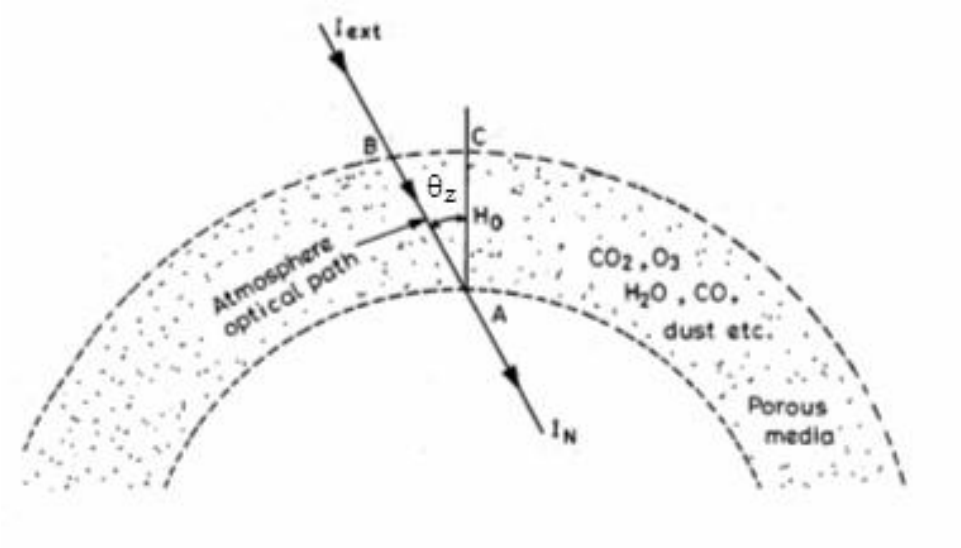

Figure 2.12: Direction of sun's ray with respect to atmosphere (Source: Dr.Ing Abebayehu Assefa's lecture note).

The following figure 2.13 shows how the sun's radiation is attenuated through Raley scattering and absorption in O_3, H_2O and CO_2:

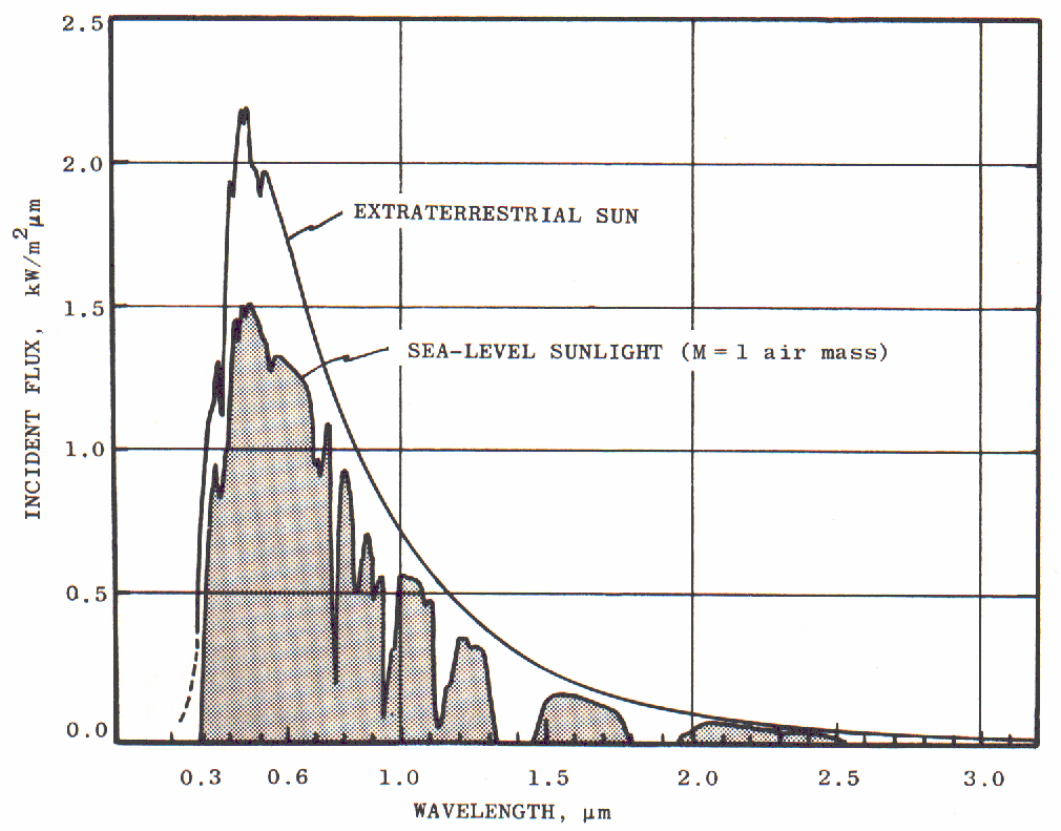

Figure 2.13: Sun's radiation is attenuated through Raley scattering and absorption in O_3, H_2O and CO_2 (Source: Duffie and Beckman, 1991).

Figure 2.13 above is for air mass, (AM), of 1. Attenuation is larger for AM 1.5 and AM 2. Since the Raleigh scattering is higher for lower wavelengths, the diffuse sky radiation has an intensity maximum at 0.4 μm, making the clear sky blue.

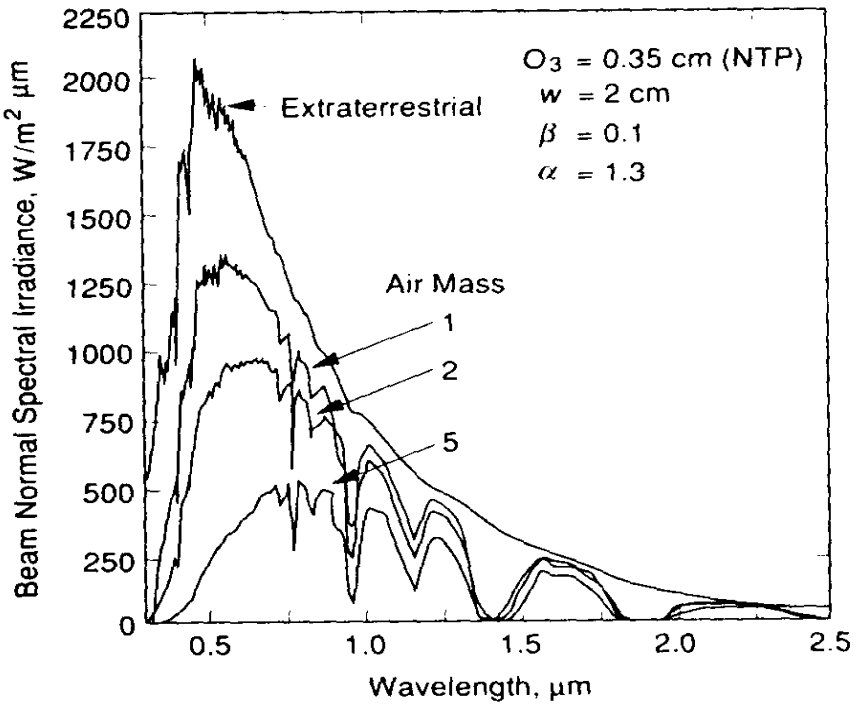

Figure 2.14: An example of the spectral distribution of beam irradiance for air masses of 0, 1, 2 and 5 (Source: Duffie and Beckman, 1991).

Extraterrestrial radiation: - is the radiation that would be received in the absence of the atmosphere. As shown in Fig. 2.15, the maximum spectral intensity occurs at about a wavelength λ = 0.48μm in the green portion of the visible spectrum. About 6.4 % of the total energy is contained in ultraviolet region (λ < 0.38μm); another 48 % is contained in the visible region (0.38μm < λ< O.78μm); and the remaining 45.6 % is contained in the infrared region (λ > O. 78μm).

The solar irradiance from the black body, either sun or earth, as a function of wavelength (μm) can be governed by Planck's law of radiation given by:

$$\epsilon_{\lambda b} = \frac{C_1}{\lambda^5\left[exp\left\{\frac{C_2}{\lambda T}\right\}-1\right]} \quad \text{..... (2.16)}$$

Where: $\epsilon_{\lambda b}$ is the spectral emissive power and represents the energy emitted per unit area per unit time per unit wave length (μm) interval at a given wave length;

C_1 = 3.742 x 10^8 w.μm^4/m^2 (3.7405 x 10^{-16} m^2w)

C_2 = 14387.9μm K (0.0143879 mK)

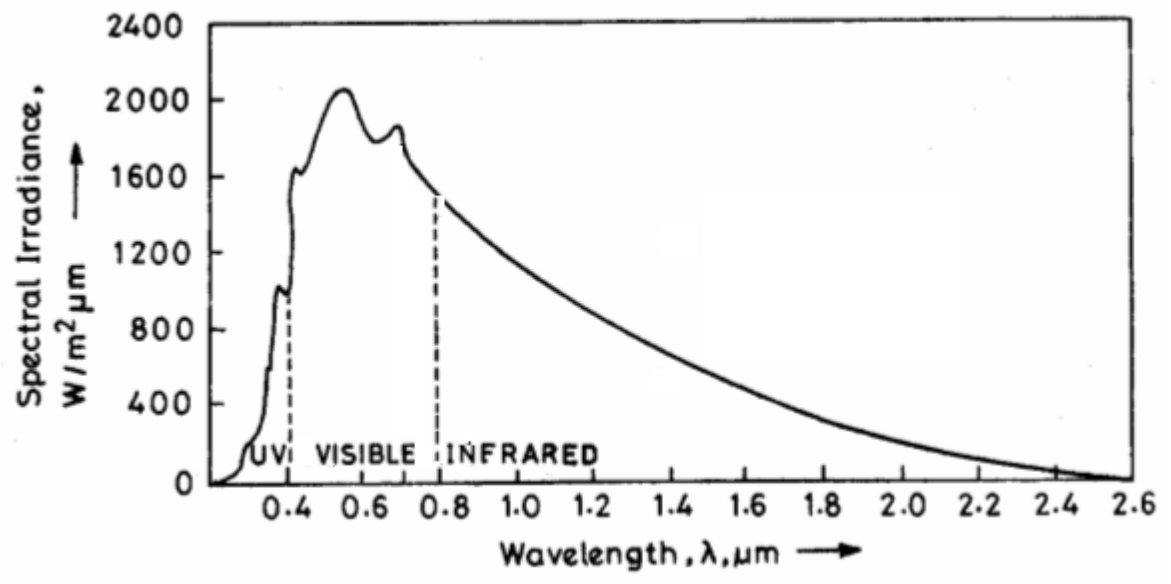

Figure 2.15: Spectral solar irradiance (Source: Duffie and Beckman, 1991).

2.2.3. Computation of Radiations (Insolations)

Total solar radiation I_T incident on a surface consists of:

I. Beam solar radiation, I_b
II. Diffuse solar radiation, I_d and
III. Solar radiation reflected from the ground and surroundings, I_r.

Normally, the beam radiation and diffuse radiation on a horizontal surface are recorded. The following formula has been developed by Liu and Jordan (1962) for evaluating the total radiation on a surface of arbitrary orientation from knowledge of beam and diffuse radiation on horizontal surface.

$$I_T = I_b R_b + I_d R_d + \rho R_r (I_b + I_d) \ldots\ldots\ldots\ldots\ldots\ldots\ldots\ldots\ldots\ldots\ldots\ldots\ldots\ldots\ldots\ldots \quad (2.17)$$

Where: $R_{b,}R_{d,}R_r\ are$ kwon as conversion factors for beam, diffuse and reflected components, respectively

The expressions for $R_{b,}R_{d,}R_r$ are as follows:

R_b:- is defined as the ratio of flux of beam radiation incident on an inclined surface to that on a horizontal surface. The flux of beam radiation incident on a horizontal surface (I_b) is given by:

$$I_b = I_N \cos\theta_z \quad \text{..... (2.18)}$$

And that on an incline surface (I_b') is given by:

$$I_b' = I_N \cos\theta_i \quad \text{..... (2.19)}$$

Where: $\theta_z and\ \theta_i\ are$ the angles of incidence on the horizontal and inclined surfaces, respectively and I_N is the intensity of beam radiation.

R_b for beam radiation can be obtained from:

$$R_b = \frac{I_b'}{I_b} = \frac{\cos\theta_i}{\cos\theta_z} \quad \text{..... (2.20)}$$

Depending on the orientation of the inclined surface, the expression for $\cos\theta_i$ and $\cos\theta_z$ can be obtained from Equations (2.2) and (2.6), respectively. The variation of R_b with respect to the N^{th} day (1-180 days) of the year for:

I. Different latitudes (ϕ = 15°, 30°, 45°, 60°);
II. Different inclination angles (β = 15°, 30°, 45°, 60°);
III. Different hour angles (ω = 0°, 30°, 45°, 60°) are shown in figures 2.16a, 2.16b and 2.16c below.

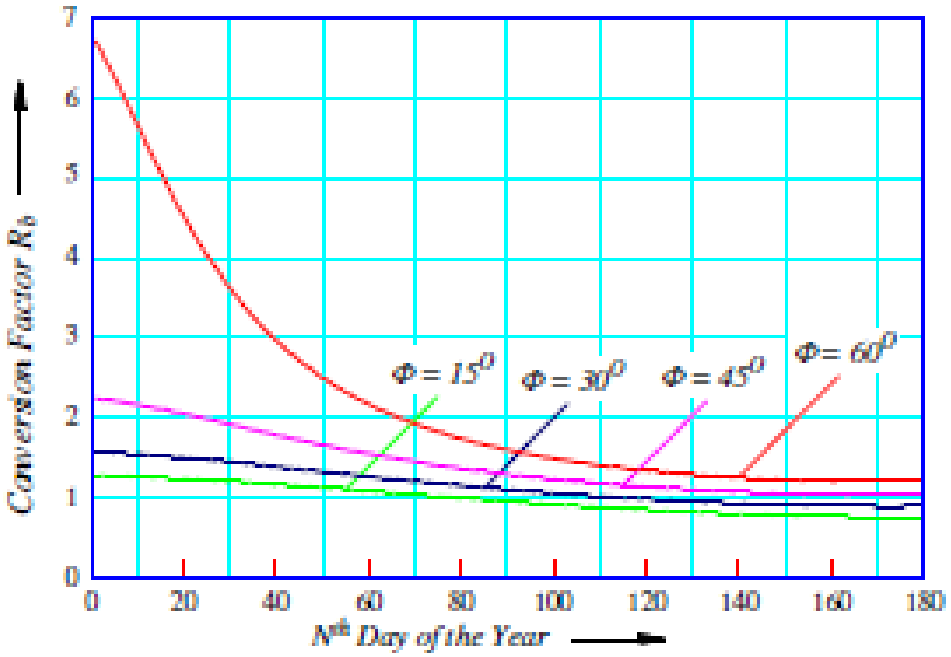

Figure 2.16a: Variation of R_b with the N^{th} day of the year for different latitudes (Source: Dr.Ing Abebayehu Assefa's lecture note).

Figure 2.16(a) above shows that the conversion factor for radiation has significant effect at higher latitude and low value of N.

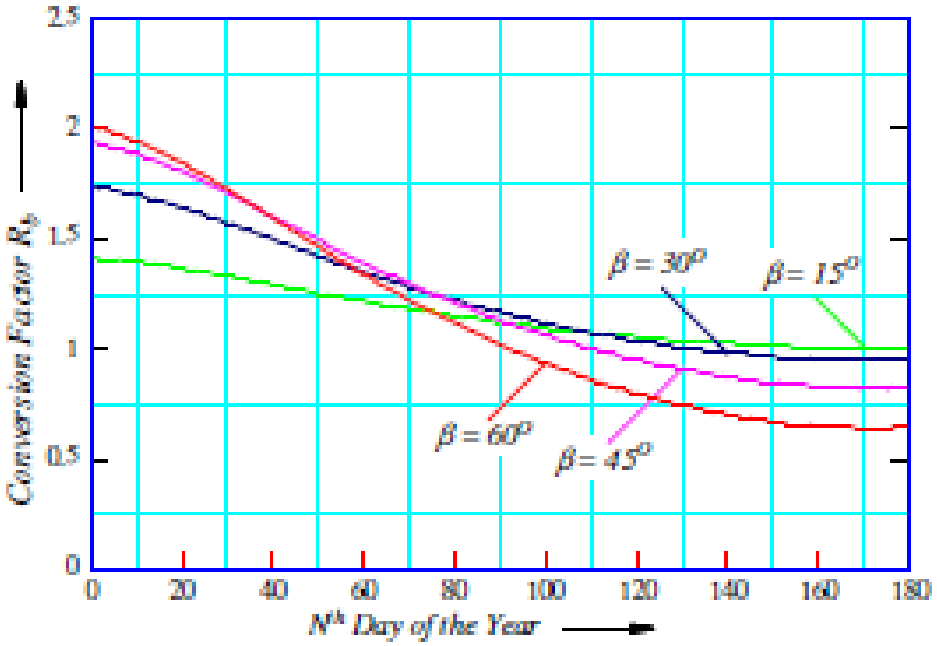

Figure 2.16b: Variation of R_b with the N^{th} day of the year for different inclination angles (Source: Dr.Ing Abebayehu Assefa's lecture note).

Figure 2.16(b) above shows that R_b depends significantly at higher inclination of the plane β and becomes less significant at lower value of β and similarly, the maximum value of R_b is observed at higher β and at low value of N.

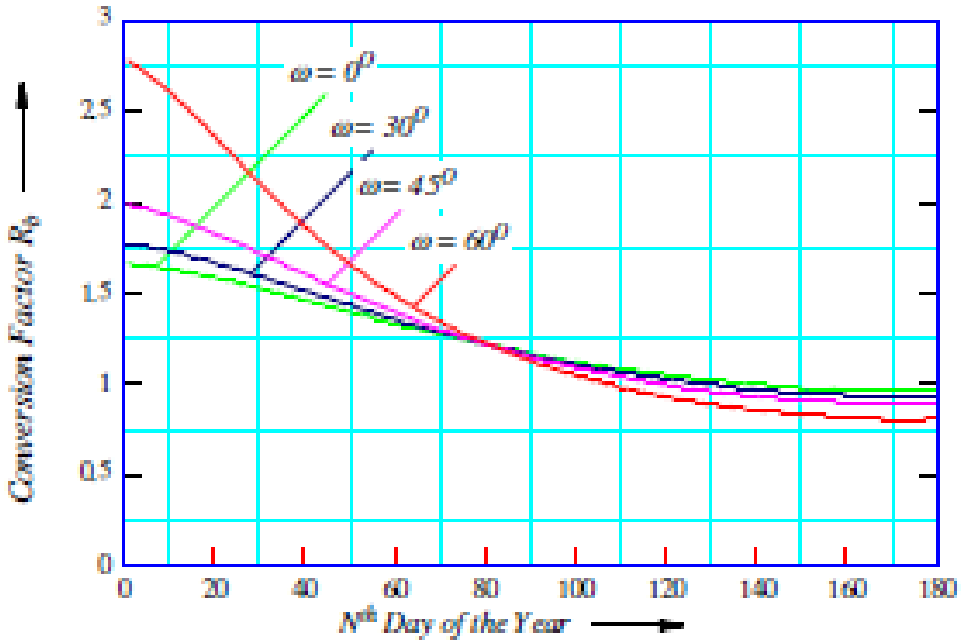

Figure 2.16c: Variation of R_b with the N^{th} day of the year for different hour angles (Source: Dr.Ing Abebayehu Assefa's lecture note).

Figure 2.16(c) above shows that R_b tends to a minimum value at higher N for various values of ω.

R_d: - is defined as the ratio of the flux of diffuse radiation falling on the tilted surface to that on the horizontal surface. This conversion factor depends on the distribution of diffuse radiation over the sky and on the portion of sky seen by the surface.

Even though a satisfactory method of estimating the distribution of diffuse radiation over the sky is yet to be found, the sky is assumed to be an isotropic source of diffuse radiation. If $(1 + cos\ \beta)/2$ is the radiation shape factor for a tilted surface with respect to the sky, then:

$$R_d = \frac{1+cos\,\beta}{2} \quad \text{..... (2.21)}$$

Rr: - is the reflected component that comes mainly from the ground and other surrounding objects. It is given by:

$$R_r = \frac{1-\cos\beta}{2} \quad \text{..... (2.22)}$$

The variation of R_d and R_r with respect to the inclination angles β = 0° – 90° is shown on figure 2.17 below. Both the beam and diffuse components of radiation undergo reflection from the ground and the surroundings. For β = 90°, $R_d = R_r = 0.5$ from Equations (2.21) and (2.22) and Fig. 2.17 below. This indicates that half of diffuse and half of reflected total radiation is received by vertical plane. For horizontal plane, $R_d = 1$ and $R_r = 0$.

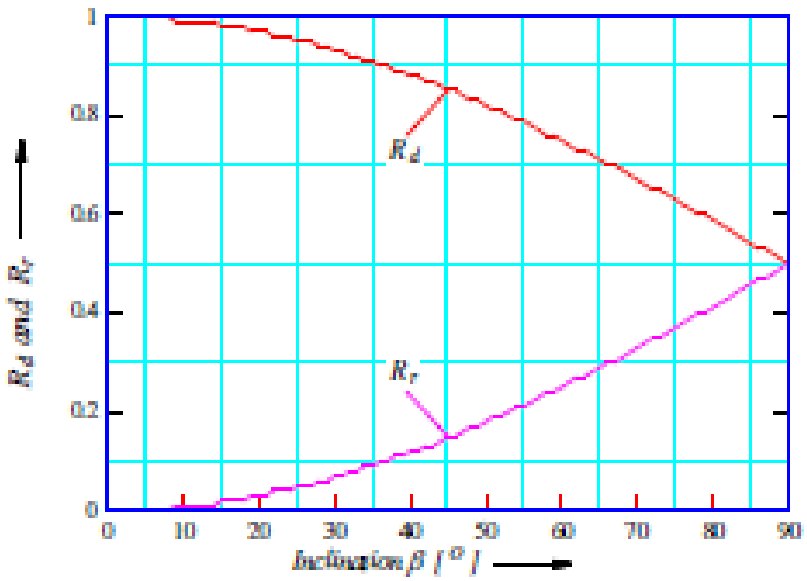

Figure 2.17: Variation of R_d and R_r with inclination angles β (Source: Dr.Ing Abebayehu Assefa's lecture note).

From Equation (2.21) and Fig. 2.17, it can be observed that all of the diffuse radiation is received by horizontal plane. In this case, β = 0° and R_r = 0°. This indicates that horizontal planes receive no reflected radiation. The effective ratio of solar energy incident on a surface to that on a horizontal surface R' is:

$$R' = \frac{I_T}{I_b+I_d} = \frac{I_bR_b+I_dR_d}{I_b+I_d} + \rho R_r \quad \text{..... (2.23)}$$

2.2.3.1. Solar Radiation on Horizontal Surface

The calculation of the extraterrestrial radiation falling on a horizontal surface at different times, hourly, daily and any time are described based on hourly, daily and any time as follows.

2.2.3.1.1. Hourly Extraterrestrial Radiation I_o

This can be calculated by any one of the following two methods:

I. By integrating the instantaneous radiation over the hour angle of interest by considering the midpoint of the hour in the following expression as:

$$I_o = I_{SC}\left[1 + 0.033\,cos\left(\frac{360N}{365}\right)\right]\cos\theta_z \left[{KJ}/{m^2.h}\right] \quad \text{..... (2.24)}$$

Where: $\cos\theta_z = \cos\emptyset\cos\delta\cos\omega + \sin\delta\sin\emptyset$

I_{sc} = solar constant in energy units [4921 kJ/m^{2}h]

ω = hour angle at the midpoint of the hour in question

N = day number of the year

I_o = extraterrestrial radiation on a horizontal surface [kJ/m^{2}h]

II. By considering the hour angles ω_1 and ω_2:

$$I_o = \left[\frac{12\times3600}{\pi}I_{SC}\right]\left[1 + 0.033\,cos\left(\frac{360N}{365}\right)\right]\times\left[\cos\emptyset\cos\delta\,(\sin\omega_2 - \sin\omega_1) + \pi 180\omega 2 - \omega 1 \sin\delta\sin\emptyset J/m2.h\right] \quad \text{..... (2.25)}$$

Where: ω_1 = hour angle at the midpoint of the hour in question

ω_2 = hour angle at the midpoint of the hour in question

I_{sc} = solar constant in power units [1367 W/m^2]

I_o = extraterrestrial radiation on a horizontal surface [J/m^{2}h]

2.2.3.1.2. Daily Extraterrestrial Radiation H_o

This is obtained by integrating the radiation falling over the day length by noting the sunrise and sunset hour angles. The expression is:

$$H_o = \left[\frac{24\times3600}{\pi} I_{SC}\right]\left[1 + 0.033\, cos\left(\frac{360N}{365}\right)\right] \times \left[\cos\emptyset \cos\delta \sin\omega_s + \frac{\pi}{180}\omega_s \sin\delta \sin\emptyset\right]\left[J/_{m^2}\right] \quad \text{(2.26)}$$

Where: ω_s = sun rise hour angle

H_o = extraterrestrial radiation on a horizontal surface [J/m^{2}day]

2.2.3.1.3. Any Time Extraterrestrial Radiation Ho

At both the equator and in the Polar Regions, the expression is:

I. At the equator, the latitude is 0° and therefore $\omega_s = \pi/2$ and therefore,

$$H_o = \left[\frac{24\times3600}{\pi} I_{SC}\right]\left[1 + 0.033\, cos\left(\frac{360N}{365}\right)\right] \times [\cos\delta]\left[J/_{m^2}\right] \quad \text{(2.27)}$$

II. In the Polar Regions, during the summer, there is no sunrise or sunset. Therefore, replacing ω with ω_s:

$$H_o = \left[\frac{24}{\pi} I_{SC}\right]\left[1 + 0.033\, cos\left(\frac{360N}{365}\right)\right] \times \left[\frac{\pi^2}{180} \sin\delta \sin\emptyset\right]\left[J/_{m^2}\right] \quad \text{(2.28)}$$

2.2.3.1.4. Estimation of Clear Sky Radiation

The intensity of beam radiation varies with weather, air quality, and altitude over sea level, and the sun's zenith angle θz. It is therefore impossible to tell the intensity without measuring it. According to Dr.Ing Abebayehu Assefa's lecture note, there exists however a formula that gives an approximate estimate at moderate elevations, clear weather and dry air by combining the Liu and Jordan's model for the transmittance of diffuse radiation as follows.

The clear sky beam radiation on a horizontal surface is:

$$I_b = I_n \tau_b \cos\theta_z \quad \text{(2.29)}$$

Where: τ_b = transmittance of beam radiation

$$I_n = I_{SC}\left[1 + 0.033 \cos\left(\frac{360N}{365}\right)\right]$$

$$\tau_b = a_o + a_1 e^{\left[-k/\cos\theta_z\right]} \quad \text{..... (2.30)}$$

$a_0 = a_0^* r_0$; $a_1 = a_1^* r_1$; and $k = k^* r_k$

Where: $a_0^* = 0.4237 - 0.00821(6 - A)^2$; $a_1^* = 0.5055 + 0.00595(6.5 - A)^2$; $k^* = 0.2711 + 0.01858(2.5 - A)^2$; $r_0 = 0.95$; $r_1 = 0.91$ *and* $r_k = 1.02$

2.2.3.1.5. Clearness Index

This important radiation parameter $\mathbf{k_T}/\mathbf{K_T}$ is defined under two time scales - hourly or daily. It is principally a measure of the radiation that is transmitted through the atmosphere and is therefore dependent only on the extraterrestrial radiation and the radiation falling at the earth's surface.

2.2.3.1.5.1. Hourly (k_T) Clearness Index

The hourly clearness index $\mathbf{k_T}$ during a particular hour is the ratio of the hourly global radiation on horizontal surface to the hourly extraterrestrial radiation on horizontal surface (during the same time period).

$$\boldsymbol{k_T} = \frac{I}{I_o} \quad \text{..... (2.31)}$$

And the monthly average hourly clearness index is given by:

$$\overline{k_T} = \frac{\bar{I}}{\bar{I_o}} \quad \text{..... (2.32)}$$

2.2.3.1.5.2. Daily (K_T) Clearness Index

The daily clearness index $\mathbf{K_T}$ gives the ratio of the daily global radiation on a horizontal surface to the daily extraterrestrial radiation on a horizontal surface. Therefore,

$$\boldsymbol{K_T} = \frac{H}{H_o} \quad \text{..... (2.33)}$$

And the monthly average daily clearness index is given by:

$$\overline{K_T} = \frac{\bar{H}}{\overline{H_o}} \quad \text{..... (2.34)}$$

2.2.4. Prediction of Solar Radiations (Insolations)

2.2.4.1. Prediction of Monthly Average Daily Horizontal Global Radiation from Sunshine Duration

The monthly mean daily global radiation on a horizontal surface may be estimated from sunshine records by the modified Angstrom correlation, as suggested by Page and others as:

$$\frac{\bar{H}}{\bar{H}_o} = a + b\frac{\bar{n}_s}{\bar{N}_s} \quad \text{(2.35)}$$

Where: $\bar{H}$ = Monthly average daily radiation on horizontal surface

$\bar{H}_o$ = Monthly average extraterrestrial radiation for the same location and time,

a, b = Empirical constants, (values are obtained by regression),

$\bar{n}_s$ = Monthly average daily hours of bright sunshine, and

$\bar{N}_s$ = Monthly average of the maximum possible daily hours of bright sunshine.

The regression parameters a and b can be obtained from:

$$a = -0.110 + 0.235\cos\emptyset + 0.323\left(\frac{\bar{n}_s}{\bar{N}_s}\right) \quad \text{(2.36)}$$

$$b = 1.449 - 0.553\cos\emptyset - 0.694\left(\frac{\bar{n}_s}{\bar{N}_s}\right) \quad \text{(2.37)}$$

2.2.4.2. Prediction of Beam and Diffuse Components of Hourly Radiation

I_d / I, the fraction of the hourly diffuse radiation on a horizontal plane, can be correlated to the hourly clearness index, $\mathbf{k}_T$, and the ratio of the total radiation to the extraterrestrial radiation for the hour. The equations for the correlation (according to Dr.Ing Abebayehu Assefa's lecture note) are:

$$\frac{I_d}{I} = \begin{cases} 1.0 - 0.249k_T & for\ k_T < 0.35 \\ 1.557 - 1.84k_T & for\ 0.35 < k_T < 0.75 \\ 0.177 & for\ \ k_T > 0.75 \end{cases} \quad \text{(2.38)}$$

2.2.4.3. Prediction of Beam and Diffuse Components of Daily Radiation

Studies of available daily radiation indicate that the average fraction which is diffuse is a function of KT. The equations for the correlation (according to Dr.Ing Abebayehu Assefa's lecture note) are:

$$\frac{H_d}{H} = \begin{cases} 0.99 & for\ K_T \leq 0.17 \\ 1.188 - 2.272K_T + 9.473\boldsymbol{K}_T^2 & for\ 0.17 < K_T < 0.75 \\ -21.865K_T^3 + 14648K_T^4 & for\ 0.17 < K_T < 0.75 \\ -0.54 + 0.632K_T & for\ 0.75 < K_T < 0.80 \\ 0.2 & for\ K_T \geq 0.80 \end{cases} \quad \text{..... (2.39)}$$

2.2.4.4. Prediction of Monthly Average Daily Horizontal Global Radiation from Sunshine Duration

The monthly average hourly global radiation on a horizontal surface can be calculated from the knowledge of the monthly average daily global radiation on a horizontal surface by using the expression proposed by Collares-Pereira and Rabl, 1979, Fig. 2.18 (according to Dr.Ing Abebayehu Assefa's lecture note) is:

$$\frac{\bar{I}}{\bar{H}} = \frac{\pi}{24}(a + b\cos\omega)\frac{\cos\omega - \cos\omega_s}{\sin\omega_s - \frac{\pi}{180}\omega_s\cos\omega_s} \text{..... (2.40)}$$

Where: $a = 0.409 + 0.5016\sin(\omega_s - 60)$; $b = 0.6609 - 0.4767\sin(\omega_s - 60)$

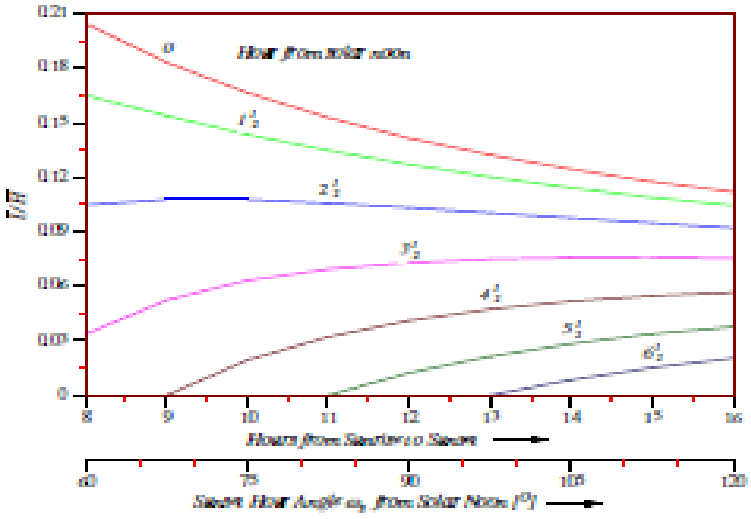

Figure 2.18: Relationship between hourly and daily total radiation on horizontal surface (Source: Dr.Ing Abebayehu Assefa's lecture note).

2.2.4.5. Prediction of Monthly Average Hourly Horizontal Diffuse Radiation from Monthly Average Daily Horizontal Diffuse Radiation

This is obtained by using the following expression of Liu and Jordan, 1960, Fig. 2.19 (according to Dr.Ing Abebayehu Assefa's lecture note) is:

$$\frac{\bar{I}_d}{\bar{H}_d} = \frac{\pi}{24}\frac{\cos\omega - \cos\omega_s}{\sin\omega_s - \frac{\pi}{180}\omega_s\cos\omega_s} \quad \text{..... (2.41)}$$

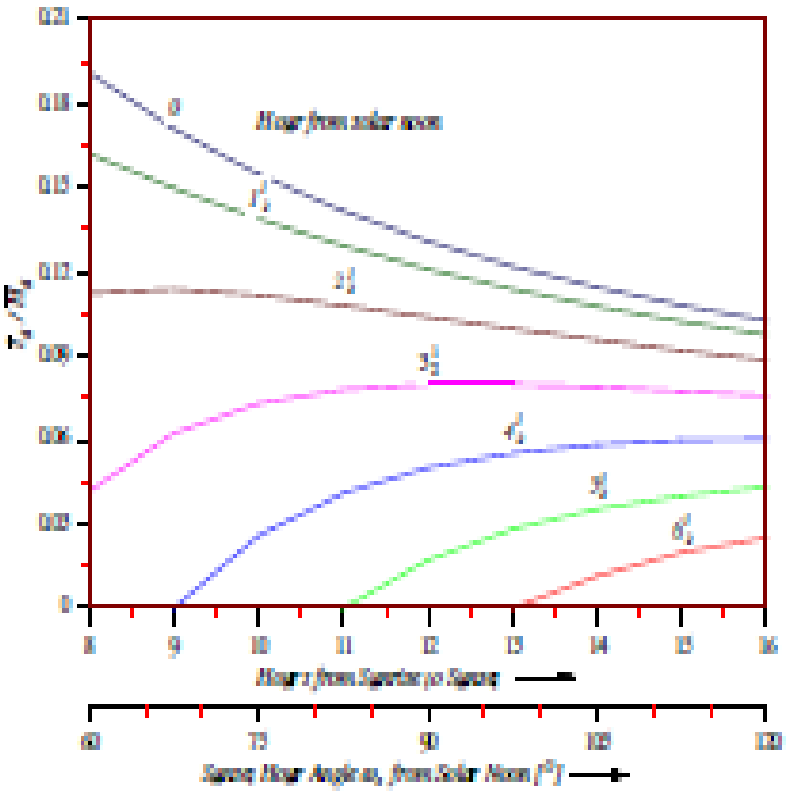

Figure 2.19: Relationship between hourly and daily diffuse radiations on horizontal surface (Source: Dr.Ing Abebayehu Assefa's lecture note).

2.2.4.6. Prediction of the Monthly Average of Daily Diffuse Radiation on a Horizontal Surface

Mainly two types of correlations have been developed. One type refers to the correlation between the ratio of monthly average of daily diffuse radiation to the monthly average of daily global radiation and K_T, the ratio of monthly average of daily global radiation to the

monthly average of daily extraterrestrial radiation, and the other type refers to correlation between the ratio of monthly average of daily diffuse radiation to the monthly average of daily global radiation and the number of bright sunshine hours.

$$\frac{\bar{H}_d}{\bar{H}} = 1.403 - 1.672\bar{K}_T \quad \textit{(2.42)}$$

And

$$\frac{\bar{H}_d}{\bar{H}} = 0.931 - 0.814\left(\frac{\bar{n}_s}{\bar{N}_s}\right) \quad \textit{(2.43)}$$

2.3. Solar Thermal Systems

2.3.1. Flat Plate Collector

The flat-plate collector is the heart of any solar energy collection system. The collector absorbs solar energy, converts it into heat and then transfers this heat to a stream of liquid or gas. It absorbs both the beam and the diffuse radiation. A flat-plate collector, as demonstrated in figure 2.20 below, usually consists of the following components:

I. Glazing - one or more sheets of glass or some other radiation transmitting material. The role of glazing is to admit the maximum possible radiation and to minimize the upward heat losses;
II. Tubes, fins or passages for conducting or directing the heat transfer fluid from the inlet to the outlet;
III. Absorber plate - flat, corrugated or grooved plate with tubes, fins or passages attached to it;
IV. Header or manifolds to admit and discharge the fluid;
V. Insulation – to minimize heat loss from the back and sides of the collector; and
VI. Container or casing which surrounds the various components and protects them from dust, moisture, etc.

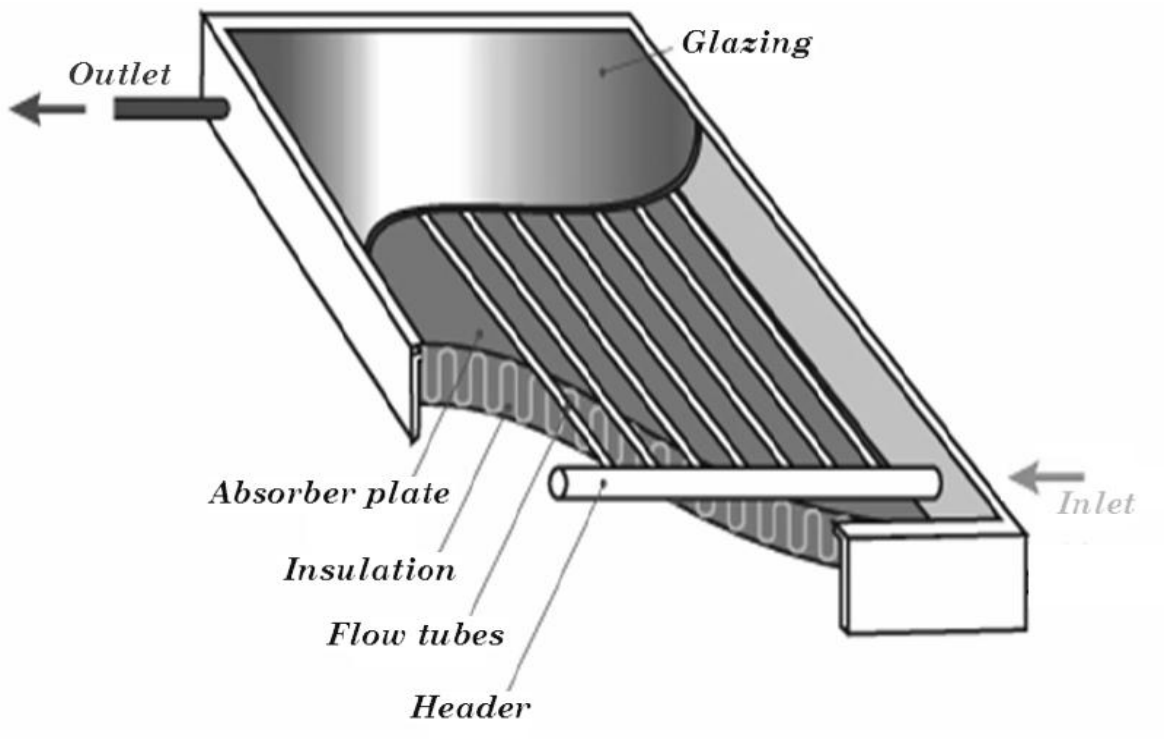

Figure 2.20: A typical liquid flate plate collector (Source: Dr.Ing Abebayehu Assefa's lecture note).

Various types of flat plate water heaters are available and the analysis of heat transfer/losses should be considered at different components of the systems that makes the complete equipment.

2.3.1.1. Heat Transfer Coefficients in Flat Plate Collector

Heat is lost to the surroundings from the plate through:

I. The glass cover (referred as top loss), and;

II. The insulation (referred as bottom loss).

These losses take place by conduction, convection and radiation which are shown in figure 2.21 below. The equivalent losses should be represented by a thermal resistance circuit.

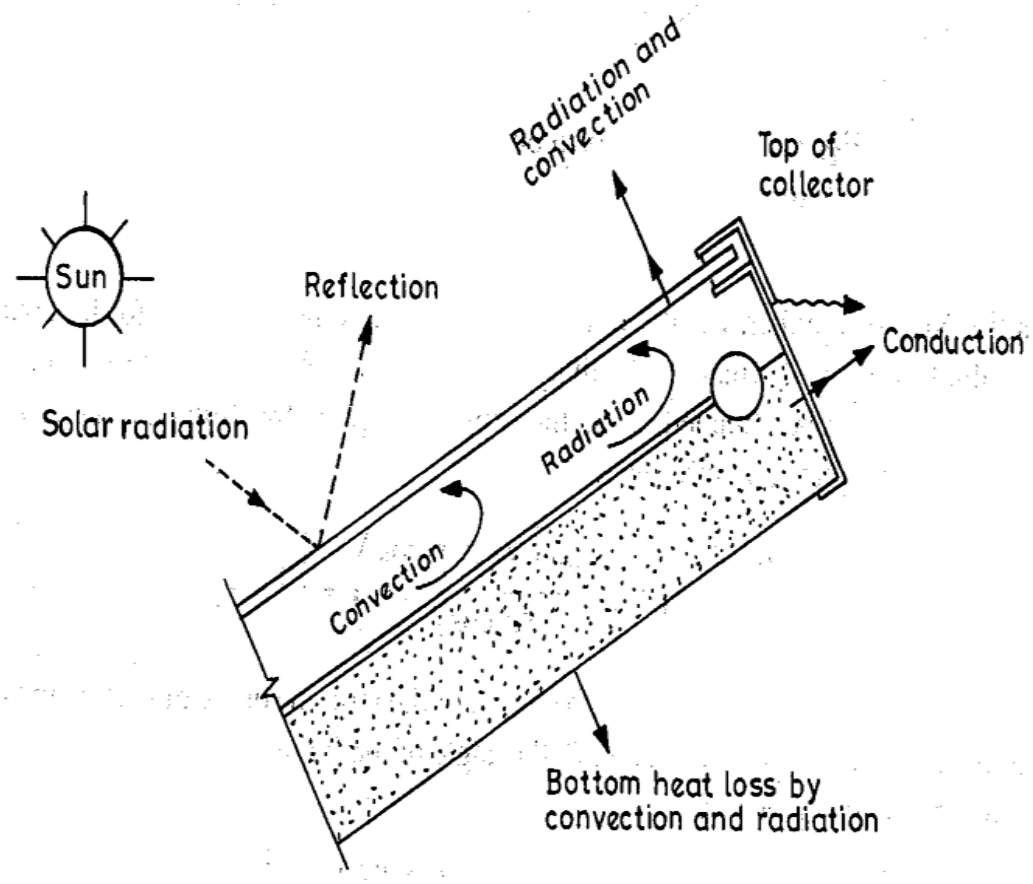

Figure 2.21: Various Heat losses from absorber to ambient (Source: Dr.Ing Abebayehu Assefa's lecture note).

There are different types of heat transfer coefficients that should be considered in thermal analysis of a flat-plate collector. Among these:

I. Top loss Coefficients(includes convective heat transfer coefficient from plate to cover, from glazing cover to ambient and radiative heat transfer coefficient from plate to cover, and from glazing cover to ambient);
II. Back loss coefficients (Heat is lost from the plate to ambient by conduction through the insulation and subsequently by convection and radiation from the bottom surface casing);
III. Edge loss coefficients (Energy lost from the side of the collector casing may be taken to have exactly the same value as that from the back, if the thickness of the edge insulation is the same as that of the back insulation [9]); and
IV. Overall Heat Loss Coefficient (The overall heat loss coefficient is the sum of the top, bottom and edge loss coefficient).

2.4. Solar Water Heating Systems

Hot water and steam form an integral part of various industrial and commercial applications and with rising oil prices, there has never been a better time to look at heating water by harnessing energy from the Sun [4].

The growing demand for energy throughout the world has caused great importance to be attached to the exploration of new sources of energy; among the unconventional sources that have been studied, solar energy now holds out much promise. Furthermore, the great depletion of oil brought attention to the fact that the dependence of any nation on oil and gas was fraught with uncertainty in the short term and must end in the long term. This means that the conventional energy resources of oil, gas, coal and uranium are finite, and will therefore be exhausted at some time in the future.

If these consumable resources are to be exhausted in the future, where shall we find our energy? The answer must lie in renewable energy sources such as geothermal energy and solar energy, including its various forms: wind, wave, offshore thermal energy conversion, bio-mass conversion, as well as the more direct forms of thermal and photo voltaic conversion.

Strictly speaking, all forms of energy are derived from the sun. However, our most common forms of energy-fossil fuels-received their solar input eons ago and have changed their characteristics so that they are now in a highly concentrated form .Since it is apparent that these stored, concentrated energy forms are now begin to supply a large portion of our energy need not from stored, but from incoming solar energy as soon as possible.

Therefore, the use of solar energy to heat water for various industrial and commercial applications has been technically feasible since solar water heaters were commonly used and hence it is a well-proven technology undergoing a vigorous rebirth today by using different materials which concentrate the energy coming from the sun and makes it more feasible.

Solar water heaters are usually of three types:

I. Box or batch type in which the collector and the storage is combined in one unit
II. Domestic unit in which the tank is placed above the absorber for maintaining the pressure head necessary for natural circulation water.

III. Large size solar water heaters where the storing tank can be placed at any convenient location and circulation is accomplished with the help of pump. Here, it is commonly used in cases where piping runs would be too long or there is no adequate position for an elevated tank. The penalty paid is the cost of the pump and its controls and the electricity needed to run them, which is not the case for other types. But a collector has a higher efficiency with an assured steady flow of water (note that the pump must be controlled so that circulation occurs only when the fluid in the collector is hotter than that in the tank). This is done by:

A. Differential thermostat (has two sensors one near the collector outlet and the other near the tank out let)
B. Thermostat set to activate the pump when the collector reaches a preset temperature
C. Switch the pump on and off manually.

The main components of a typical solar water heating system are:

I. Solar Collectors, which functions as the primary heating source;
II. Insulated hot water tank: for storing hot water;
III. Insulated piping, regulate the temperature flow of water between components; and
IV. Air vent: to release trapped air from hot water tank.

Figure 2.22: Components of a typical solar water heater (Source: Web: www.tatabpsolar.com)

Based on experience over a decade in stalling large capacity systems, requiring different features that enable to customize and design solar water heating systems to suit specific site/industry requirements are carried out.

The technology to heat water using solar energy is based on two simple principles:

I. Thermo-siphon action, which is based on a simple principle that hot water is less dense and hence tends to rise above colder water.
II. Black body absorption, which is a well known fact that a black body absorbs heat which can be used to heat water.
III. The Sun's rays heats the black powder coated copper fins (larger surface area) which in turn heats the cold water in the copper tubes. The heated water slowly rises in the copper pipes thro thermo-siphon action and eventually gets stored in the hot water storage tank.
IV. This principle ensures that no electricity is used in the entire system.

According to Thammasat (2008), solar collector oriented due south in the northern hemisphere and tilted at an angle of $\pm 5^{o}$ more or less than the local geographic latitude is best recommended to heat the water to the maximum temperature for the site.

Generally, a flat plate collector can be used for heating water. Water circulating through the tubes of a flat plate collector receives heat from the solar energy absorbed and the heated water is stored in an insulated storage tank. The mode of circulation of heated water from the collector to an insulated storage tank can be either by natural circulation (thermosiphon) or forced circulation (using pump). A solar water heating system shown in figure 2.23 below has the following main components:

I. A flat plate collector;
II. A heat exchanger, and
III. An insulated storage tank.

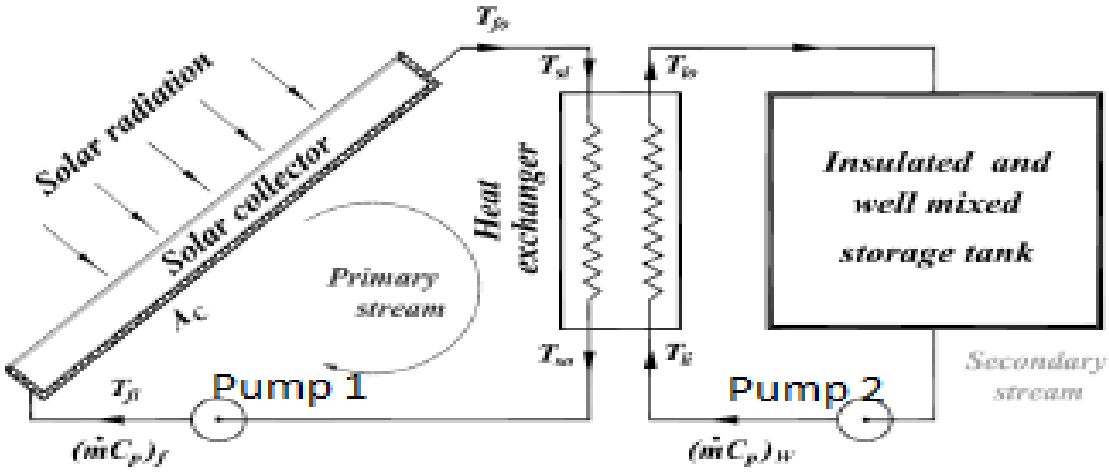

Figure 2.23: Schematic view of solar water heating system (Source: Dr.Ing Abebayehu Assefa's lecture note).

In figure 2.23 above, pump 1 is used in the collector loop (primary stream) to circulate the fluid through the collector and another pump 2 is used to circulate the water in the outer loop (secondary stream) between the storage tank and a heat exchanger.

2.4.1. Transient Analysis of Solar Water Heater

A cross-section of the flat-plate collector and the thermal resistance and capacitance of the simplified collector model are given in figure 2.24 and figure 2.25.The transient thermal performance of the solar collector is evaluated by applying energy balance on its components. The solar radiation energy incident on the collector surface which is inclined at an angle β to the horizontal, defined in terms of the global radiation $\mathbf{I}_t$, the diffuse radiation $\mathbf{I}_d$, the beam radiation factor $\mathbf{R}_b$, the diffuse radiation factor $\mathbf{R}_d$, the ground reflectivity factor $\mathbf{R}_r$ and the ground reflectivity ρ is given by equations 2.20, 2.21 and 2.22 above.

$$I_N = I_b R_b + I_d R_d + \rho R_r (I_b + I_d) \ldots\ldots\ldots\ldots\ldots\ldots\ldots\ldots\ldots\ldots\ldots\ldots\ldots\ldots \quad (2.44)$$

Where: $R_{b,} R_{d,} R_r \; are$ known as conversion factors for beam, diffuse and reflected components, respectively

The flux collected per unit time is given by:

$$I_C = I_N (\tau_g \alpha_p) \ldots\ldots\ldots\ldots\ldots\ldots\ldots\ldots\ldots\ldots\ldots\ldots\ldots\ldots\ldots\ldots\ldots\ldots\ldots\ldots\ldots\ldots \quad (2.45)$$

Where: $R_{b,}R_{d,}R_r\ are$ known as conversion factors for beam, diffuse and reflected components, respectively

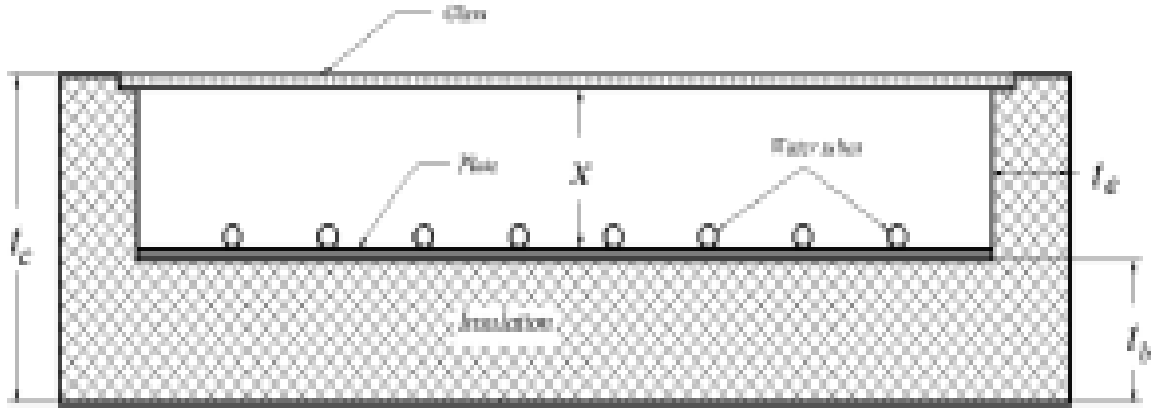

Figure 2.24: Cross-Section of the Flat-plate Collector (Source: Dr.Ing Abebayehu Assefa's lecture note).

2.4.1.1. Transient Analysis of the Absorber Plate

The plate temperature T_p at any time $(t + \Delta t)$ can be determined from conditions at time t and the energy absorbed by the plate and energy losses.

$$\left(mc_p\right)_p \frac{dT_p}{dt} = A_c I_c - A_c U_{pg}\left(T_p - T_g\right) - A_w U_{pw}\left\{T_p - \frac{T_{wo}+T_{wi}}{2}\right\} - A_c U_{pab}\left(T_p - T_A\right) - A_1 U_{pae}\left(T_p - T_a\right) \quad \text{..... (2.46)}$$

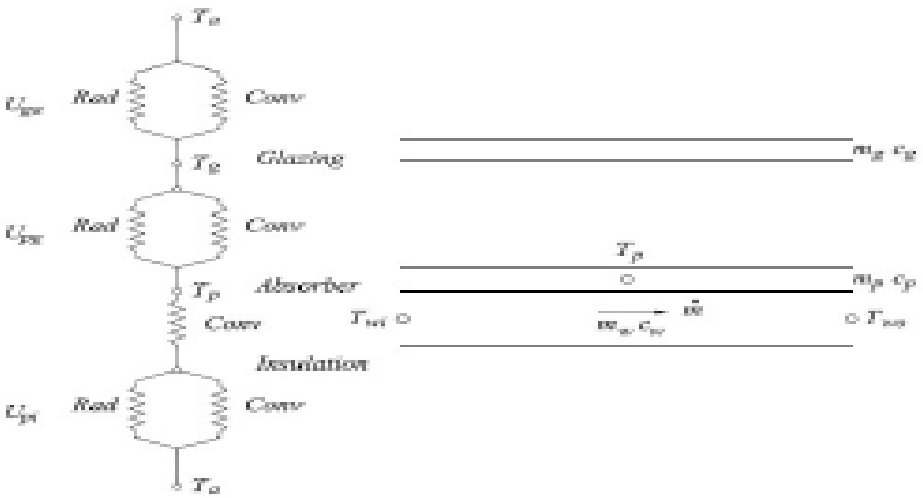

Figure 2.25: Thermal Resistance and Capacitance of the Collector (Source: Dr.Ing Abebayehu Assefa's lecture note).

The plate temperature Tp_1 at any time $(t+\Delta\tau)$ is estimated from energy absorbed during the time interval $\Delta\tau$ and the energy losses at the same time interval as:

$$T_{p1} = \underbrace{\frac{A_c I_c}{(mc_p)_p}\Delta\tau}_{A_{11}} + \underbrace{\left\{1.0 - \left(\frac{A_c U_{pg}}{(mc_p)_p} + \frac{A_w U_{pw}}{(mc_p)_p} + \frac{A_c U_{pab}}{(mc_p)_p} + \frac{A_1 U_{pae}}{(mc_p)_p}\right)\Delta\tau\right\}}_{A_{12}} T_{po}$$
$$+ \underbrace{\left(\frac{A_c U_{pg}}{(mc_p)_p}\Delta\tau\right)}_{A_{13}} T_{go} + \underbrace{\left(\frac{A_w U_{pw}}{2(mc_p)_p}\Delta\tau\right)}_{A_{14}} T_{wo0} + \underbrace{\left(\frac{A_w U_{pw}}{2(mc_p)_p}\Delta\tau\right)}_{A_{15}} T_{wi0}$$
$$+ \underbrace{\left\{\left(\frac{A_c U_{pab}}{(mc_p)_p} + \frac{A_1 U_{pae}}{(mc_p)_p}\right)\Delta\tau\right\}}_{A_{16}} T_{a0}$$

$$T_{p1} = A_{11} + A_{12}T_{p0} + A_{13}T_{g0} + A_{14}T_{wo0} + A_{15}T_{wi0} + A_{16}T_{a0} \quad \text{..... (2.47)}$$

2.4.1.2. Transient Analysis of the Glazing/Glass Cover

Making energy balance on the glass cover, assumed single glazed collector, its temperature at any time $(t+\Delta\tau)$ is determined from data at time t and energy absorbed and lost from the glass cover during the time interval $\Delta\tau$ is as follows:

$$(mc_p)_g \frac{dT_g}{dt} = A_c I_c(1-\tau_g) + A_c U_{pg}(T_p - T_g) - A_c U_{ga}(T_g - T_a) \quad \text{..... (2.48)}$$

Upon integration, equation (2.48) yields the temperature of the glass cover, after time interval of $\Delta\tau$, as:

$$T_{g1} = \underbrace{\frac{A_c I_c(1-\tau_g)}{(mc_p)_g}\Delta\tau}_{A_{21}} + \underbrace{\left\{1.0 - \left(\frac{A_c U_{pg}}{(mc_p)_g} + \frac{A_c U_{ga}}{(mc_p)_g}\right)\Delta\tau\right\}}_{A_{22}} T_{go} + \underbrace{\left(\frac{A_c U_{pg}}{(mc_p)_g}\Delta\tau\right)}_{A_{23}} T_{po}$$
$$+ \underbrace{\left(\frac{A_c U_{ga}}{(mc_p)_g}\Delta\tau\right)}_{A_{24}} T_{a0}$$

$$T_{g1} = A_{21} + A_{22}T_{g0} + A_{23}T_{p0} + A_{24}T_{a0} \quad \text{..... (2.49)}$$

2.4.1.3. Transient Analysis of the Water Stream

Application of similar approach yields an expression for the temperature of hot water leaving the solar collector as:

$$\left(mc_p\right)_w \frac{dT_{wo}}{dt} = A_w U_{pw}\left\{T_p - \frac{T_{wo}+T_{wi}}{2}\right\} - \left(\dot{m}c_p\right)_w (T_{wo} - T_{wi}) \quad \text{..... (2.50)}$$

$$T_{w01} = \underbrace{\left(\frac{A_w U_{pw}}{\left(mc_p\right)_w}\Delta\tau\right)}_{A_{31}} T_{po} + \underbrace{\left\{1.0 - \left(\frac{A_w U_{pw}}{\left(mc_p\right)_w} + \frac{\left(\dot{m}c_p\right)_w}{\left(mc_p\right)_w}\right)\Delta\tau\right\}}_{A_{32}} T_{wo0} - \underbrace{\left\{\left(\frac{A_w U_{pw}}{2\left(mc_p\right)_w}\right) - \left(\frac{\left(\dot{m}c_p\right)_w}{\left(mc_p\right)_w}\right)\right\}}_{A_{33}} \Delta\tau T_{wi0}$$

$$T_{p1} = A_{31}T_{p0} + A_{32}T_{wo0} + A_{33}T_{wi0} \quad \text{..... (2.51)}$$

Application of similar approach yields an expression for the temperature of hot water leaving the solar collector as equations (2.47), (2.49) and (2.50) are derived from energy balance on the absorber plate, the glass cover and the water stream, respectively. The given sets of equations are non-linear due to temperature dependent radiant and convective heat transfer coefficients. The solutions are, therefore, determined by an integration scheme that linearises these equations within a set time step.

2.4.1.4. Transient Analysis of the Storage Tank

The temperature of the water at the inlet of the collector is evaluated by taking the hot water extracted from and the heat losses across the storage tank into account. In the model, the level of water in the storage tank is to be controlled by a float valve keeping the mass of water in the storage constant. After making energy balance in the time interval $\Delta\tau$, the storage tank temperature is evaluated from:

$$\left(\rho c_p\right)_w V_s \frac{dT_s}{dt} = \left(\dot{m}c_p\right)_w (T_{wo} - T_{wi}) - U_{Ls}A_s\{T_s - T_a\} - \text{..... (2.52)}$$

$$T_{s1} = \underbrace{\left\{1.0 - \left(\frac{A_s U_{Ls}}{(\rho_w c_p)_w V_s}\right)\Delta\tau\right\}}_{A_{41}} T_{s0} - \underbrace{\left\{\left(\frac{(\dot{m}c_p)_w}{(\rho_w c_p)_w V_s}\right)\Delta\tau\right\}}_{A_{42}} (T_{wo0} - T_{wi0}) + \underbrace{\left\{\left(\frac{A_s U_{Ls}}{(\rho_w c_p)_w V_s}\right)\Delta\tau\right\}}_{A_{43}} T_{a0}$$

$$T_{s1} = A_{41}T_{s0} + A_{42}((T_{wo0} - T_{wi0}) + A_{43}T_{a0} \quad \text{..... (2.53)}$$

The temperature of the absorber plate varies across the width of the fin, having a maximum on the center line between the fluid ducts.

The transient simulation of the solar water heater can be carried out. It is used to predict the monthly and annual performance of the solar water heating system. The parameters read from input files at the beginning of the simulation process include:

I. Latitude of the site, azimuth and slope of the solar collector;
II. Geometric dimensions and thermo physical properties of the absorber plate, the glazing and the insulation;
III. Thermo physical properties of water;
IV. Storage capacity, daily hot water consumption pattern and hot water delivery and cold water supply temperatures, and;
V. Beam and diffuse solar radiation and ambient temperature for every hour of the day.

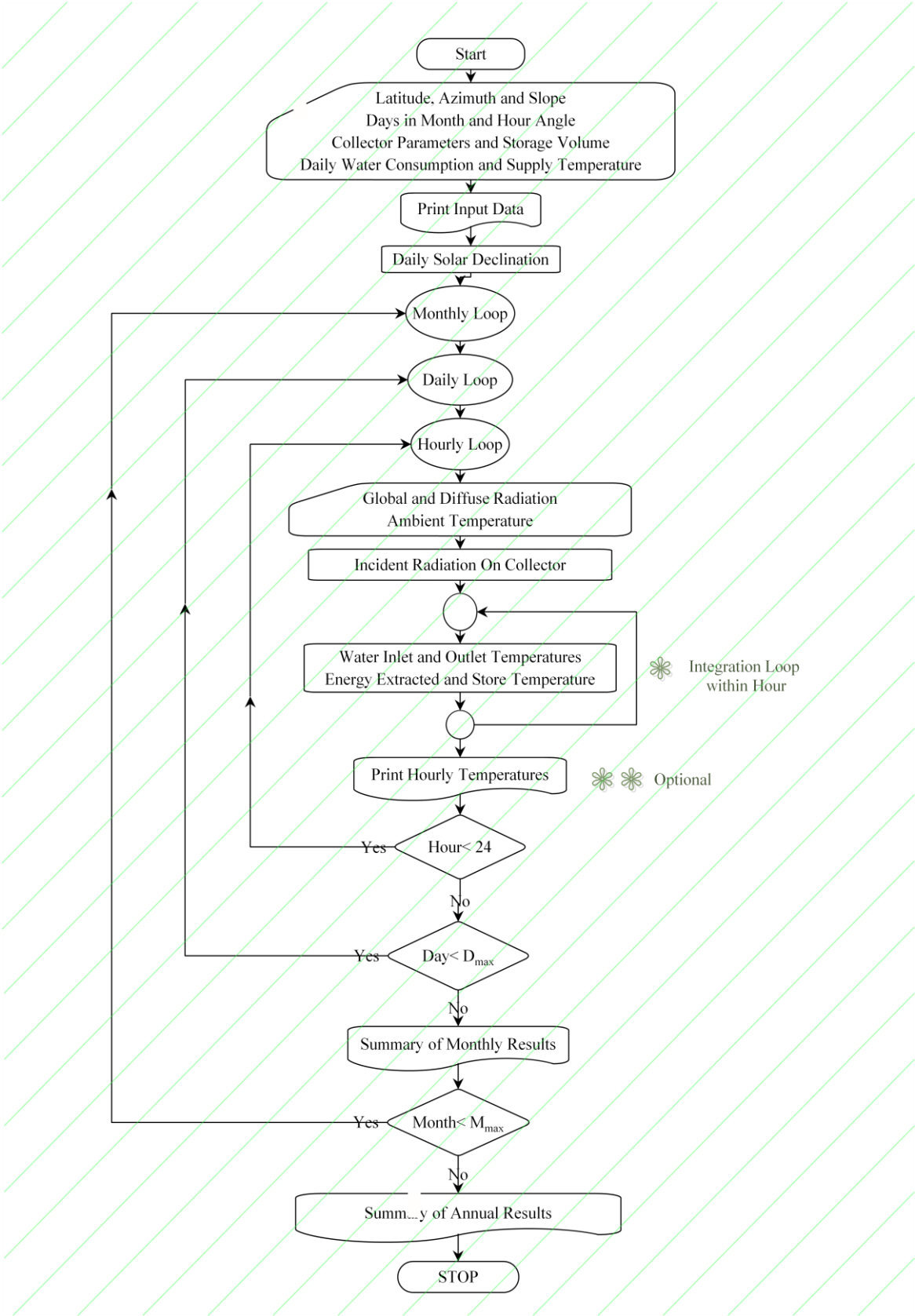

Figure 2.26: Flow chart of Simulation Programme (Source: Dr.Ing Abebayehu Assefa's lecture note).

Solution Method;

I. The year-round transient analysis of the collector model is performed using the given solar radiation data and the solar collector parameters.
II. The fraction of the total daily hot water load that occurs in the hour should also be specified in the simulation process.
III. The temperature variations of the collector panel, the glass cover, the water stream leaving the collector and the storage tank are estimated from Equations (2.47), (2.49), (2.51) and (2.53), starting on January 01 at 01:00 AM.

The following steps are applied in the determination of the temperature variations over the year.

Step 1:

Evaluate temperatures T_{p1} of the plate, T_{g1} of the glass cover, T_{wo1} of the water at outlet from the collector and T_{s1} of the storage tank at time applying Equations (2.46), (2.49), (2.51) and (2.53), respectively, starting the system simulation by assuming the following initial temperatures for the various components of the solar collector model.

I. Ambient temperature Ta0 = value read from solar radiation data on January 01 at 01:00 AM;
II. Glass temperature $T_{g0} = T_{a0} + 0.25$;
III. Plate temperature $T_{p0} = T_{a0} + 1.0$;
IV. Temperature of water at collector inlet $T_{wi0} = T_{a0}$; and
V. Temperature of water at collector outlet $T_{wo0} = T_{a0} + 0.5$

Step 2:

Since the assumed temperatures for the various components in Step 1 are too crude, they have to be refined by taking average values of the assumed temperatures and the evaluated temperatures at time $(t+\Delta\tau)$ and substituted for temperature values at time t. Steps 1 and 2 are performed only for January 01 at 01:00 AM.

Step 3:

Temperature variations Tp_1, Tg_1, Two_1 and Ts_1 during a period of 24 hours over the year are then estimated by substituting the new values of Tp_1, Tg_1, Two_1 and Ts_1, respectively, for Tp_0, Tg_0, Two_0 and Ts_0 for the next time interval.

The following relations are used in the above equations:

$$A_1 = p(t_c - t_b) \;\; and \;\; A_w = \pi d_i NL \quad \text{..... (2.54)}$$

$$U_{pg}\left\{\left(0.06 - 0.017\frac{\theta}{90}\right)\frac{k_a}{x}G_{rx}^{\frac{1}{3}}\right\} + \epsilon_{pg}\sigma\left(T_p^2 + T_g^2\right) * \left(T_p + T_g\right) \quad \text{..... (2.55)}$$

Where: $$G_{rx} = \frac{g\beta_v(T_p - T_g)x^3}{v^2} \quad \text{..... (2.56)}$$

And the volume expansion coefficient β_v is given by:

$$\frac{1}{\beta_v} = \frac{(T_p + T_g)}{2} \quad \text{..... (2.57)}$$

The overall emittance factor for the absorber-glass cover is obtained from the relation:

$$\epsilon_{pg} = \left[\frac{1}{\epsilon_p} + \frac{1}{\epsilon_g} - 1\right]^{-1} \quad \text{..... (2.58)}$$

$$U_{pw} = \left[\frac{k_w R_e P_r}{4L}\right] ln\left[\frac{1}{1 - \frac{2.654}{P_r^{0.167}\left(R_e P_r \frac{d_i}{L}\right)^{0.5}}}\right] \quad \text{..... (2.59)}$$

$$U_{pab} = \frac{k_i}{t_b} \quad and \;\; U_{pae} = \frac{k_i}{t_e} \quad \text{..... (2.60)}$$

Where (Nomenclature):

A_c = Area of a collector [m^2]

I_b = Beam radiation on horizontal surface [W/m^2]

C_p = Specific heat capacity [kJ/kg K]

I_d = Diffuse radiation on horizontal surface [W/m^2]

g = Gravity of the earth [m/s^2]

I_t = Global radiation on horizontal surface [W/m^2]

G_{rx} = Grashof number at position x [-]

$I_c = I_N (\tau_g \alpha_p)$ = Solar irradiation on a collector surface [W/m^2]

k_a = Thermal conductivity of air [W/m K]

k_i = Thermal conductivity of insulation [W/m K]

L = Distance between cover and absorber [m]

$\dot{m}_a$= Mass flow rate of air [kg/s]

$(m\ c_p)_a$ = Mass x specific heat of air [kJ/K]

$(m\ c_p)_g$ = Mass x specific heat of glass [kJ/K]

$(m\ c_p)_p$ = Mass x specific heat of collector plate [kJ/K]

p = Perimeter of collector [m]

P_r = Prandtl number [-]

R_b = Beam radiation factor [-]

R_d = Diffuse radiation factor [-]

R_e = Reynold number [-]

T_a = Ambient temperature [°C]

t_b = Back insulation thickness [m]

t_c = Depth of collector [m]

t_e = Edge insulation thickness [m]

T_g = Glass cover temperature [°C]

T_p = Plate temperature [°C]

T_s = Storage temperature [°C]

Twi = Temperature of water at collector inlet [°C]

Two= Temperature of water at collector outlet [°C]

U_{LS} = Heat transfer coefficient of the storage tank [kW/m^2]

U_{ga}= Glass to ambient heat transfer coefficient [kW/m^2]

U_{pg}= Collector plate to glass heat transfer coefficient [kW/m^2]

U_{pa}= Collector plate to air heat transfer coefficient [kW/m^2]

α_p = Solar absorptance of collector plate [-]

σ = Stefan-Botzman constant [5.67x10^{-8} W/m^2 K]

τ_g = Solar transmittance of glazing [-]

β= Inclination of the solar collector [°]

Δτ = Integration time step [s]

2.5. Cement Production Process

2.5.1. Description of Clinker Production Process

Regardless of whether the process route is wet or dry, the heating of the raw materials in clinker production in a cement industry follows certain stages:

I. Drying and pre-heating (20 - 900^{o}c): release of free and chemically bound water;
II. Calcinations (600 - 900°C): Initial reactions with formation of clinker materials and intermediate phases with the release of carbon dioxide;
III. Sintering (1250 -1450°C): in a liquid state, where the free lime reacts with the other components to form calcium silicates, aluminates and alumino ferrite (the principal ingredients of Portland cement).This sintered product is known as cement clinker and this process stage is also referred to as “burning” or “clinkering”; and

IV. Cooling: where the temperature of the liquid is reduced from 1450 to 1100°C to form stable crystals within the kiln followed by cooling to about 250°C in a clinker cooler.

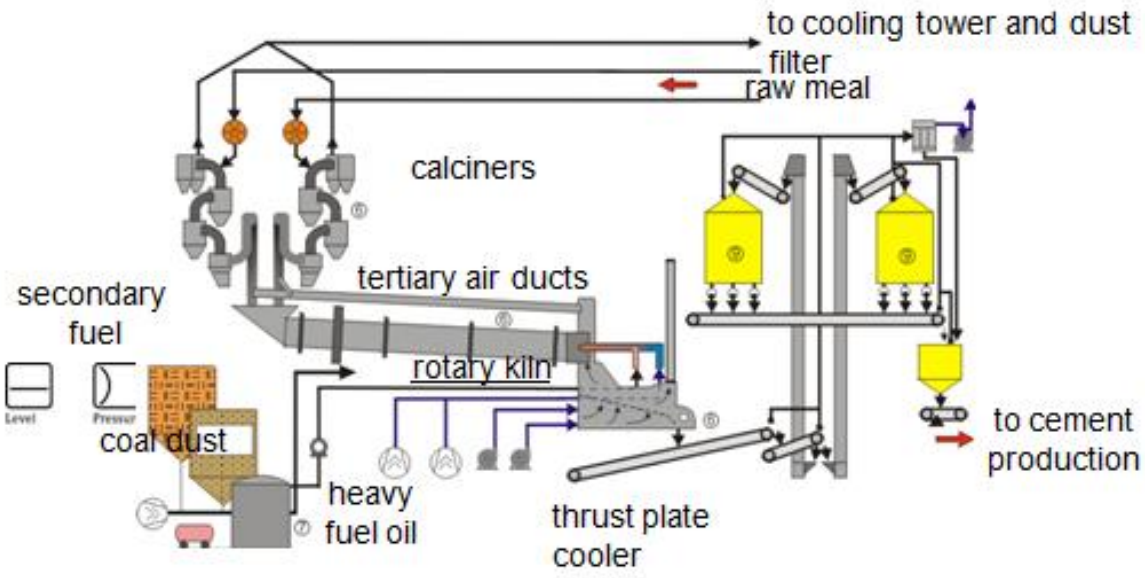

Figure 2.27: Typical Clinker Production Process (Source: Operation manual)

A typical pre-heater kiln processing diagram is given in Figures 2.28 and 2.29 below showing the broad variation in chemical composition and temperature with time and position within the kiln system.

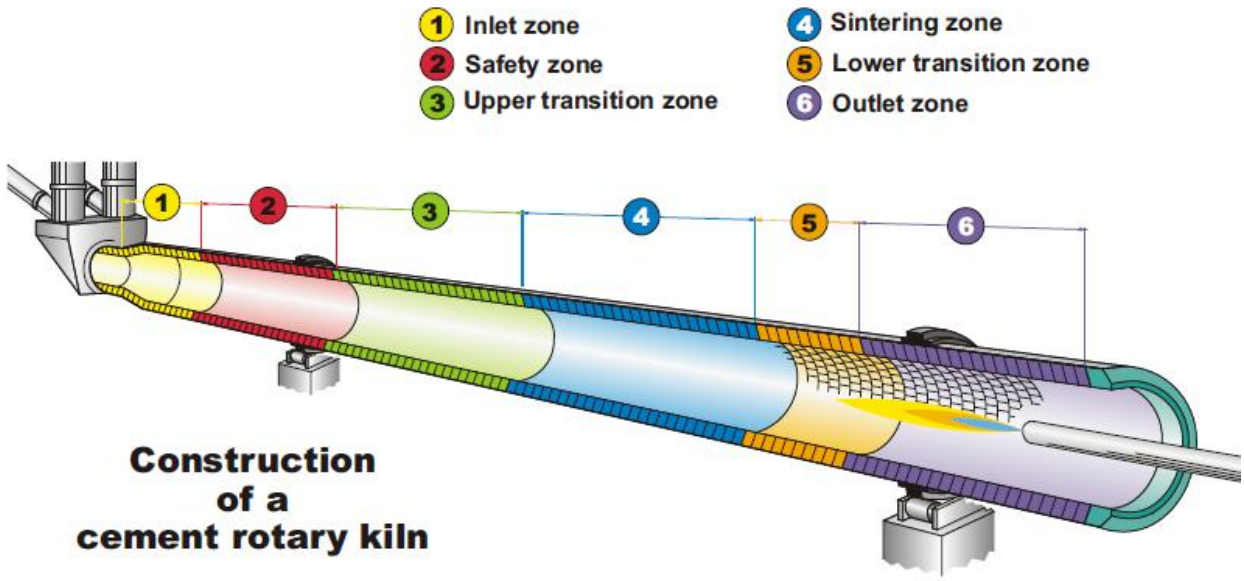

Figure 2.28: Zones of typical Kiln (Source: Magnesita Refractories GmbH)

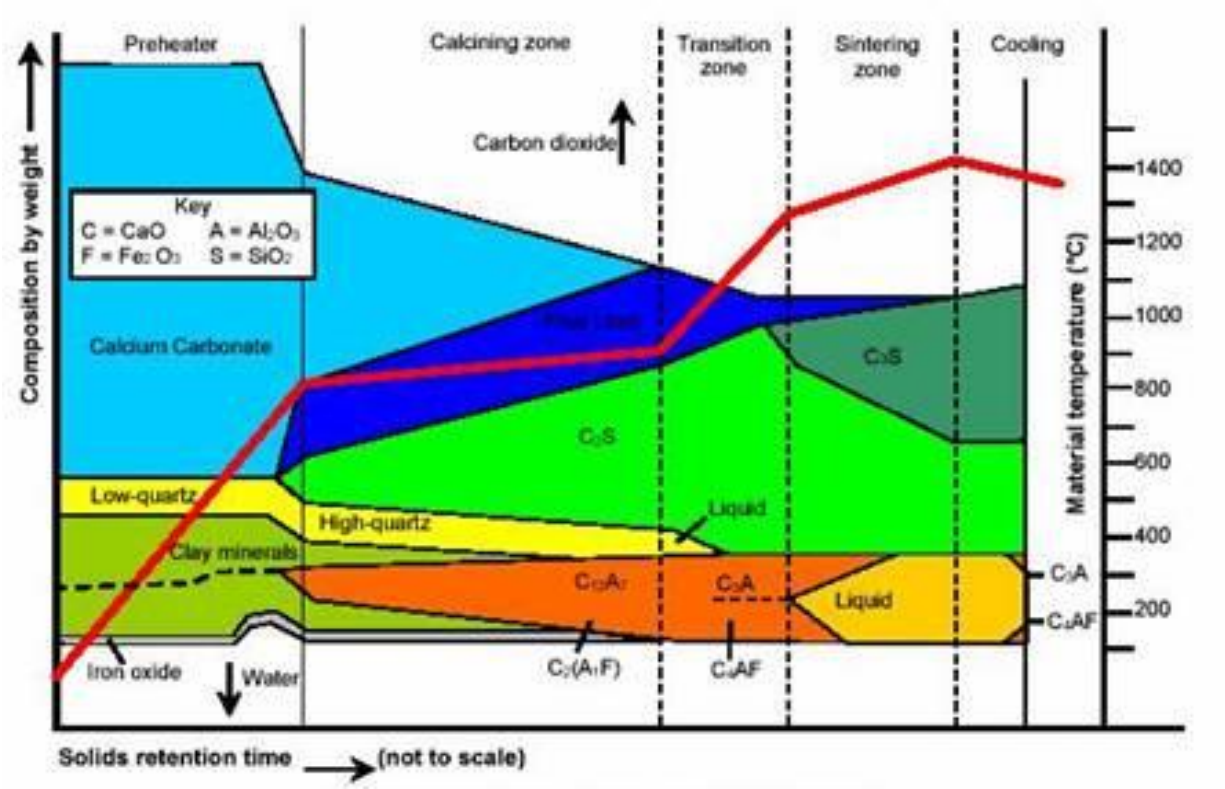

Figure 2.29: Typical pre-heater kiln processing diagram (Source: Operation manual)

However, cement manufacturing center is an energy intensive activity and the choice of fuels affects both the environmental releases and the economics of the process.

Total energy cost can represent 65-75% of the variable costs of the process. The pre-heater tower supports a series of vertical cyclone chambers through which the raw material passes on the way to the kiln.

To save energy modern cement plants preheat the raw material before they enter the kiln. Rising more than 200 feet, hot exit gases from the kiln heat the raw meal as they swirl down the cyclone string.

The pyro-processing stage is generally regarded as the heart of the cement-making process. It is the stage in which most of the operating costs of cement manufacture appear, and is also therefore the stage where most of the opportunities for process improvement exist.

There are many different kiln system designs and enhancements, but they are all in essence performing the following material transformation, in order from the feed end:

I. Evaporating free water, at temperatures up to 100°C.

II. Removal of adsorbed water in clay materials 100° to 300°C.

III. Removal of chemically bound water 450° to 900°C.

IV. Calcinations of carbonate materials 700° to850°C.

V. Formation of C_2S, aluminates and ferrites800° to 1,250°C.

VI. Formation of liquid phase melt >1,250°C.

VII. Formation of C_3S 1,330° to 1,450°C.

VIII. Cooling of clinker to solidify liquid phase 1,300° to 1,240°C.

IX. Final clinker microstructure frozen in clinker <1,200°C.

X. Clinker cooled in cooler 1,250° - 100°C.

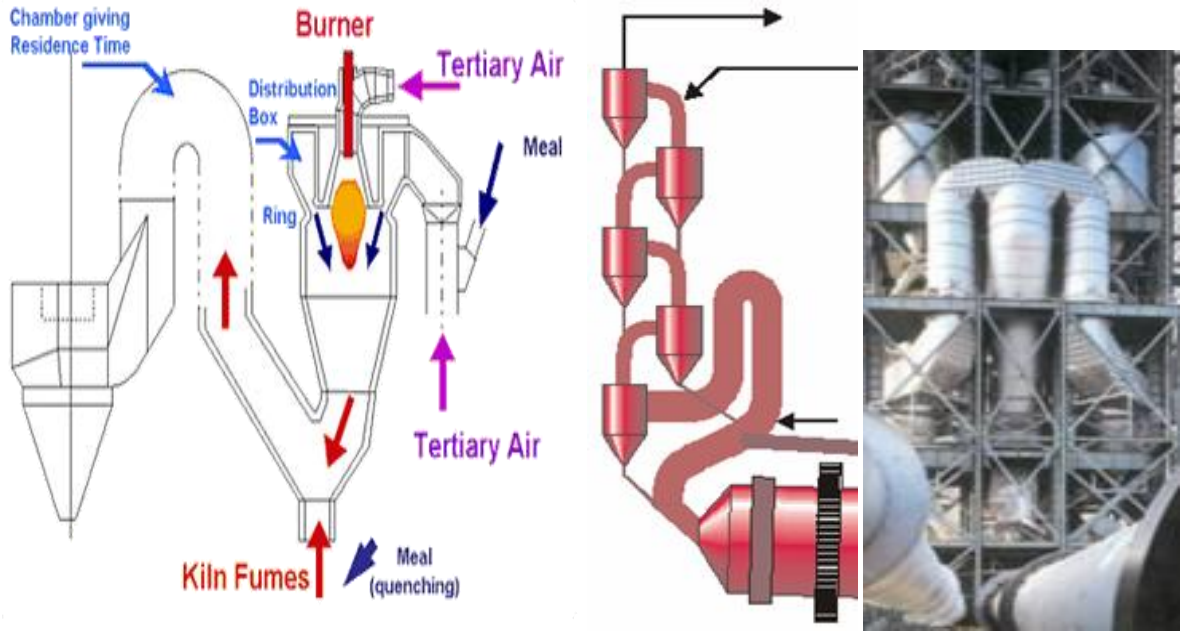

Figure 2.30: Typical Cyclone pre-heater and Pre-Calciner kiln processing diagram (Source: Operation manual)

In pre-calciner kilns, the combustion air for burning fuel in the pre-heater no longer passes through the kiln, but is taken from the cooler region by a special tertiary air duct to a specially designed combustion vessel in the pre-heater tower. Typically, 60% of the total fuel is burnt in the calciner, and the raw meal is over 90% calcined before it reaches the rotary kiln section. Since the calciner operates at temperatures around the calcination temperature of raw meal (800°C to 900°C), there may not be a flame as such.

The calciner efficiency is dependent on uniform air flow and uniform dispersion of fuel and raw meal in the air. Typically, average residence times calculated on gas flow for early units

were about 1 to 2 seconds for coal and oil, and 2 to 3 seconds for natural gas. In recent years, though, there has been a trend toward larger calciner vessels to reduce some of the combustion problems of the earlier designs and provide greater flexibility for using lower grade fuels.

Pre-calciner kilns can have very large outputs in excess of 10,000 tpd, with specific fuel consumption below 3MJ/kg (700kcal/kg). There are many different configurations, with one, two, or three pre-heater towers operating with one or two calciner vessels in either an in-line configuration or separate line configuration. Some designs include a separate pre-combustion chamber.

An in-line calciner has kiln exhaust gases and tertiary air making up the combustion air (reduced oxygen levels) for the calciner, while the separate line system has tertiary air only with 21% oxygen forming the combustion air.

A separate line system has a better combustion environment and may be preferred for difficult fuels. It has a further advantage when converting pre-heater kilns to pre-calciners in that there is minimal interference with the operating pre-heater kiln during the construction phase for the new separate line pre-heater tower and tertiary air duct.

Pre-calciner kiln systems can operate only in conjunction with grate coolers, as there is no provision for tertiary air off-take with planetary coolers. L/D (length to Diameter) ratios are typically low at 10 to 14, and kiln speeds are in the order of 3.5 rpm. Kiln residence time is typically 20 to 25 minutes.

From the pre-heater, the raw material enters the rotary kiln at the upper end. It slides down the cylinder through progressively hotter zones towards the flame. At the lower end of the kiln, fuels such as pulverised coal or natural gas feed a flame that reaches 1870°C (3400°F).

The clinker at the bottom of the kiln reaches a temperature of 1450°C and becomes partially molten.

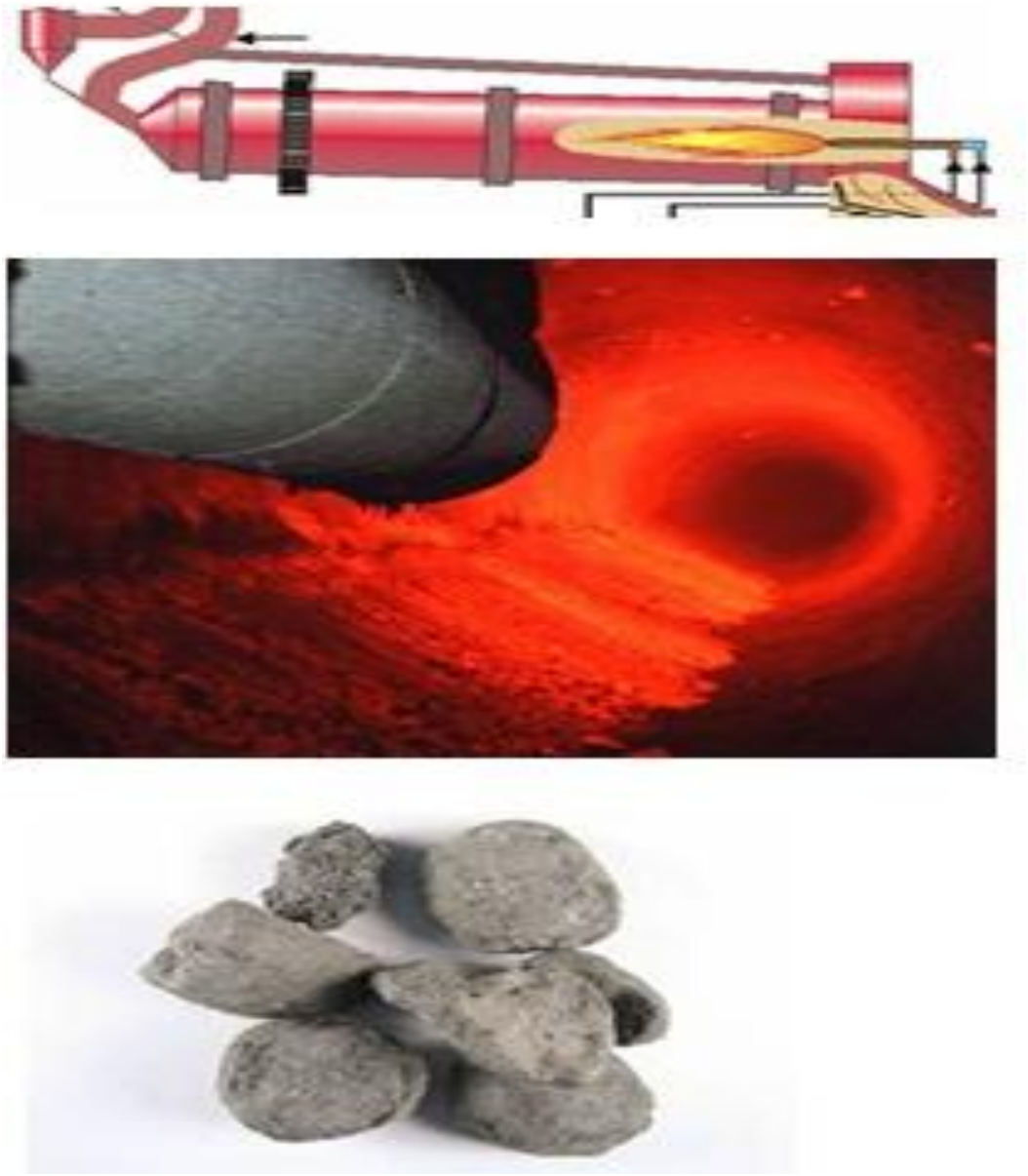

Figure 2.31: Typical burning in the kiln and clinker stones formation (Source: Operation manual)

The intense heat triggers chemical and physical changes. The Calcium and Silica Oxides are converted to Calcium Silicate or Clinker stones.

Cooling of clinker takes place at two locations:

I. In the kiln after the material passes the burning zone region, and
II. In the specially designed clinker coolers after the material falls out of the kiln.

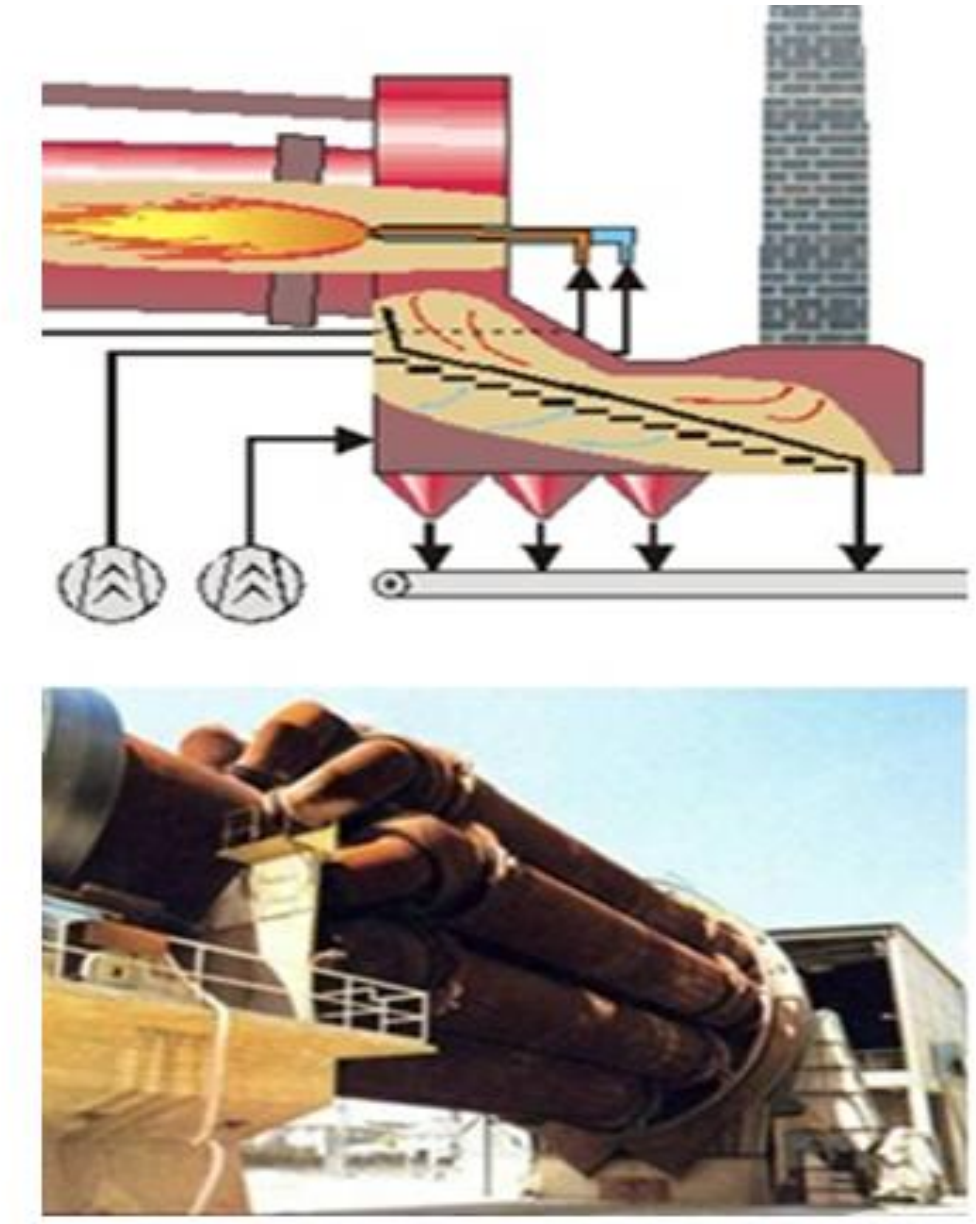

Figure 2.32: Typical clinker coolers locations (Source: Operation manual)

The rate of cooling can be critical to the clinker quality and performance of cement. The rate of cooling in the kiln is determined by the flame and resulting heat flux, flame temperature, and speed of material flow through the kiln. As the clinker temperature exiting the kiln is normally 1,200°C to 1,250°C, the clinker characteristics have been already largely established before the, clinker enters the cooler. A long flame gives slow heat-up and slow cooling of the kiln charge before it falls from the kiln.

This will tend to produce clinker with large alite and belite crystals, resulting in a coarse-grained clinker matrix with poor reactivity and poor grindability.

Slow cooling can also result in reversion of C_2S from the 'α' phase to the less reactive β form, or in extreme cases even to the un-reactive γ form, and can even allow C_3S to revert to C_2S and CaO. All of these have a negative impact on cement strength.

A further quality problem can arise if there are high levels of MgO in the clinker, because slow cooling allows large periclase crystals to form such that when these hydrate slowly in concrete, the expansion can cause the concrete to rupture.

There are two main types of coolers used in cement clinker production.

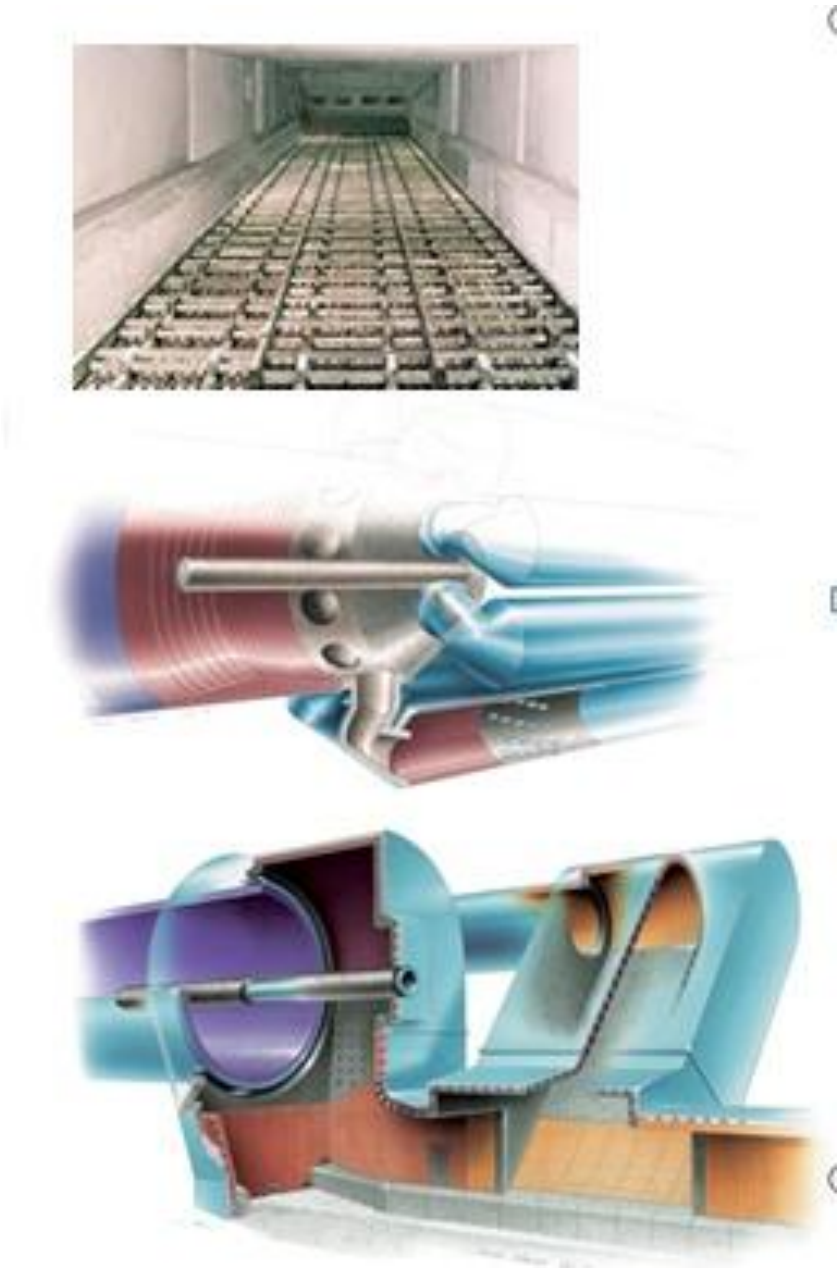

Figure 2.33: Clinker coolers (Source: Operation manual)

These are the satellite (or planetary) type and the oscillating grate type. The 1990s saw tremendous advances in clinker cooler technology that greatly improved heat efficiency and potential output from a given kiln system.

Clinker coolers perform the function of:

I. Transporting clinker from the kiln to the clinker delivery system;
II. Cooling the clinker to a safe temperature for subsequent transport;
III. Finalizing the clinker mineralogy through rapid cooling; and
IV. Preheating combustion air by heat exchange with hot clinker.

After cooling the clinker has a temperature between 80°C and 200°C. The clinker stones are stored in domes or silos prior to milling to keep down the dust levels. Typically the clinker stone will have a max size of 50mm.

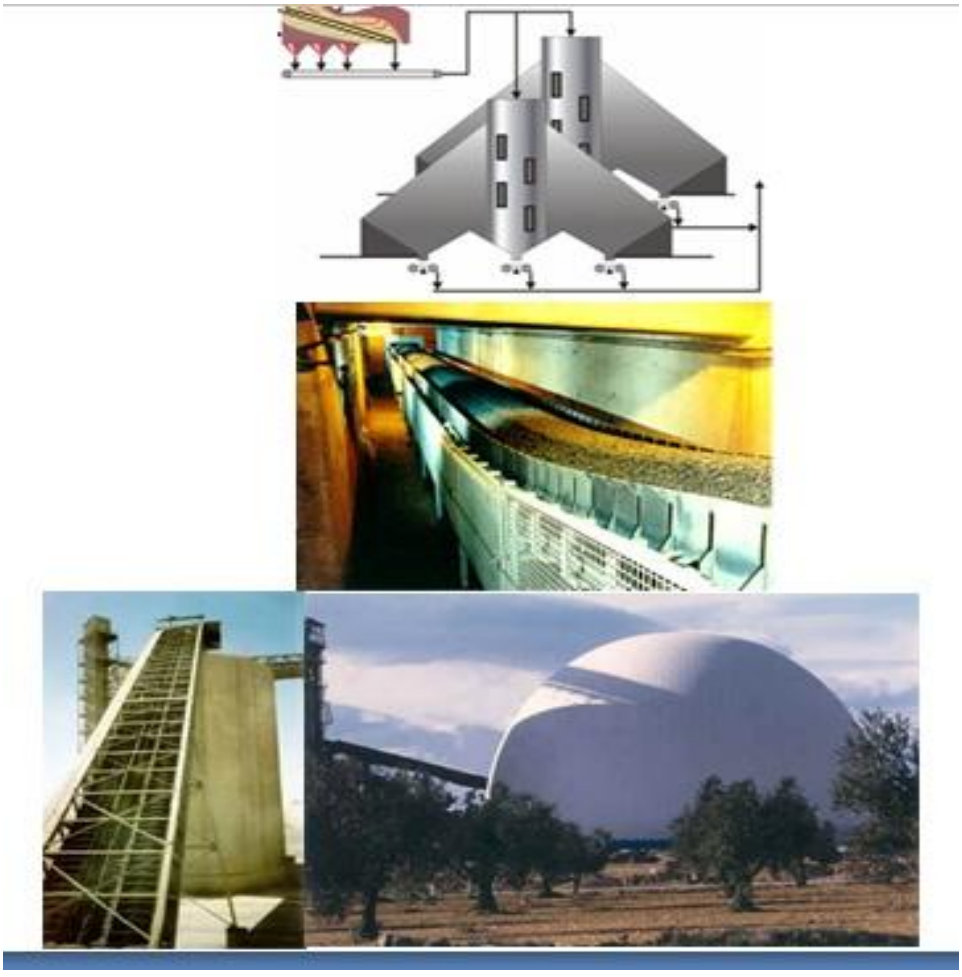

Figure 2.34: Clinker transport and storage (Source: Operation manual)

CHAPTER THREE

MATERIALS USED AND METHODOLOGY EMPLOYED TO TEST AND MEET THE OBJECTIVE/ PROVE THE HYPOTHESIS STATED

3.1. Introduction

The aim of this chapter is to discuss the materials/equipments and testing methods used in the practical analysis of the engine-generator set performance in order to meet the objective/prove the hypothesis stated. Testing procedures are also described. All experimental work was performed in Mugher Cement Factory.

3.2. Materials Used for Performance Testing

3.2.1. Engine

The installed engine is a four cycle, six cylinder inline, water cooled and turbocharged with a pressure type pump that can generate the maximum power of 818 Hp at 1500rpm. In this thesis, the installed engine, which has a problem of delay in getting its full power, especially during start up due to low coolant temperature, is currently used in Mugher Cement Factory. The installed drive engine data (Figure 3.1) are presented as follow:

I. Manufacturer: Cummins
II. Engine Number: 41125773
III. Model: KTAA19-G6A
IV. Serial Number: 5046296
V. Maximum Power: 818Hp/610Kw at 1500 rpm
VI. Manufacture Date: 2009 11
VII. Valve lash: 0.36 intake and 0.69 exhaust

3.2.2. Electric Water Heater

The parameters of heater used to test the improvement of delay time, in attaining full power, in line with circulating coolant water are:

I. Voltage: 220V
II. Power: 4000W

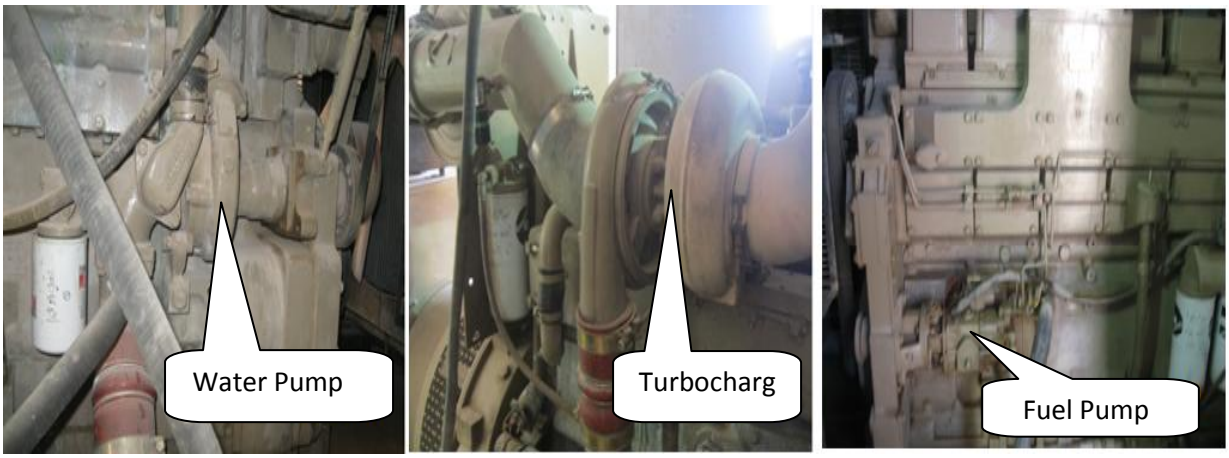

Figure 3.1: Components of installed engine (Source: Picture taken on site)

3.2.3. Generator

The installed generator can produce the voltage of 400V and the maximum power of 500Kw at 902Acurrent at sea level with a frequency of 50Hz. But, the current total output of the generator is tested to be the maximum of 180Kw, which is very much less than the design capacity with the power factor of 80%. The installed generator data (Figure 3.2) are presented as follow:

I. Manufacturer: ENGGA
II. Type: EG355L-500N
III. Voltage: 400V
IV. Continuous Duty: 625KVA
V. Rating: 500Kw at 902A
VI. Standby Duty: 687.5KVA
VII. Rating: 550Kw at 902A
VIII. Cos φ : 0.8
IX. Phase: 3
X. Frequency: 50Hz
XI. Speed: 1500rpm

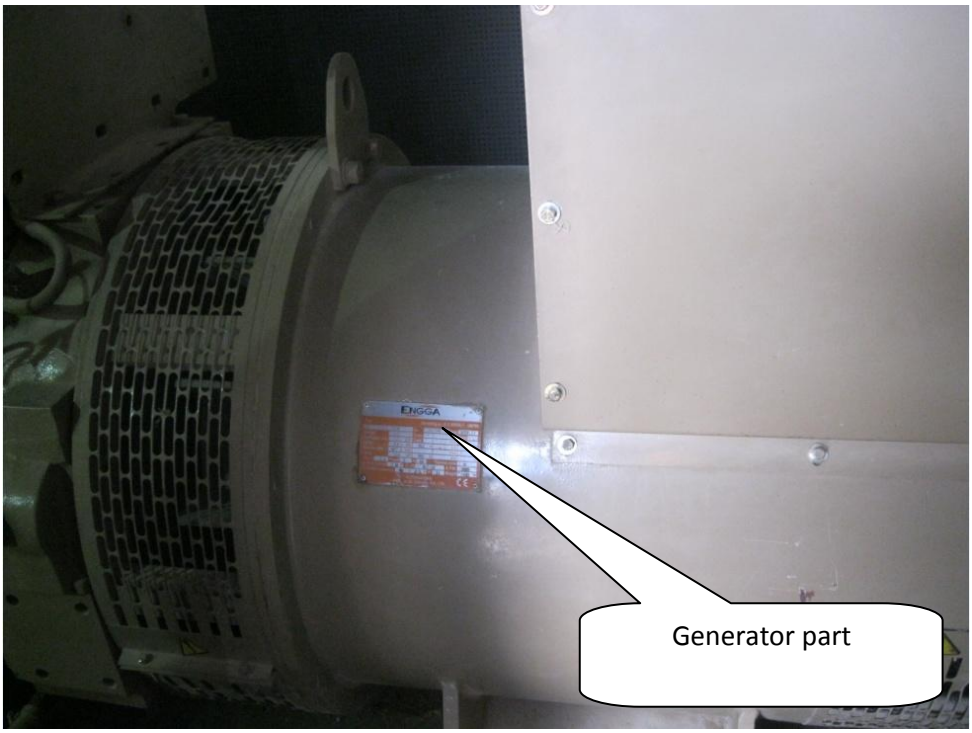

Figure 3.2a: Installed Generator (Source: Picture taken on site)

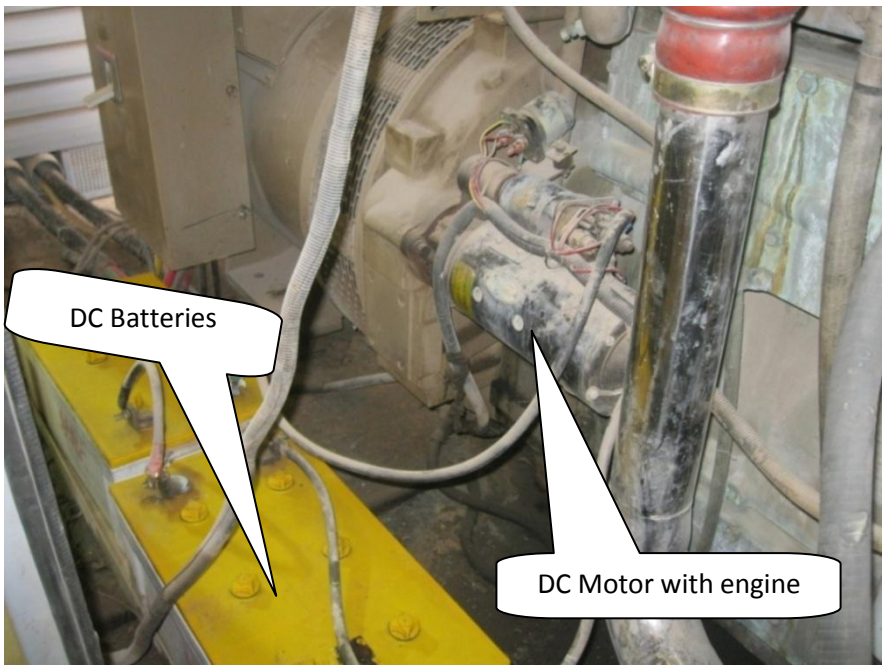

Figure 3.2b: Installed DC battery with engine starter DC motor (Source: Picture taken on site)

Figure 3.2: Installed Genset (Source: Picture taken on site)

The controller displays both the engine and generator performance parameters in a digital and standard symbolic manner (Figure 3.3). The control procedure, protection parameters and

display parameters can be modified, such as measuring, control, protection, telecommunication, remote control capability and so on by satisfying automatic control requirements. Generator Set Controller Data are presented as follow:

I. Manufacturer: Harsen Industries Limited (JNH)

II. Type: GU320B

Figure 3.3a: Installed genset and controller (Source: Picture taken from manufacturer manual)

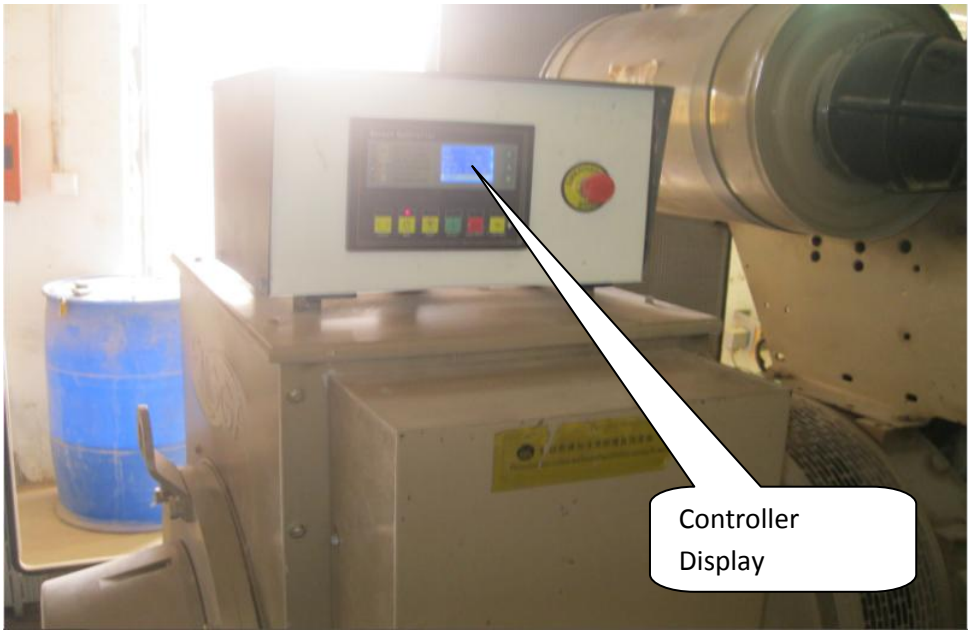

Figure 3.3b: Installed controller (Source: Picture taken on site)

Figure 3.3c: Generator Switch Gear (Source: Picture taken on site)

Figure 3.3: Generator set controllers (Source: Manufacturer manual and Pictures taken on site)

Features of the installed controller are described as follows:

I. It measures and displays all generator set output parameters including speed (rpm), engine oil pressure, engine coolant (water) temperature, direct current source voltage, operating hours of the engine, true root mean square display of voltage, current, power, and so on to ensure the accuracy of the data.
II. The push buttons on the panel face are used to select the control mode, start operating sequence, alternate display parameters and modify protection parameters, incorporates light emitting diodes (LED) that display entire operating mode and fault indication.

As per the installed controller output display reading, the maximum coolant temperature had been less than 26°C. The installed engine needs minimum 75°C to attain its full capacity and absorb the high draw starting current requirement of kiln system drive motors as per literature review under section 2.1.

To attain the required engine rated power running temperature, it is required to run minimum for more than 20 minutes depending on the ambient and seasonal conditions as per literature review under section 2.1, which may lead the kiln system equipment, which works under

high thermal stress mentioned under section 2.2.1 in literature review, to thermal deformation.

3.2.4. Electro Mechanical Components of Generator Systems

The following electromechanical components are integrated with the installed generator:

I. Circuit breaker
II. Transformer/Step up/generator-transformer
III. Medium voltage switch gear

Circuit Breaker (Figure 3.3c) is used to connect generator load to the step up transformer after the generator reach full load.

Step up transformer is a transformer that transforms generated voltage (380/400Volt) by generator to medium voltage (6 Kilo Volt) for connection to a medium distribution feeder.

Figure 3.4: Step up transformer (Source: Picture taken on site)

The plant gets supply from the main grid 15 Kilo Volt. Then Mugher Cement Factory reduces 15 Kilo Volt to Medium voltage (6 Kilo Volt) by medium step down transformer which is under the control of this factory. The reduced medium voltage sent to the main medium distribution system of the organization. The medium voltage (6 Kilo Volt) is connected to medium voltage bus bar from where the power is distributed to different plant stations. In the main station, there are two switchgears. One switch gear is used to control the main supply that come from main grid, whereas the second switchgear is used to control the supply that come from the standby generator when the main grid supply fails.

The 15 kilo volt main-station transformation line principle is depicted as follows:

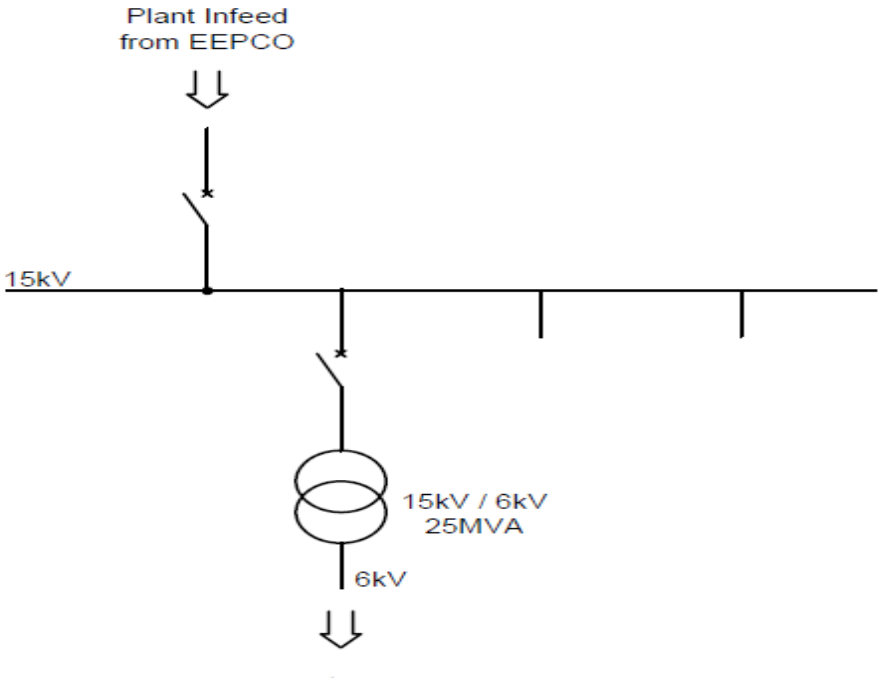

Figure 3.5: Transformation of 15kilo volt to 6kilo volt (Source: Picture taken from operating manual)

The incoming cable from main grid leads to the 15 kilo volt main-station as shown above in figure 3.5. In case of power cut off from the main grid, the protection relay of the incomer and outgoing feeder will open both circuit breakers.

The 6kV main-station transformation line principle is depicted as follows:

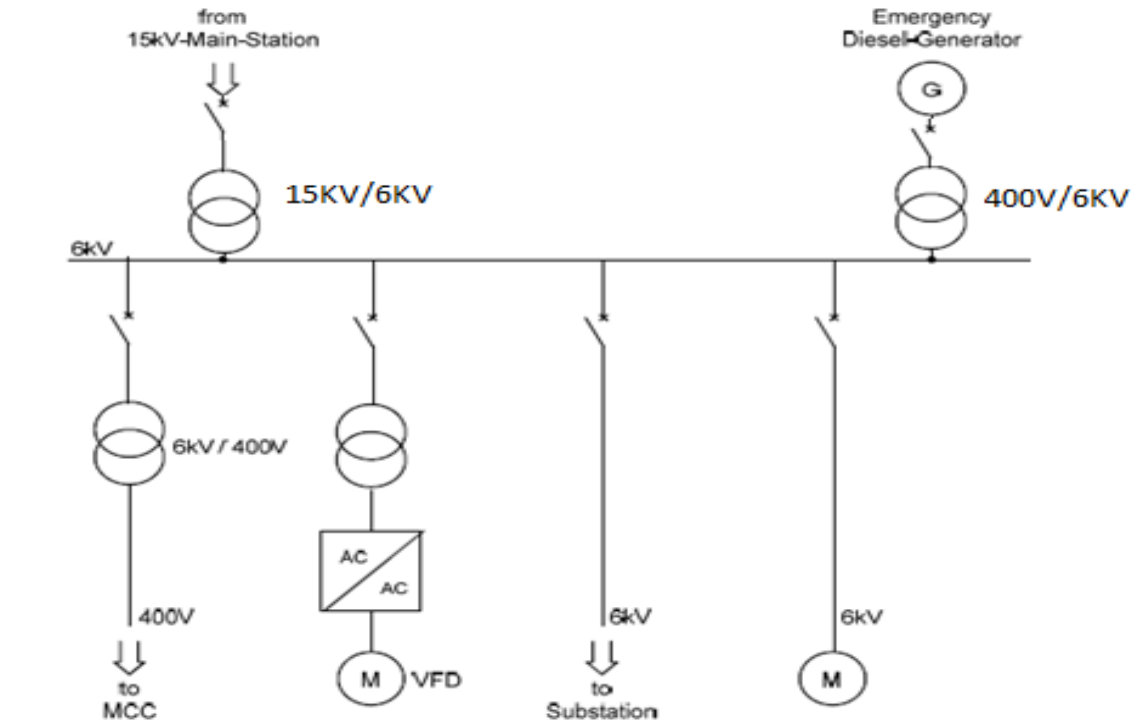

Figure 3.6: Transformation of Voltages (Source: Picture taken from operating manual)

The cable from the 15kilo volt-main-station leads to 6kilo volt from the Main-Transformer to the incoming circuit breaker. The above sketch shows the typical outgoing feeders, such as to distribution transformers 6kilo volt to 400 volt, feeding the 400 volt motor control cabinets (MCC's), or to transformers of variable frequency drives (VFD), or to next subordinate 6kilo volt substation like limestone-crushing-plant units, or directly to 6kilo volt motors.

In case of power cut, the protection relay of each circuit breaker panel will open the circuit breaker so that the incoming and all outgoing-feeders will be open.

To switch over to emergency supply, operators of the main-station will:

1. First they start the diesel generator set,
2. Pull out the circuit breaker truck of the incomer panel from the grid,
3. Push in the circuit breaker truck of the incomer panel of the emergency generator and
4. Switch on this circuit breaker and all necessary outgoing feeders to transformers and also substations switches will be switched ON.

As soon as the power of the main grid is back, the same movements in the opposite way will be carried out:

I. Switch OFF the circuit breaker of the incomer panel of the emergency generator and at the same time all outgoing feeders will be switch off by their protection relay,
II. Pull out the circuit breaker truck of the incomer panel of the emergency generator
III. Push in the circuit breaker truck of the incomer panel from the main grid,
IV. Switch ON the circuit breaker of the incomer panel from the main grid.
V. Switch ON all outgoing feeders to transformers and stations, and
VI. Finally, turn off the emergency generator set can be turned off.

The installed system has no control panel which shall provide an automatic switching power supply between the national grid and the installed diesel driven electric generator during power cut in and out that can provide an easy switching-back to supply to the national grid that permits an immediate re-start-up of the plant.

3.2.5. Temperature and Speed Testing Tools

To check the specified parameters of the generator set system, the infrared temperature measuring instrument and the revolution speed measuring tools are used as depicted in figure 3.7 on site.

Figure 3.7a: **Infrared thermometer (PeakTech 4980 type) used to measure ambient and coolant temperatures (Source: Picture taken on site)**

Figure 3.7b: Revolution speed measuring (MONARCH PLT200 type) tool used to measure speed of engine and generator (Source: Picture taken on site)

Figure 3.7c: Temperature measuring using PeakTech 4980 type infrared thermometer (Source: Picture taken on site)

Figure 3.7d: Revolution speed measuring using (MONARCH PLT200 type) (Source: Picture taken on site)

Figure 3.7: Measuring instruments used (Source: Picture taken on site)

3.3. Methodology

To investigate the improvement achieved or prove the hypothesis stated, electric water heater is used to heat engine coolant. The analysis of the system, without heater and with heater, has been done by using:

I. Installation of electric water heater is carried out as per figure 3.8 below set up,
II. Controller performance display readings,
III. Performance measuring instruments and
IV. Temperature reading data before and after installation of electric water heater have been recorded and analyzed by using some statistical methods, particularly to analyse the improvements achieved or the severity of the existing problem.

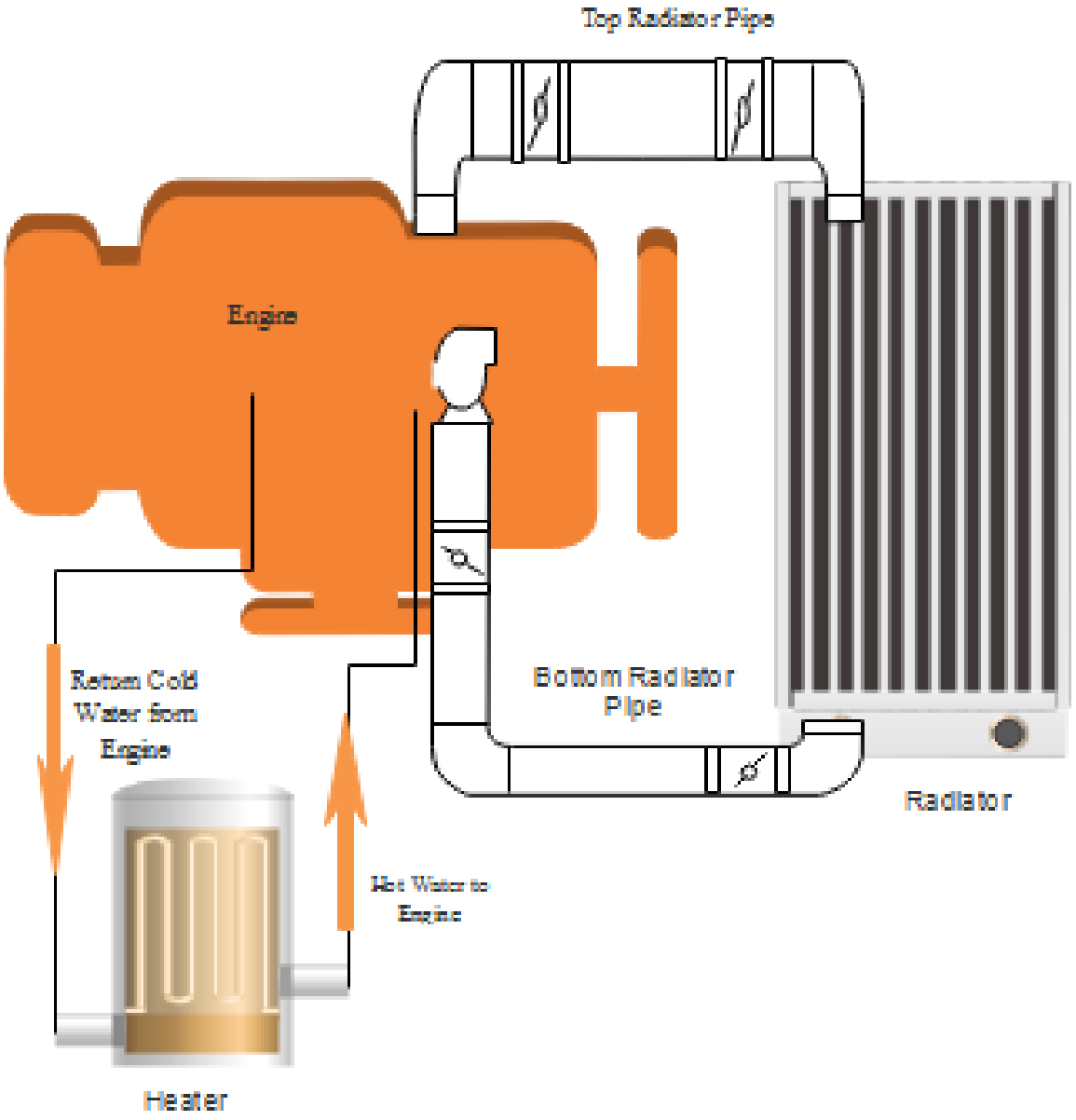

Figure 3.8: Set up of electric water heater used for testing

To equip the system with renewable energy technology, particularly with solar energy, design of appropriate solar collector to be installed has been carried out based on the formulas and literatures depicted in chapter two above by optimizing with the existing facilities. The procedures followed are:

I. Solar collector sizing and selection has been carried out
II. Determination of the monthly average daily global insolation for the required solar water heater has been determined
III. Total collector area has been calculated

IV. Operating principles, layout and equipments required has been described
V. Tilt angle and position of the collector has been decided
VI. Absorber plate has been sized
VII. Requirement of absorber coating (black–paint spray) has been identified
VIII. Cover plate has been sized
IX. Insulation requirement has been identified
X. Tube sizing and flow patterns has been identified
XI. Pump selection has been carried out
XII. Energy storage tank has been sized
XIII. The algorithm/flowchart of the transient analysis of the system has been developed.

3.4. Data

In order to measure the improvement of engine efficiency during starting up period of main grid failure, temperature data are collected from the genset controller and testing/measuring instruments both before and after installation of electric heater. The electric heater is used to justify and check that heating up of engine coolant, either by solar or electric heater, has an impact on its delay performance, after start up, in attaining its full power. These data have been collected when this experiment was made on site in Mugher Cement Factory. The data contain readings of temperature [°C] instruments and controller (Table 3.1 and 3.2).

Table 3.1: Sample of engine coolant temperature record data before the installation of heater

S.No.	Date of Record	Time of Record	Temperature[°C]
1.	17-09-2015	18:00	26
2.		19:00	25
3.		20:00	25
4.		21:00	25
5.		22:00	24
6.		23:00	24

S.No.	Date of Record	Time of Record	Temperature[°C]
7.		24:00	23
1.	18-09-2015	01:00	23
2.		02:00	23
3.		03:00	23
4.		04:00	23
5.		05:00	22
6.		06:00	22
7.		07:00	22
8.		08:00	22
9.		09:00	22
10.		10:00	22
11.		11:00	22
12.		12:00	22
13.		13:00	22
14.		14:00	22
15.		15:00	22
16.		16:00	22
17.		17:00	22
18.		18:00	22

The above data had been recorded and collected before the installation of heater for the third Line Emergency Diesel Generator Set of Mugher Cement Factory for the period of 17 to 18 September 2015 for the specified engine and generator type to be analyzed. Note that the time is put on 24:00 hour bases system to match with the time system this factory uses.

Table 3.2: Sample of engine coolant temperature record data after the installation of heater

S.No.	Date of Record	Time of Record	Temperature[°C]
1.	06-10-2015	06:00	39
2.		07:00	40
3.		08:00	40
4.		09:00	40
5.		10:00	40
6.		11:00	40
7.		12:00	39
8.		13:00	39
9.		14:00	39
10.		15:00	39
11.		16:00	40
12.		23:00	40
13.		24:00	40
14.		02:00	40
15.		03:00	39

S.No.	Date of Record	Time of Record	Temperature[°C]
16.		06:00	40
1.	07-10-2015	02:00	40
2.		10:20	41
3.		11:00	41
4.		12:00	40
5.		13:00	41
6.	21-10-2015	07:00	43
7.		08:00	43
8.		09:00	43

The above data had been recorded and collected after the installation of heater for the third Line Emergency Diesel Generator Set of Mugher Cement Factory on the dates of 6, 7 and 21 October 2015 for the specified engine and generator type to be analyzed. Note that the time is put on 24:00 hour bases system to match with the time system this factory uses.

CHAPTER FOUR

RESULTS AND DISCUSSIONS

4.1. Trends of Generator Set Performance before and after Heater Installation

The aim of this thesis is to investigate whether pre-heating of engine coolant can improve its performance especially during start up in attaining its full capacity and consequently save the driven production equipment from high thermal deformations that works in different ranges of combustion and cooling temperatures and also keeps the quality of the semi-processed products partly. In this case, attempt is made to investigate the improvement achieved by tuning the engine without any heater and with different combinations of heaters in the following topics.

4.1.1. Trends of Generator Set Performance before Heater Installation

From table 3.1, it can be observed that the maximum engine coolant temperature record observed is 26°C. The installed engine needs minimum 75°C to attain its full capacity to absorb the high draw starting current requirement of kiln system drive motors as per literature review under section 2.1.

The temperature readings are taken from both the controller display unit and also results of infrared thermometer used are compared with the result of the display especially at the thermostat inlet points as per figure 3.7c before installation of heater also.

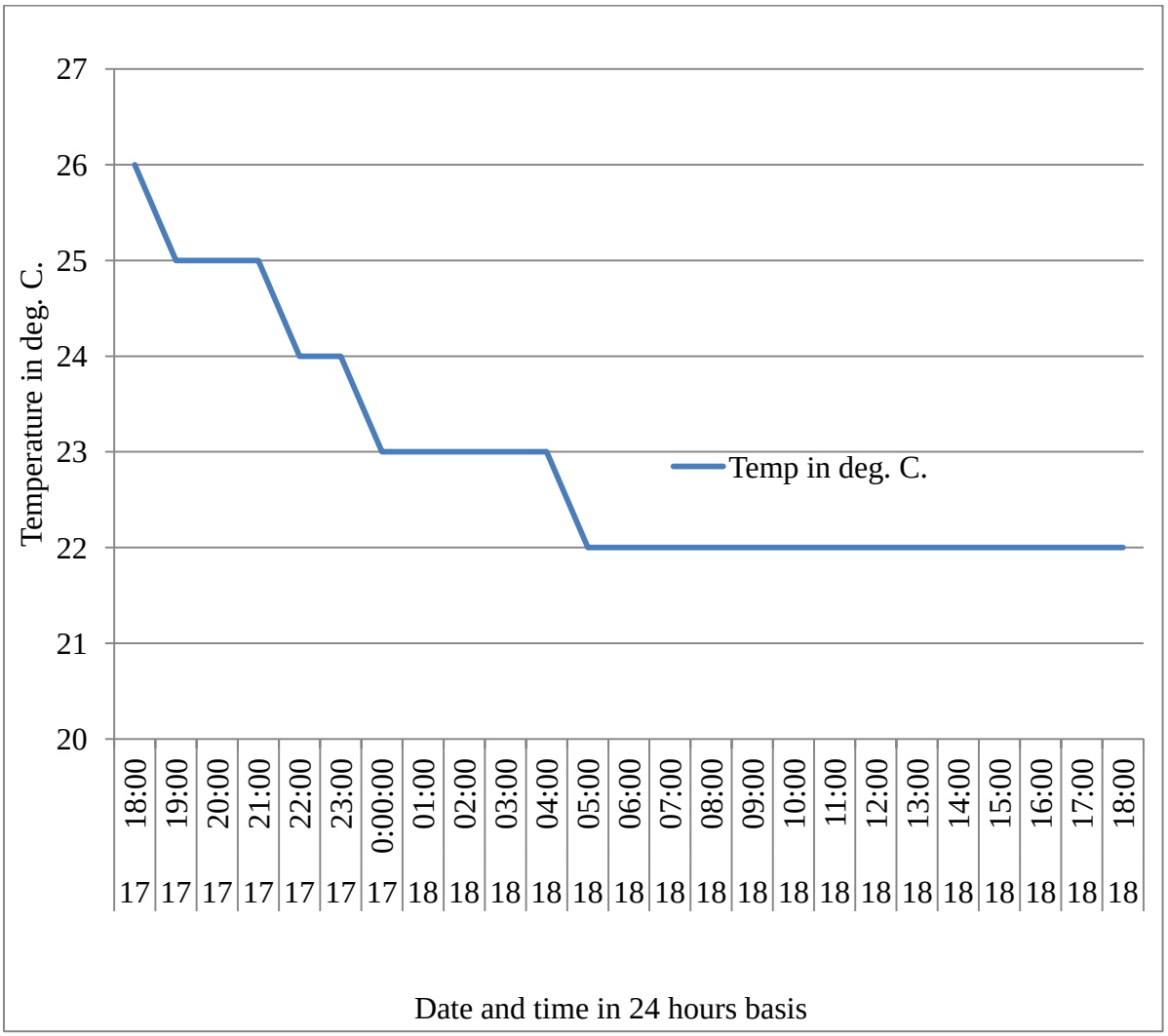

Figure 4.1: Engine temperature reading before electric heater installation

To attain the required engine rated power running temperature, it is required to run minimum for more than 20 minutes depending on the ambient and seasonal conditions as per literature review under section 2.1, which may lead the kiln system equipment to thermal deformation due to high thermal stress mentioned under section 2.5.1 in literature review to thermal deformation and also loss of clinker product quality due to non-procedural/out of standard burning and cooling pattern. The semi-processed material also coagulate and lead to deformation of clinker transport equipments like pan conveyors and due to boulder formation crusher and related parts will be loaded unnecessarily.

4.1.2. Trends of Generator Set Performance after Electric Heater Installation

From table 3.2, it can be observed that the maximum engine coolant temperature record observed using the specified heater under this section (supported by figures 4.2 and 4.3) is

43°C up to 45.3°C, observed early in the morning at 07:00 on the depicted table mentioned. The installed engine needs minimum 75°C, thermostat opening temperature, to attain its full capacity to absorb the high draw starting current requirement of kiln system drive motors as per literature review under section 2.1.

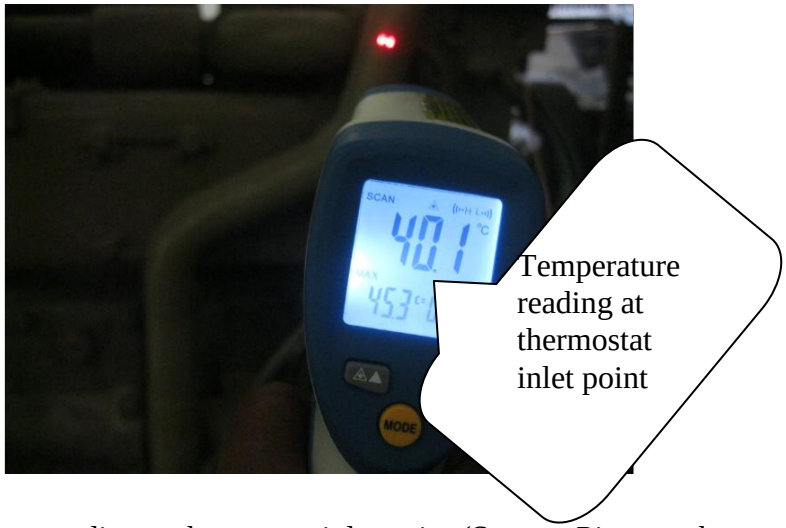

Figure 4.2: Temperature reading at thermostat inlet point (Source: Picture taken on site)

Figure 4.3: Temperature reading on an engine block/cylinder head (Source: Picture taken on site)

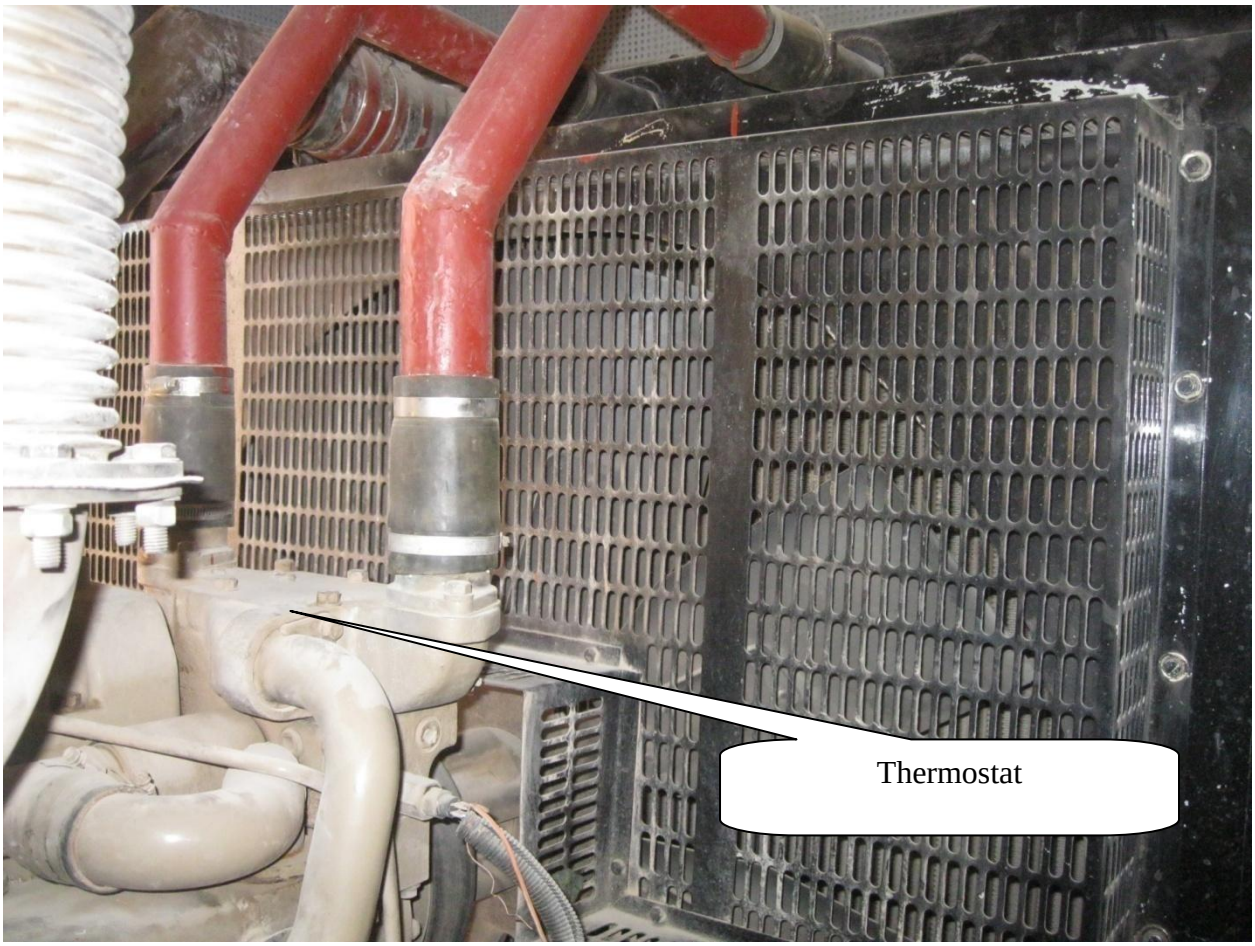

Figure 4.4: Location of Thermostat (Source: Picture taken on site)

To attain the required engine rated power running temperature, it is observed practically that after installation of heater, the required minimum running time has been observed to be 5-10 minutes depending on the ambient and seasonal conditions as per literature review under section 2.1, which indicates an improvement by halving the delay time. Still the improvement is not enough. The time should be less than or equal to 3 minutes to save the kiln system equipments from thermal deformation due to high thermal stress deformation mentioned under section 2.5.1 in literature review and also reduction of loss of clinker product quality due to non-procedural burning and cooling pattern.

To improve the circulating coolant temperature and the pre-heating time requirement, Mugher Cement Enterprise has installed electrical water heater. The parameters of heater installed in line with circulating coolant water are:

III. Voltage: 220V

IV. Power: 4000W

Figure 4.5: Installed Electric Water Heater (Source: Picture taken on site)

The heater is taped from the bottom of the radiator line that leads to the intake side of water pump, which is integral with the engine part that take drive from the power take off point of the engine gear train, which in turn drives the alternator that charges the DC battery of the starting system. The other output end of the heater is directly mounted on the engine block on the output side of the pump by hose.

From table 3.2 above and figure 4.6 below, it can be seen that a great improvement have been achieved in delay time of engine in attaining its rated power that can save major processing equipments.

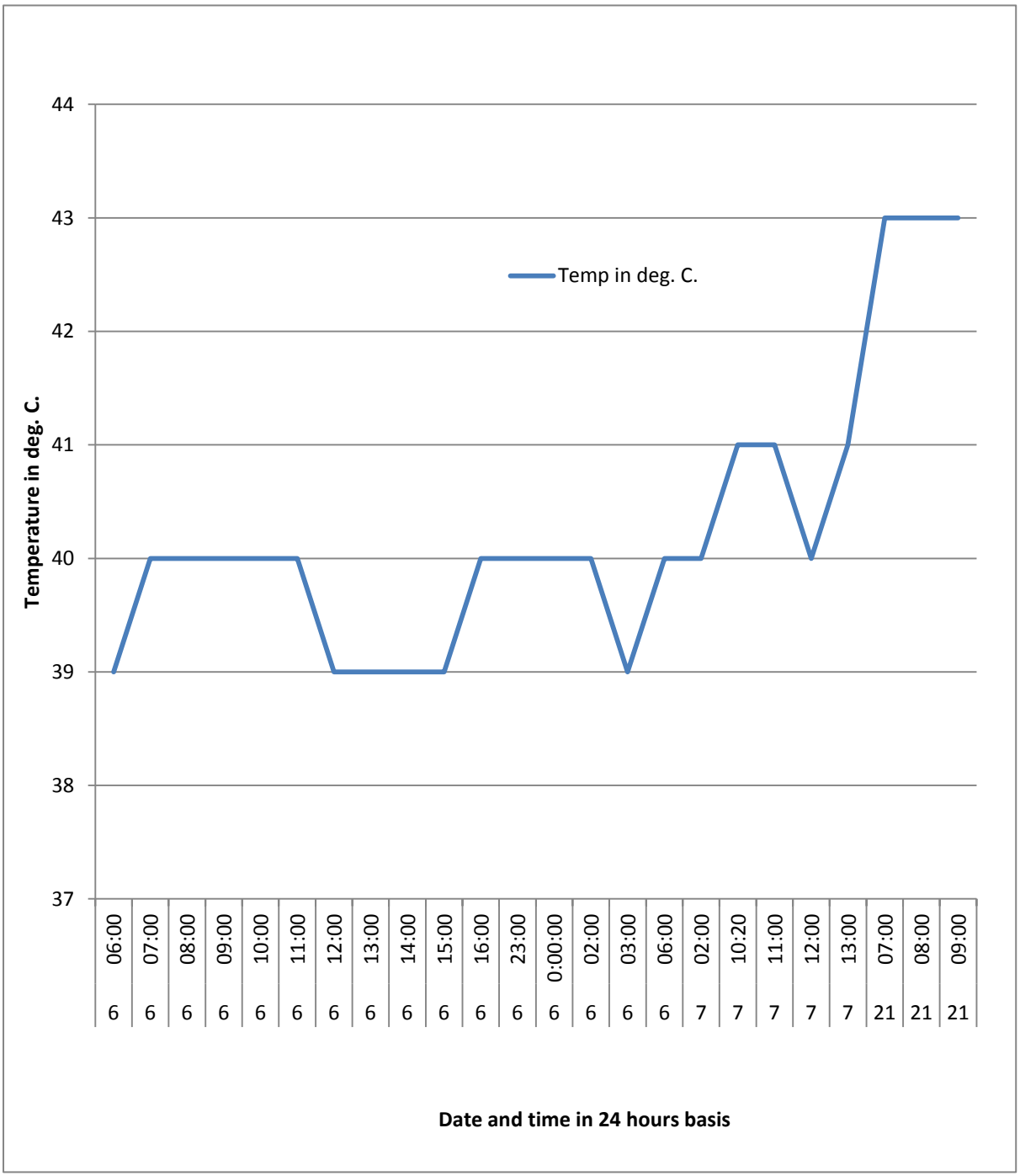

Figure 4.6: Engine temperature reading after electric heater installation

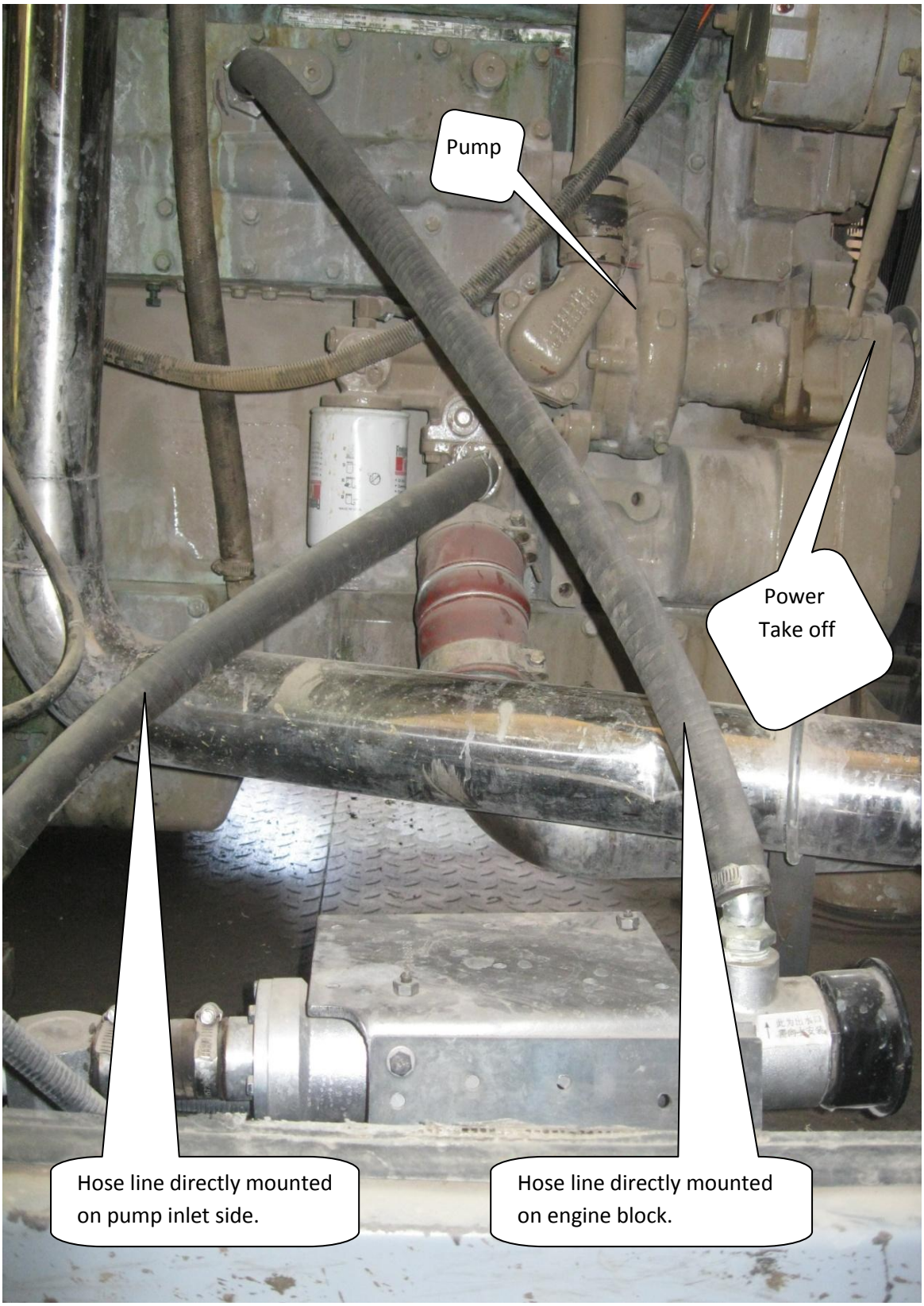

Figure 4.7: Location of water pump and its drive and hose connection points from heater sides (Source: Picture taken on site)

4.2. Selection and Sizing of Heaters

The design data to be used to carry out the design of solar water heater are:

I. Latitude of the location: 9.687° N of equator
II. Longitude: 37.987° E
III. Altitude/elevation: 2496m above sea level
IV. Amount of water to be heated: 100 liters
V. Amount of water required for engine: 35 liters
VI. Inlet cold water temperature: 20°C
VII. Outlet hot water temperature: 55°C
VIII. Inclination of collector: 12°
IX. Specific heat capacity of water: C = 4.180KJ/kg°c
X. Density of water ρ=1000kg/m^3

4.2.1. Solar Collector Sizing and Selection

Solar collector sizing is planned to be carried out in Mugher Cement Factory, a state owned cement producing industry in Ethiopia. Its geographic location is (9°40'60"=9.687°) N latitude, (37°58'60"=37.987°) E longitude at an altitude/elevation of 2496m above sea level, 90 kilo meter away west of the capital city, Addis Ababa. The factory has an average daily production capacity of five thousand tone of clinker with three production lines.

4.2.2. Determination of the Monthly Average Daily Global Insolation for the Required Solar Water Heater

The collector is designed based on the assumption that is to be mounted in Mugher, for which ϕ=9.687^0. It is to have an inclination of 12° [11].

To determine the monthly average daily global insolation, it is preceded as follows. The monthly average daily global insolation ($\bar{H}$) as obtained from reference [11] on the month of May for the year 1988 is $\bar{H}$=19.45 MJ/m^2.day for Addis Ababa which is approximated for Mugher to be equal for sizing purpose).

The monthly average daily extraterrestrial insolation on a horizontal surface in May at Mugher (9.687^0 latitude) as calculated from equations indicated on literature review in which,

ϕ=9.687^0

$\delta = 23.45 sin\left[\frac{360}{365}(284+N)\right]$ =18.8° (Representative angle indicated on Table 2.1)

n = representative day of May = May 15 for which n=135 as counted from January 1.

$\omega_s = \cos^{-1}(-\tan\phi\tan\delta) = 86.67°$ (For Mugher site).

Form equation (2.26):

$$\overline{H_O} = \left[\frac{24\times 3600}{\pi} I_{SC}\right]\left[1+0.033\cos\left(\frac{360N}{365}\right)\right] \times\left[\cos\phi\cos\delta\sin\omega_s + \frac{\pi}{180}\omega_s\sin\delta\sin\phi\right]\left[J/_{m^2}\right]$$

$\overline{Ho}$=282 WH/m^2.day = 36.9MJ/(m^2.day). Therefore, $\overline{K_T} = \frac{\bar{H}}{\bar{H}_o}$=0.527 from equation (2.34).

From equation (2.42), $\frac{\bar{H}_d}{\bar{H}} = 1.403 - 1.672\bar{K}_T$,

$\bar{H}_d = \overline{H}$(1.403-1.672$\bar{K}_T$) = 19.45(1.403-1.672x0.527) = 10.15 MJ/(m^2.day)

The monthly average daily beam insolation on the horizontal surface is obtained by using the equation $\overline{H_b} = \bar{H} - \overline{H_d}$= 19.45-10.15 = 9.3 MJ/(m^2.day)

Using equation (2.20), $R_b = \frac{I_b'}{I_b} = \frac{\cos\theta_i}{\cos\theta_z}$, equation (2.6),

$$\cos\theta_z = \cos\phi\cos\delta\cos\omega + \sin\delta\sin\phi, \textit{ and} \text{ equation (2.5),}$$

$$\cos\theta_i = (\cos\phi\cos\beta + \sin\phi\sin\beta)\cos\delta\cos\omega + \sin\delta(\sin\phi\cos\beta - \cos\phi\sin\beta)$$

$$R_b = \frac{I_b'}{I_b} = \frac{\cos\theta_i}{\cos\theta_z} = 0.98$$

From equation (2.22)

$$R_r = \frac{1-\cos\beta}{2} = 0.011$$

From equation (2.21)

$$R_d = \frac{1+\cos\beta}{2} = 0.989$$

From Appendix D of reference [12] for a characteristic surface surrounding the collector of concrete, for the case of the generator set building as per figure 4.20, ρ_r=0.22

The monthly average daily insolation on a tilted surface is the sum of the entire beam, diffuse and reflective as follows from equation (2.17)

$$\overline{H_T} = \overline{H_b}R_b + \overline{H_d}R_d + \rho R_r(\overline{H_b} + \overline{H_d})$$

$\overline{H_T} = 9.3x0.98 + 10.15x0.989 + 0.22x0.011\ (9.3+10.15) = 19.2$ MJ/(m^2.day)

The above results obtained are used to design the collector to be used which fits the specifications required of capacity= 100 liters.

The collector is to be mounted at Mugher where latitude is 9.6870. These specifications, given above are set to meet the requirement of hot water by the generator installed for 24 hour service to maintain a temperature of 45 to 55°C all day.

4.2.3. Total Collector Area

Here, the simple and approximate way of estimating the absorber area is used. In this method, the following inputs are used.

The minimum cold water temperature is 20°C. This is estimated from table 3.1.The water heater is to deliver 100 liters of water per day at 55°C. The collector efficiency is of the order of 0.5. This could also be confirmed by previous experiments conducted on collector of the same type in Addis Ababa University.

The mean daily available insolation on a surface inclined at about 12° to the horizontal and facing equator (South) at Mugher (latitude = 9.687°) for the average year round use is obtained above to be:

$\overline{H_T} = 9.3x0.98 + 10.15x0.989 + 0.22x0.011\ (9.3+10.15) = 19.2$ MJ/(m^2.day)

The mean daily energy requirement will be

$Q_L = mc\Delta T = \rho vc\Delta T$

Where volume of water v=0.1m^3

Mass of water m

Specific heat capacity of water c = 4.180KJ/kg°c

Density of water $\rho=1000kg/m^3$

Q_L=14630KJ/day=14.630MJ/day.

The useful insolation energy for the specified efficiency is

$Q_u=\overline{H_T}\eta$ = 19.2 x 0.5 = 9.6 MJ/(m^2.day)

The total collector area required is

$$A_T = \frac{Q_L}{Q_U} = \frac{14.63}{9.6} = 1.524 m^2$$

The collector is made in the size of A_c = Area of a collector [m^2] = 2mx1m =$2m^2$. This dimension is selected so that two persons can handle it easily and this size confirms to the size of the sheet metal available in the local market.

Thus, the total number of collector required is

$$\frac{A_T}{A_C} = \frac{1.524}{2} = 0.762 \approx 1$$

Hence, a total of one (1) collector is required.

4.2.4. Operating Principles, Layout and Equipment

Here, the system consists of a solar collector, a circulation system and one storage tank. Engine cooling water from a circulation source is circulated directly through the collector and engine from the tank. The pump circulates water from the tank through the collector and engine. The engine maintains the required temperature throughout the day. If any water level decreases, fresh cold water will be added to the tank. The design of the system is expected to be fully controlled by the controller, as schematically described in figure 4.8 below, even if some of the works are the way forward.

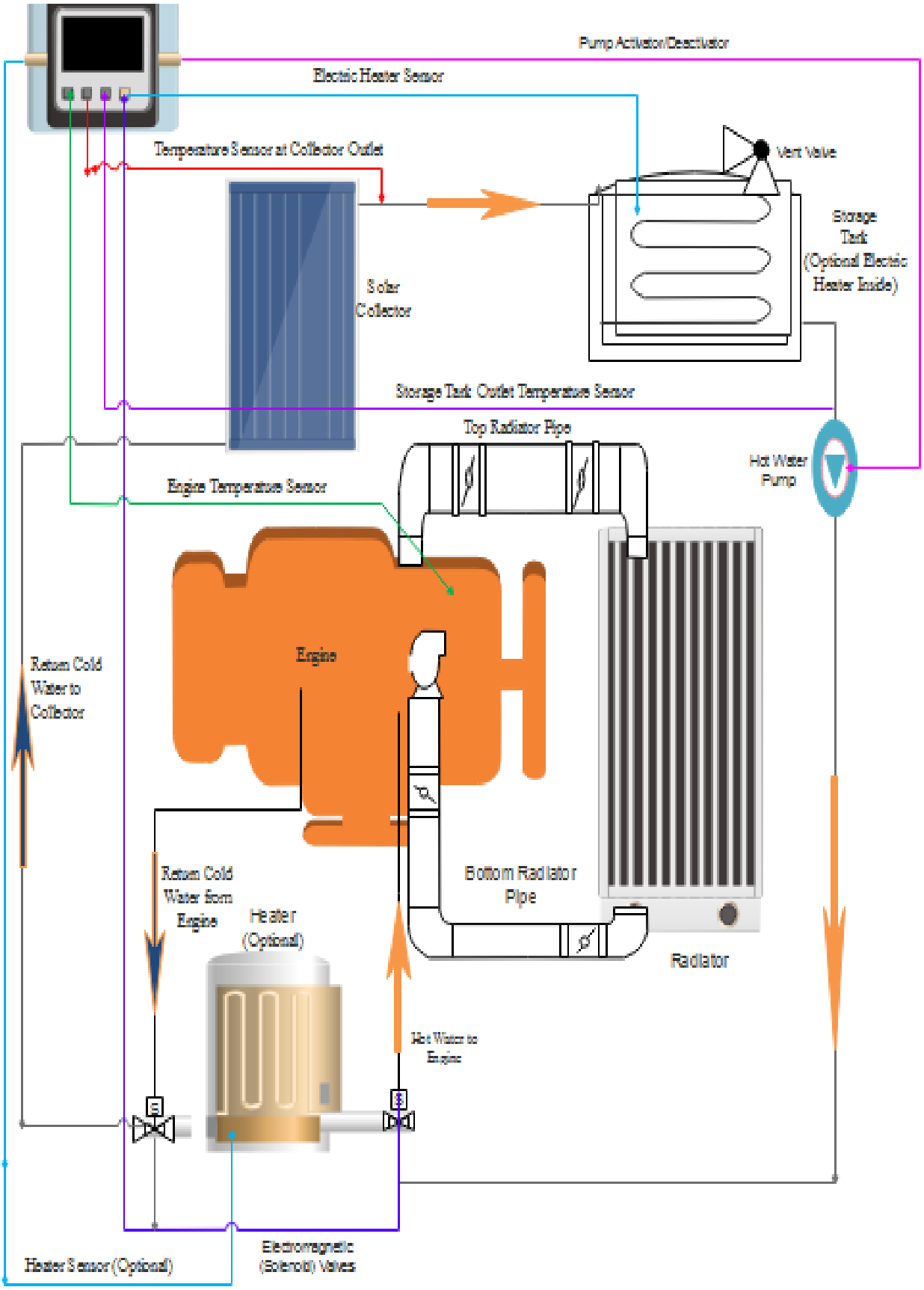

Figure 4.8: Complete System set up.

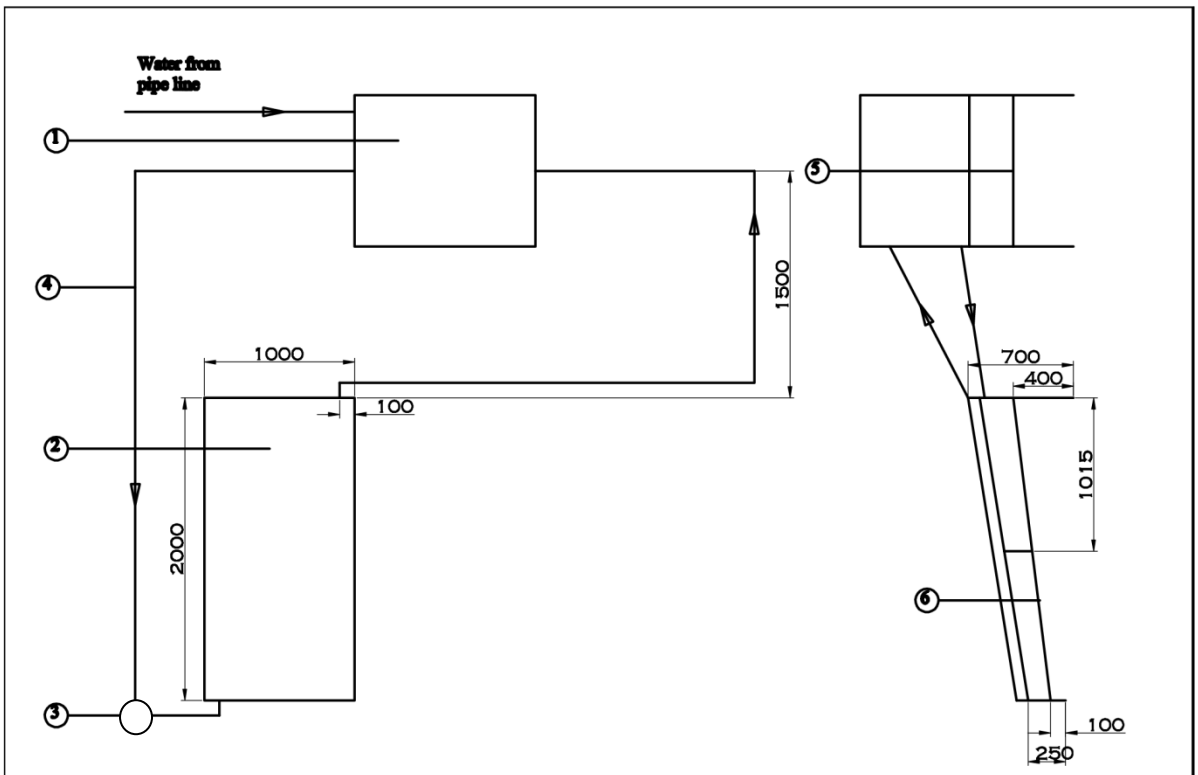

No.	PART NAME	QTY.	MATERIAL	DIMENSION.	REMARK.
6	Support steel	1	Mild steel		
5	Tank support	1	Mild steel		
4	Pipe		Galvanized steel	1 in.dia	
3	Pump	1	Standard		0.25Hp
2	Collector	1	Mild steel	2mx1m	
1	Tank	1	Mild steel	Ø370mm x 900x 4mm	

DR BY:
TADESSE MELETA

CH BY:-
DR.ING. DEMISS ALEMU

A.A.UNIVERSITY INSTITUTE OF TECHNOLOGY ENERGY CENTER

DR.NO:-1

SCALE:
1:10

DATE:

TITLE:
COLLECTOR LAYOUT

Figure 4.9: Collector layout.

4.2.5. Tilt Angle and Position of the Collector

The collector is to be installed in a clear site that face South at an optimal title angle of 12°, a little above the latitude of Mugher. This is done due to the fact that domestic hot water requirement is year round in about the same daily amounts. Thus, this arrangement is for about the same daily gain in all seasons. Relatively constant daily insolation strikes a South facing collector tilted at an angle equal to the local latitude. The orientation should be due south, towards the equator, to take the advantage of the greater heating effect of the afternoon sun.

4.2.6. Absorber Plate

The most difficult choice in designing and building a liquid type flat-plate collector is the selection of an absorber plate. Absorber plates can be made of copper, aluminum, steel, or plastics. But here it is made of steel taking into account the durability and cost of the material.

The arrangement and design of the absorber plate is shown in figure 4.10 below. The absorber plate consists of flat metal sheet (corrugated) with galvanized pipes welded to it as shown in the drawing with the necessary spacing between the pipes. Here, the pipes are welded to the sheet metal intermittently. The dimensions of the absorber plate are given in the drawing.

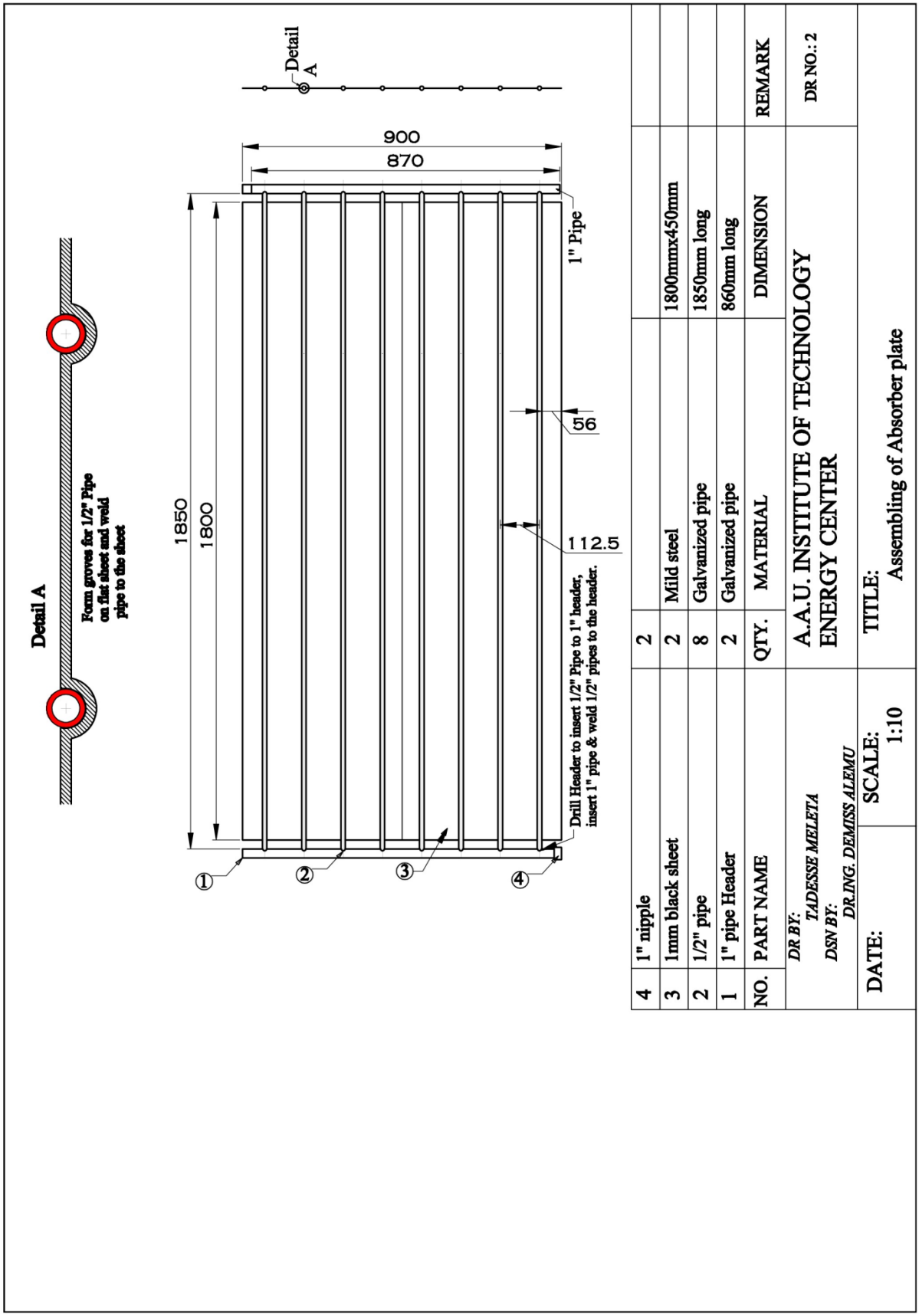

Figure 4.10: Assembly of absorber plate.

4.2.7. Absorber Coating (Black–Paint Spray)

The primary function of the absorber surface or coating is to maximize the percentage of sunlight retained by the absorber plate. The black material is used because of its high absorptance. It also maximizes the absorptance of solar energy and minimizes the radiation emitted by the plate.

Any surface reflects and absorbs varying proportion of the sunlight striking it. The percentage it absorbs is called its absorptance α. It is the opposite of emittance ε, the tendency of a surface to emit long wave thermal radiation. An ideal absorber coating would have $\alpha = 1$ and $\varepsilon = 0$, so that it would absorb all sunlight striking it and emit no thermal radiation. But there is no such substance, and it is assumed that the black paints have both α and ε close to 1. Note that it is necessary; to clean the absorber plates thoroughly before the application of the black paint spray. That is, it is necessary to use an acid bath to ensure maximum adhesion.The size of the black paint required is three ounces.

4.2.8. Cover Plate

A cover plate is a transparent sheet placed above the absorber plate. It is used to reduce convective and radiative heat losses from the absorber. Short wave sunlight penetrates the cover plate, glass sheet in this case, and is converted to heat in the absorber. The cover plate, glass sheet, retards the escape of heat. It absorbs the thermal radiation from the hot absorber, returning some of it to the collector, and prevents the escape of warm air. Commonly used transparent materials include glass, Plexiglas, fiber glass reinforced polyester, and thin plastic films. They vary in their ability to transmit sunlight and trap thermal radiation. They also vary in weight, ease of heating, durability and cost.

Glass is used for this specific purpose as it is very good solar transmittance and is almost totally opaque to thermal radiation, that is, long wavelength radiation emitted by the absorber plate. Furthermore, it is readily available and installation techniques are familiar for most persons.

The glass cover plate must be able to expand and contract while maintaining a tight seal against moisture and air leakage. It is made to rest on rubber as there is potentially severe heat on metal, see figure 4.11 below on the next page.

A critical choice in the design of a solar collector is the number of cover plates to use. Additional cover prates provide extra barriers to retard the outward flow of heat and ensure higher collector temperatures. But the more cover plates, the greater the fraction of sunlight absorbed and reflected by them and the smaller the percentage of solar energy reaching the absorber surface. Considering these factors and the additional cost incurred by having more cover plates, the glass sheet of 2m x1m x 3mm is used for this specific purpose.

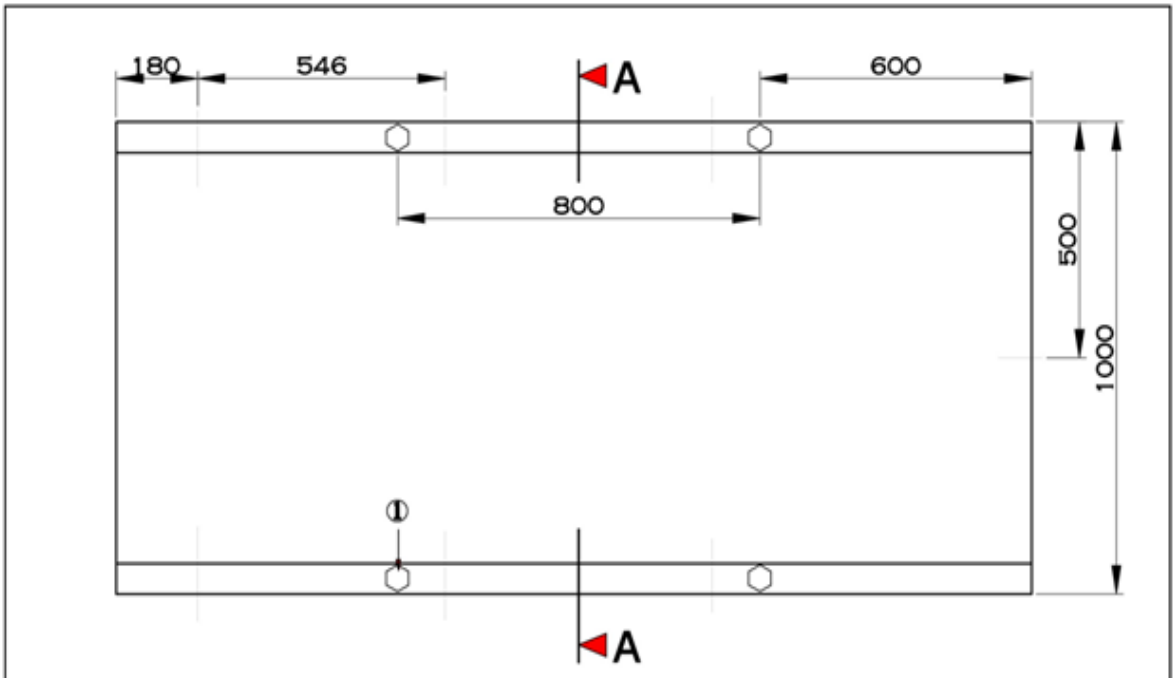

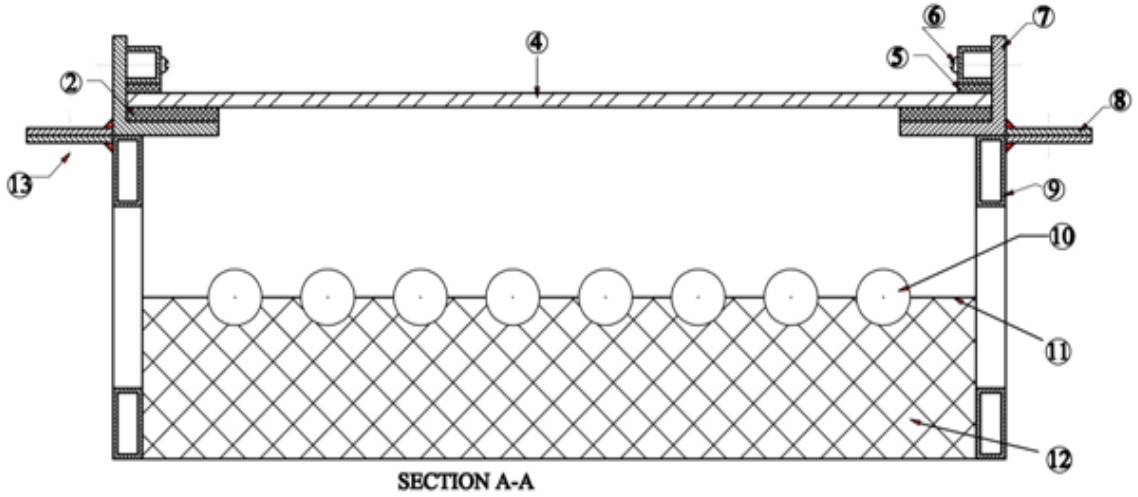

SECTION A-A

13	Nut	5	M5
12	Insulation		
11	Absorber plate	2	1800mmx450mm
10	Pipe	8	Ø1/2"x1854mm
9	RHS30x10x1.5	4	2000mm
8	Sheet metal	4	2020mmx20mmx2mm
7	Angle iron	2	2000mmx25mmx25mmx3mm
6	Metal sheet screw	10	M5x15mm
5	rubber	2	2000mmx10mmx3mm
4	Glass	1	2000mmx1000mmx3mm
3	U-tube	2	2000mmx10mmx10mmx1.5mm
2	Rubber	2	2000mmx22mmx3mm
1	Bolt	5	M5
No.	PART NAME	QTY.	SPECIFICATION.
TITLE:- Collector Arrangement and its Sealings			
DESIGNED BY: TADESSE MELETA	CHECKED BY: DR.ING.DEMISS A.		
A.A.U. INSTITUTE OF TECHNOLOGY ENERGY CENTER			DR.NO:-3

Figure 4.11: Collector arrangement and its sealings.

4.2.9. Insulation

Insulating material, fiberglass is placed at the back and sides of the collector to reduce parasitic heat losses. That is insulation is added in order to cut heat losses out. The insulation material should be protected from water and should be of closed-cell construction. It should also be non-flammable. Fiberglass is used because of its stability at high temperatures as it can fulfil the above conditions stated and has lightweight.

The perimeter of the absorber must be insulated to reduce heat losses at the edges. Temperatures along the perimeter of the absorber are generally lower than at the middle because of the losses, which can be reduced by massive insulation around the edges. But extra insulation is avoided as it seriously reduces the absorber surface exposed to the sun. Metal sheets of thickness 1mm with the anti-rust applied on them, is used as a protective casing around the outside of the insulation.

4.2.10. Tube Sizing and Flow Patterns

The flow passage conduct the working fluid, water, through the collector by using the galvanized pipe welded to the absorber plate intermittently. The flow passage does not extend over the entire absorber plate surface, and heat is conducted along the absorber plate to reach the fluid, water. The tubes are spaced 10 centimetres apart, the absorber surface between them acts like a fin, with radiant energy impinging on the surface, being conducted toward the tubes, and being transferred from the tube inner surface by convection to the water.

Flow tubes in the collector is thermally welded to the collector plate in such a way that there is good thermal conductance as welded contacts reduce the contact resistance between the tube and plate. The flow tubes are routed through the collector in parallel paths from an inlet to an outlet header. See figure 3.9 for the arrangement of headers, their size and flow patterns.

4.2.11. Pump Selection

A forced circulation system is required for this arrangement of generator set under consideration. The pump is selected for a flow rate of 1.1 litre/(min.m^2) which is nearly the same as the natural circulation system. Besides these, the engine requires enough coolant to function properly and the head of the location of collector relative to engine should be considered for selection of the pump.

Based on the above specifications and considering other factors necessary for its selection, a pump of 0.25 Hp is used for this purpose.

4.2.12. Energy Storage Tank

Solar systems can also provide heat when the sun is not shining. On sunny days, a properly sized system should be able to collect more energy than is needed to met the daytime heating load, and the excess energy can then be stored for later use. Here the water tank is used for heat storage purpose.

In the storage system, it is necessary to have:

I. A heat storage material
II. A container and
III. Provision for adding and removing heat.

A storage tank is made to be well insulated to minimize heat loss. Heat is also lost as water is moved into and out of storage. These losses include:

I. Losses between the collector and the storage tank (charging losses)
II. Losses between the storage tank and the heating load (discharge losses)

To minimize these losses

I. The ducting or piping from collector to storage tank is made to be well insulated and have weather protection and
II. The piping or ductwork from storage to load is made to be as short as possible and well insulated.

The size of the storage tank is based on the daily demand of hot water and also on the radiation intensity available at the place. A rectangular structure of size of 450mm x 450mm x 500mm is used as the storage tank. Furthermore, to preserve heat it is provided with 10cm thick fiber glass insulation, which is also protected by a mild steel sheet of 1.5mm thick. If necessary a small immersion heater and cheap safety thermostat can be fitted into the storage tank.

The cold water enters at the bottom through a galvanized pipe connected to a float value system. The hot water delivery pipe takes off 30cm below the water level so as to insure good flow rate. See figure 4.12 below for the storage tank.

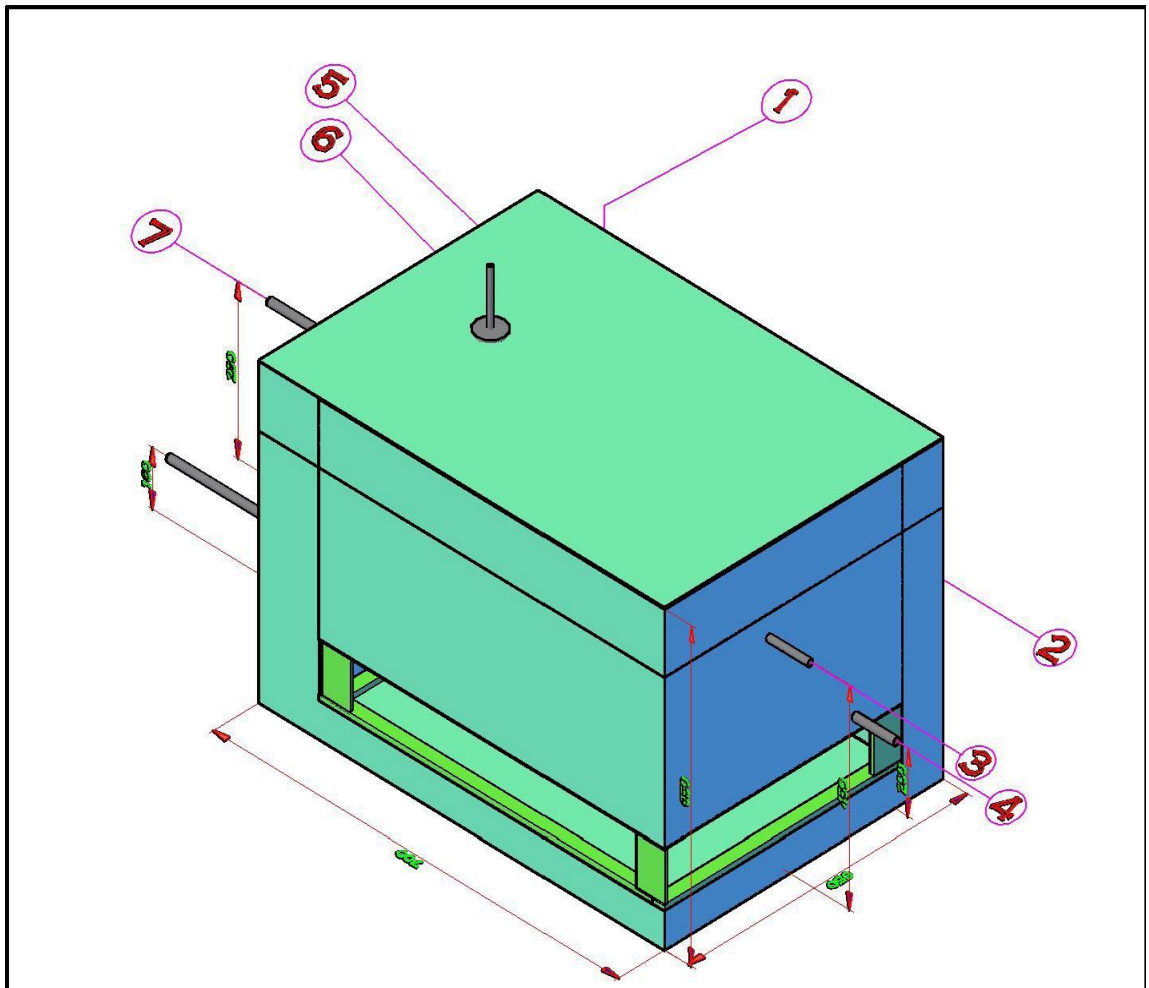

No.	PART NAME	QTY.	MATERIAL	DIMENSION.	REMARK.
9	Support	1	RHS50x10	450x500x100	
8	outlet pipe	1	Galvanized pipe		
7	Discharge pipe	1	Galvanized pipe		
6	Manual inlet	1	Mild Steel		
5	Air vent	1	Galvanized pipe		
4	Pipe from line	1	Galvanized pipe		
3	Inlet pipe	1	Galvanized pipe		
2	Insulation cover	1	Mild Steel	700x650x650	
1	Tanker	1	Mild Steel	500x450x4500	

DR BY: TADESSE MELETA
CHECKED BY: DR.ING. DEMISS ALEMU

A.A.U INSTITUTE OF TECHNOLOGY
ENERGY CENTER.

DR.NO:-11

DATE:

SCALE: Not to Scale

TITLE: Storage Tank

Figure 4.12: Storage Tank.

Here, other drawings related to this project are presented as follows:

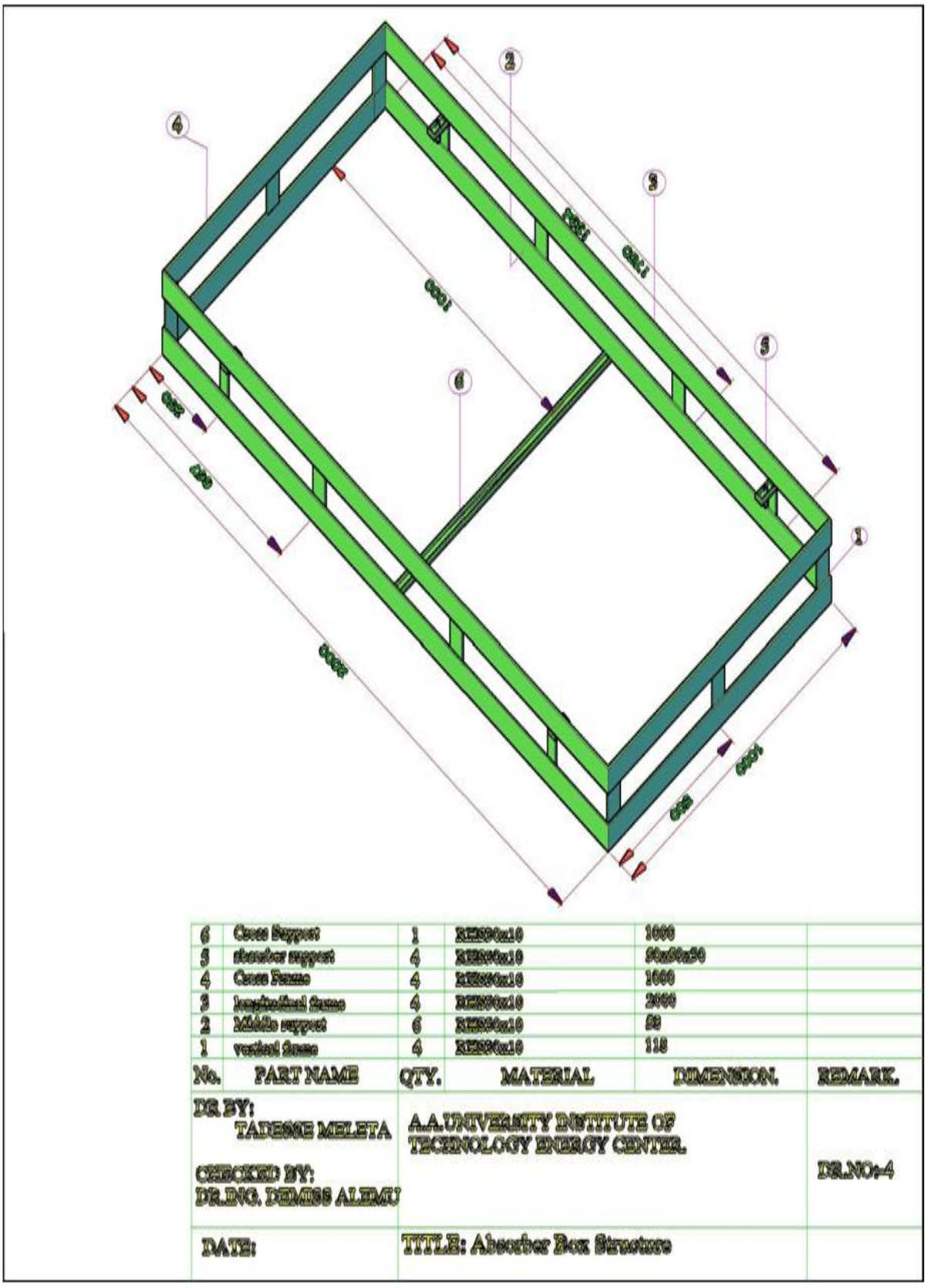

Figure 4.13: Absorber Box Structure.

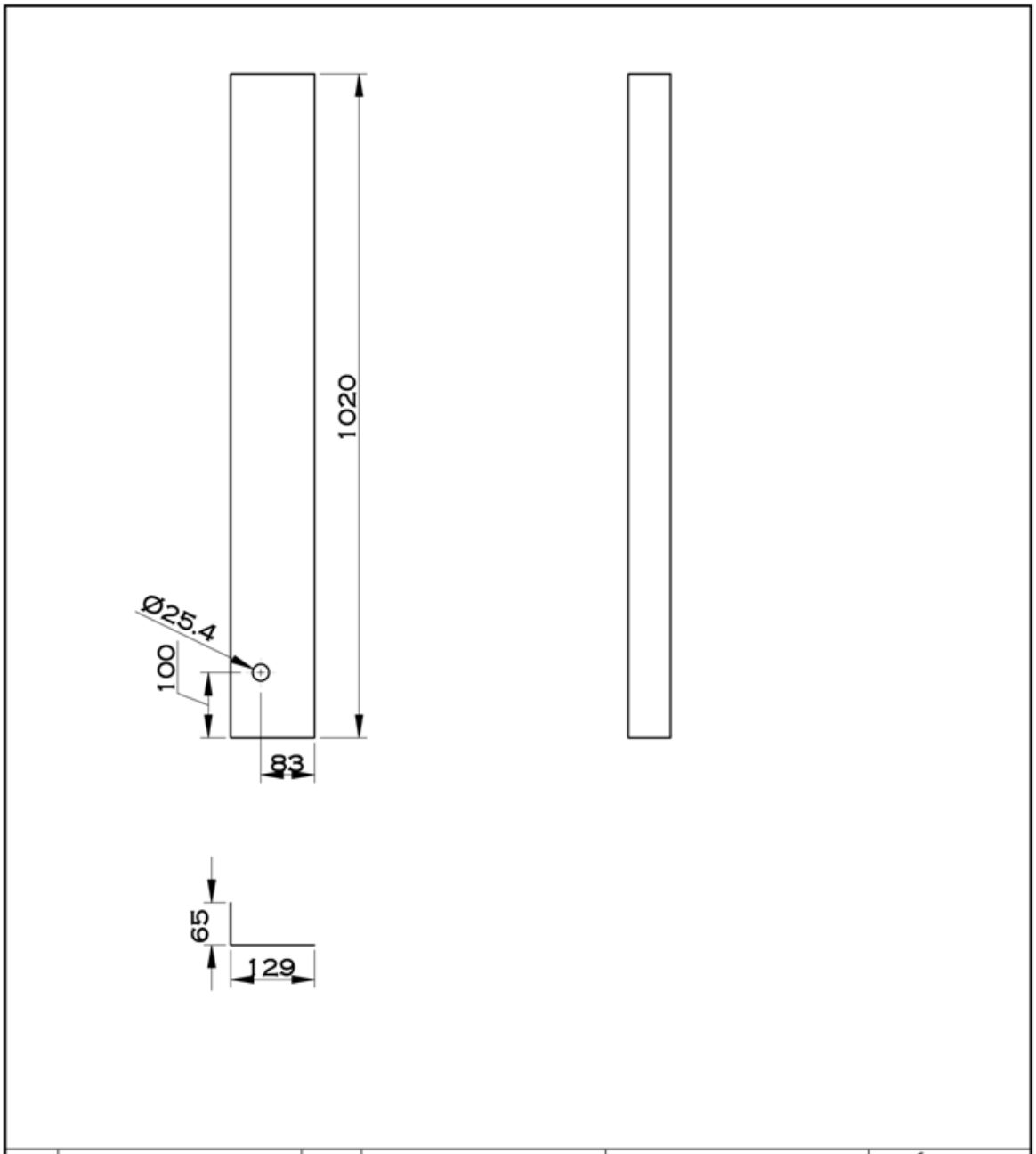

No.	PART NAME	QTY.	MATERIAL	DIMENSION.	REMARK.
1	Front Cover	1	Mild steel	1000x129x130x1	6 is rqd

DR BY: TADESSE MELETA CHECKED BY: DR.ING. DEMISS ALEMU	A.A.UNIVERSITY INSTITUTE OF TECHNOLOGY ENERGY CENTER	DR.NO:-5
DATE:	SCALE: 1:10	TITLE: *Front Cover*

Figure 4.14: Front Cover Structure.

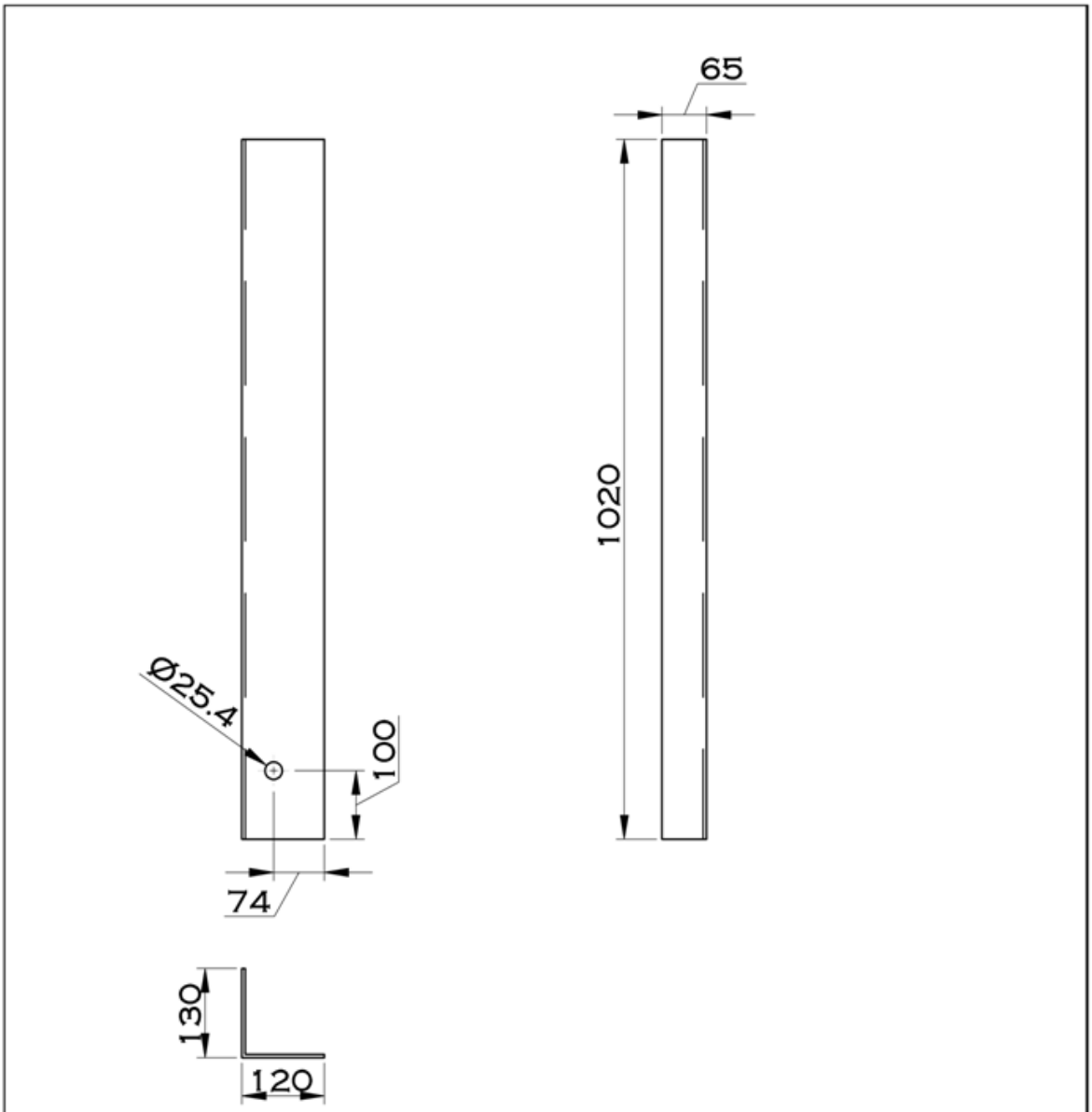

1	Front Cover	1	Mild steel	1000x130x120	
No.	PART NAME	QTY.	MATERIAL	DIMENSION.	REMARK.
DR BY: TADESSE MELETA CHECKED BY: DR.ING. DEMISS ALEMU		A.A.UNIVERSITY INSTITUTE OF TECHNOLOGY ENERGY CENTER			DR.NO:-6
DATE:	SCALE: 1:10	TITLE: *Front Cover from side*			

Figure 4.15: Front Cover Structure from Side.

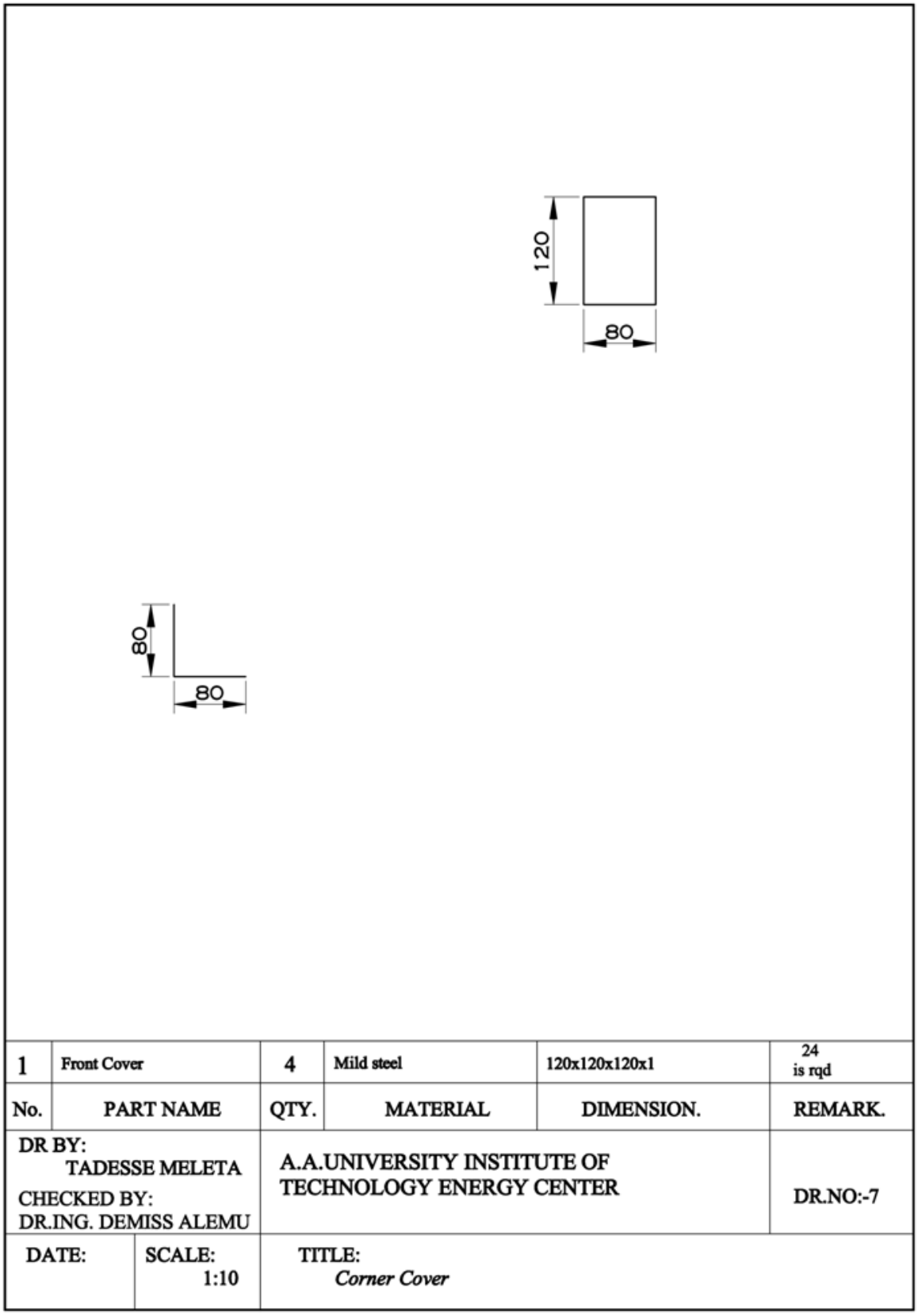

1	Front Cover	4	Mild steel	120x120x120x1	24 is rqd
No.	PART NAME	QTY.	MATERIAL	DIMENSION.	REMARK.
DR BY: TADESSE MELETA CHECKED BY: DR.ING. DEMISS ALEMU		A.A.UNIVERSITY INSTITUTE OF TECHNOLOGY ENERGY CENTER			DR.NO:-7
DATE:	SCALE: 1:10	TITLE: *Corner Cover*			

Figure 4.16: Corner Cover Structure.

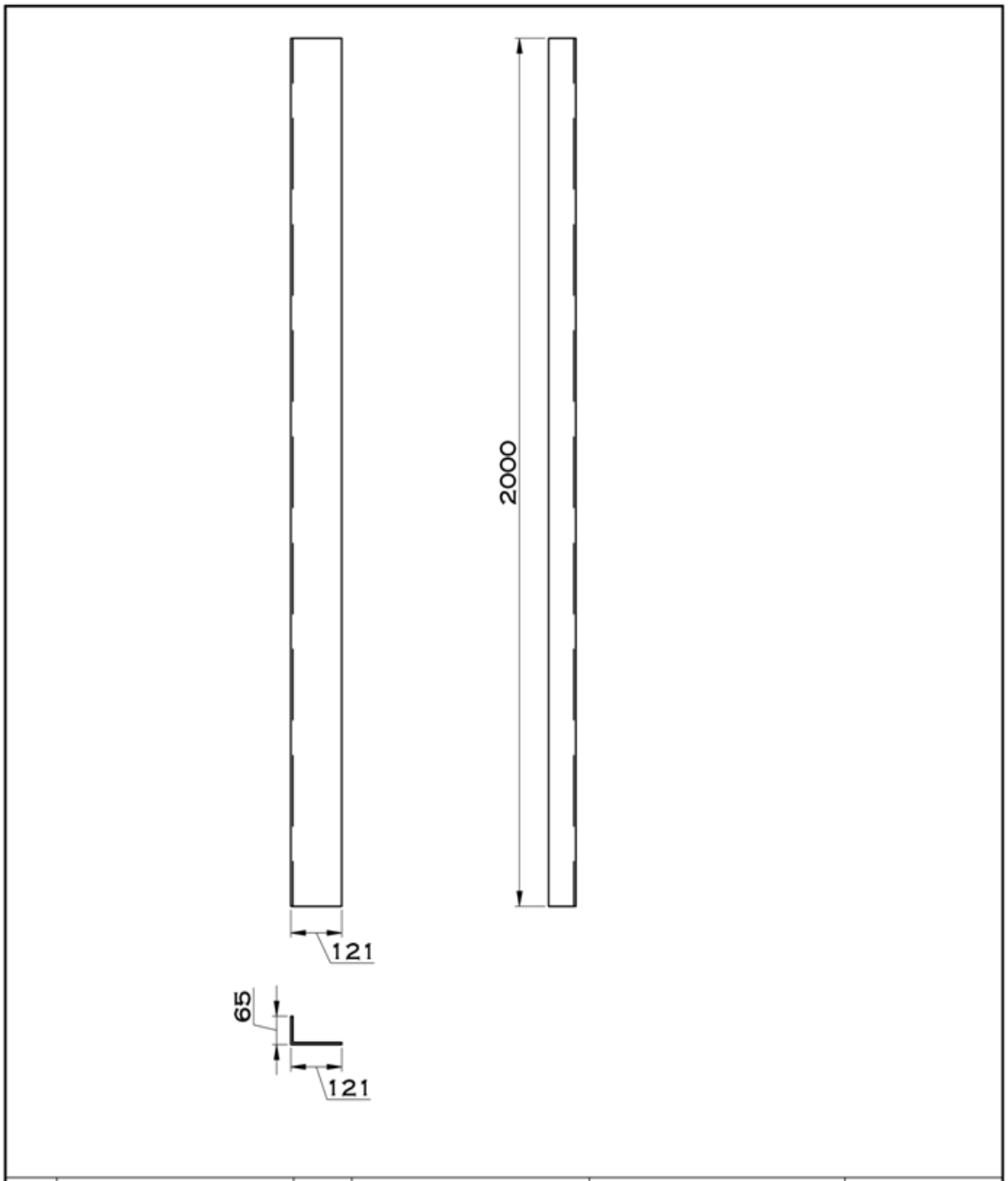

1	Side Cover	1	Mild steel	2000x121x65	
No.	PART NAME	QTY.	MATERIAL	DIMENSION.	REMARK.
DR BY: TADESSE MELETA CHECKED BY: DR.ING. DEMISS ALEMU		A.A.UNIVERSITY INSTITUTE OF TECHNOLOGY ENERGY CENTER			DR.NO:-8
DATE:	SCALE: 1:10	TITLE: *Side Cover*			

Figure 4.17: Side Cover Structure.

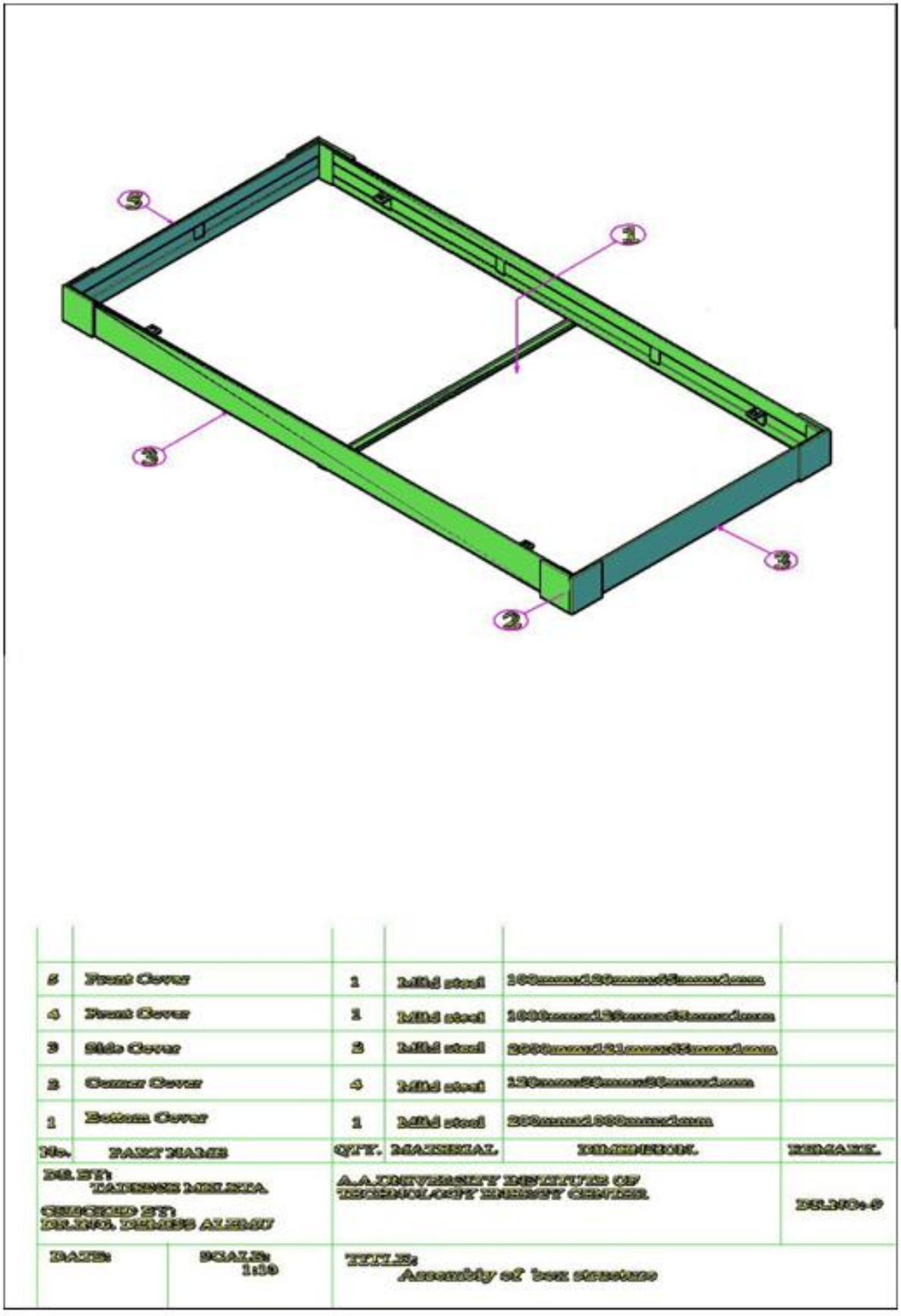

Figure 4.18: Sheet Metal Covered Structure.

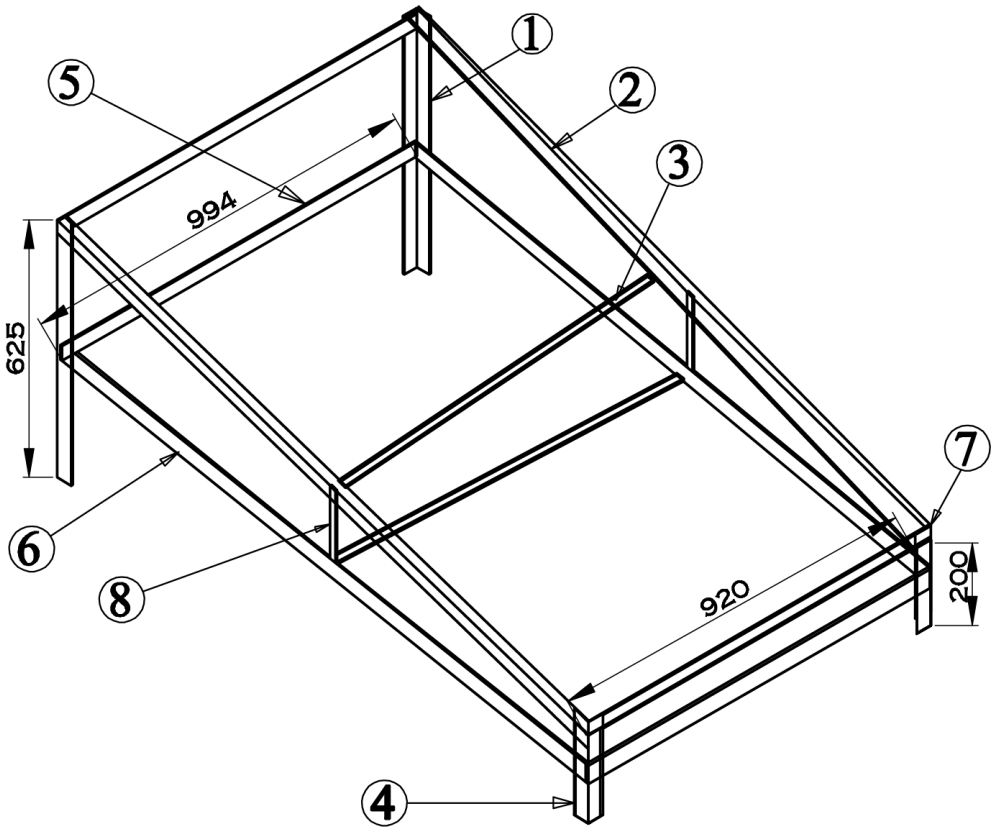

No.	PART NAME	QTY.	MATERIAL	DIMENSION.	REMARK.
8	Vertical Support	2	Mild steel	RHS30x10x212.6mm	
7	Frame (RHS)	2	Mild steel	40mmx40mmx40mmx3mm	
6	Side reinforcing structure (RHS)	2	Mild steel	1994mmx30mmx10mm	
5	reinforcing structure (RHS)	2	Mild steel	988mmx30mmx10mm	
4	Supporting leg (angle iron)	2	Mild steel	208.5mmx40mmx40mmx12°	
3	Support	3	Mild steel	920mmx30mmx10mm	
2	Frame (angle iron)	2	Mild steel	2000mmx40mmx40mm	
1	Supporting leg (angle iron)	2	Mild steel	622mmx40mmx40mmx12°	

DR BY: TADESSE MELETA CHECKED BY: DR.ING. DEMISS ALEMU	A.A.UNIVERSITY INSTITUTE OF TECHNOLOGY ENERGY CENTER	DR.NO:-10
DATE:	SCALE: 1:10	TITLE: Collector Supporting Structure

Figure 4.19: Collector Supporting Structure.

4.3. Trends of Generator Set Performance after Combined Electric and Solar Heater Installation

From the performance improvements observation of table 3.1, 3.2 and measuring instruments results, the generator set shows that its performance has been clearly improved by using heater to heat the coolant. Besides these, it can be deduced, even if it is not yet tested, that coupling of the solar thermal technology can further improve its performance.

The solar water heater with the flat solar collector can heat water not less than 65°C if it is properly oriented, cleaned and made from quality products that best suits the solar thermal technology (Ong, 2011). Based on this, a solar water heater of 100 litre capacity that can best fits the specific situation of this thesis is designed and presented above for the case of Mugher Cement Factory Diesel Engine Driven Electric Generator.

The algorithm/flowchart of the transient analysis of the system has been developed. The transient analysis of the system using appropriate software, manufacturing and erection/installation of the solar collector designed for this thesis is noted to be the way forward that should be carried out to investigate and prove the hypothesis stated in the future.

The collector set is expected to be mounted on the following building (Figure 4.20).

Figure 4.20: Generator set building (Source: Picture taken on site)

The building is exposed to shadings of other buildings of existing plants that may hinder proper irradiance of the panel. The switch gears of the end loads are nearby this building that enables the operators to select proper load according to engine-generator output capacity and severity of the equipments exposure to thermal load.

CHAPTER FIVE

CONCLUSIONS AND RECOMMENDATIONS

5.1. Conclusions

All types of diesel engine driven electric generators are not designed for emergency electric generation purpose because of the delay nature of diesel engines in attaining optimum operating temperature.

To find out the problems of the delay of the diesel engine driven emergency electric generator in attaining its rated power capacity in a shorter time that suits the purpose for which it is intended and seek solution, different data and methodology are used. Among these, engine tuning is carried out with and without electric water heater to meet the objective or prove the hypothesis stated.

From table 3.1, it can be observed that the maximum engine coolant temperature record observed is 26°C. The installed engine needs minimum 75°C to attain its full capacity to absorb the high draw starting current requirement of kiln system drive motors. Again from the analysis made, to attain the required engine rated power running temperature, it is required to run minimum for more than 20 minutes depending on the ambient and seasonal conditions for the case of without electric water heater, which may lead the kiln system equipment to thermal deformation due to high thermal stress.

To improve the circulating coolant temperature and the pre-heating time requirement, electric heater has been installed. From table 3.2 and figure 4.6 above, it can be seen that a great improvement have been achieved in delay time of engine in attaining its rated power that can save major processing equipments. From this table, it can be observed that the maximum engine coolant temperature record observed using the specified heater is 43°C. To attain the required engine rated power running temperature, it is observed practically that after installation of heater, the required minimum running time has been observed to be 5-10 minutes depending on the ambient and seasonal conditions, which indicates an improvement by halving the delay time. Still the improvement is not enough. The time should be less than or equal to 3 minutes to save the kiln system equipments from thermal deformation due to high thermal stress.

From the performance improvements observation of table 3.1, 3.2 and measuring instruments results, the generator set shows that its performance has been clearly improved by using heater to heat the coolant. Besides these, it can be deduced, even if not tested, that coupling of the solar thermal technology can further improve its performance.

The designed solar collector is to be installed in Mugher Cement Factory, a state owned cement producing industry in Ethiopia. Its geographic location is (9°40'60"=9.687°) N latitude, (37°58'60"=37.987°) E longitude at an altitude/elevation of 2496m above sea level. The collector is to be installed in a clear site that face South at an optimal title angle of 12°, a little above the latitude of Mugher.

The monthly average daily insolation on a tilted surface is the sum of the entire beam, diffuse and reflective is calculated to be *19.2* MJ/(m^2.day)

The above results obtained are used to design the collector to be installed which fits the specifications required for the capacity of 100 liters. These specifications, given above are set to meet the requirement of hot water by the generator installed for 24 hour service to maintain a temperature of 45 to 55°C all day.

The minimum cold water temperature is 20°C. This is estimated from table 3.1.The water heater is to deliver 100 liters of water per day at 55°C. The collector efficiency is of the order of 0.5. This could also be confirmed by previous experiments conducted on collector of the same type in Addis Ababa University.

The mean daily energy requirement of the amount of water is obtained to be 14.630MJ/day. The useful insolation energy for the specified efficiency is 9.6 MJ/(m^2.day)

The total collector area required is $1.524m^2$. The collector is made in the size of A_c = Area of a collector [m^2] = 2mx1m =$2m^2$. This dimension is selected so that two persons can handle it easily and it confirms to the size of the sheet metal available in the local market.Thus, the total number of collector required is one (1).

A forced circulation system is required for this arrangement of generator set under consideration. The pump is selected for a flow rate of 1.1 litre/(min.m^2) which is nearly the same as the natural circulation system. Based on the specifications and considering other factors necessary for its selection, a pump of 0.25 Hp is used for this purpose.

Solar systems can also provide heat when the sun is not shining. A storage tank is made to be well insulated to minimize heat loss. The size of the storage tank is based on the daily demand of hot water and also on the radiation intensity available at the place.

Generally, the specific objectives of this thesis, that is, designing and adopting proper solar water heating technology, together with electric heater, for the circulating coolant of emergency electric generator drive diesel engine that shortens preheating time in attaining its thermostat opening temperature of 75°C, for this specific case, has been indicated in a trend from tables 3.1 and 3.2 and analysis of the performance parameters improvement achieved in a lesser time to avoid the rotary kiln and related drive/driven systems thermal gradient deformation immediately after the main grid failure of a cement industry is an indication of the applicability of the result/objective of this thesis. Hence, the objective has been met or hypothesis stated has been proved.

5.2. Recommendations

The main problem in the conversion process of the installed emergency electric generator in this factory is the delay of the conversion process system, including drive engine, in attaining full load during start up to avoid the rotary kiln and related drive systems from thermal gradient deformation immediately after unexpected main grid failure.

It has been deduced by default from the depicted tables of 3.1, 3.2 and instrumental measurement data taken that the delay of the system in attaining its rated capacity is due to low start up operating temperature of drive engine including the circulating coolants and lubricants.

The performance of the engine's coolants and lubricants shall be improved by providing a hotter circulating coolant always readily available by installing a water/coolant heater either electric heater, solar thermal technology heater or the combination of both to reach the engine's thermostat opening temperature within a shorter period of pre-heating time without delay.

Besides these, utilization of exhaust heat that can be obtained through the production process options can be utilized to solve the existing diesel engine driven emergency generator problems. These can be done either by utilizing the hot water that comes out from the screw

compressors available in this factory and also by heating and cooling the water by using the kiln/cooler exhaust gases.

The hot water that come out from compressor can be utilized by installing a proper treatment like filters to remove debris from hot water that comes out after cooling lubricants, the heat recovered from screw compressors can be used to reduce energy costs when used for this specific application as an alternative option.

By utilizing the heat exchanger installed in the air-end cooling oil circuit of the compressor, it is possible to generate hot water for this purpose with correct planning pre-requisite [13].

Again, with correct planning pre-requisite it is also possible to utilize the kiln/cooler exhaust gas by examining proper taping points and optimization of the inlet temperature to the engine requirement by utilizing suitable technologies and techniques because of high exhaust temperatures at most exhaust line points.

In the stages of the heat recovery for both options recommended above, the cold/hot water should be checked for optimum inlet temperature for the engine in a safety heat exchanger. If the water is too hot, it should be cooled down in the connecting cooling/hot water circuit preventing an overheating of the engine systems in the event of high temperatures. Within the system, excess heat should be discharged through system coolers (after-cooler/inter-cooler and oil cooler). To maintain an optimum inlet temperature for the engine, additional after cooler should be installed, if necessary, directly in the cooling/hot water system for installations with heat recovery system.

Generally, the research shall contribute reliability for industry's production processing equipment, especially the key equipment that operate at high process temperature, by avoiding rapid cooling that causes the thermal gradient deformation and leads to complete equipment damage and consequently loss of production, revenue and employee lay off.

The finding/investigation of this research can be used as the potential of making the diesel engine driven electric generator or other vehicles and construction equipments engine in attaining their full load immediately, without longer period of pre-heating time requirement, for the intended purpose by adopting similar technologies for institutions that require immediate back up and reduce fuel consumptions.

Furthermore, it is a better thinking looking at heating water by harnessing energy from the sun in industrial and commercial applications to overcome the rising oil prices and think over other alternative sources of energy, specifically renewable energy technologies and seek better solutions for the existing problems like the case of this research in Mugher Cement Factory and promoting green energy technology.

Finally, this system needs further investigation such as piping connection and other electrical and instrumentation control mechanisms design incorporation to make it fully functional and realistic. It also needs testing of performance parameters after installation of the designed solar water heater. The transient analysis of the system using appropriate software, manufacturing and installation of the solar collector designed for this thesis is noted to be the way forward that should be carried out to investigate and prove the hypothesis stated as per Figure 4.8 complete system set up.

.

REFERENCES

1. Barney L. Capehart, Craig B. Smith, Wesley M. Rohrer Jr. Taylor & Francis Group, "Handbook of Energy Efficiency and Renewable Energy" Edited by Frank Kreith and D. Yogi Goswami, CRC Press 2007
2. Thammasat"Model-based analysis for Experimental Parameter Identification of Micro DC Motor". Thammasat Int. J. Sc. Tech., Vol.13, No.1, January-March 2008.
3. http://www.express-press-release.net
4. http://www.tatabpsolar.com
5. Dipl.-Ing.Walter H.Duda, "Cement Data HandBook", Volume 1, 3rd Edition, Berlin, Bauverlag, 1985.
6. Draft Regulatory Guide DG-1172, "Application and Testing of Safety-Related Diesel Generators in Nuclear Power Plants," U.S. Nuclear Regulatory Commission, Washington, DC, November 2006.
7. Ong K.S., "Experimental comparative performance testing of solar water heaters". Int. J. Low-Carbon Technologies, June 2011.
8. Duffie, J.A. and Beckman, W.A., Solar Engineering of Thermal Processes, 1991.
9. Dr.Ing Abebayehu Assefa's lecture notes).
10. www.retscreen.net
11. ESME JOURNAL No.2; June 1997
12. H.P. GARG, Design and Performance of a Large Size Solar Water Heater, Solar Energy, 1973, Vol.14.
13. KAESER Compressors, Compressed Air Seminar Handbook.